UNIVERSITÀ DEGLI STUDI DI NAPOLI
FEDERICO II

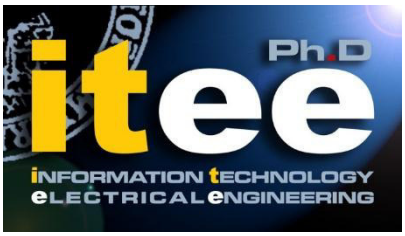

UNIVERSITÀ DEGLI STUDI DI NAPOLI FEDERICO II

PH.D. THESIS

IN

INFORMATION TECHNOLOGY AND ELECTRICAL ENGINEERING

OPTIMAL SIZING OF DISTRIBUTED ENERGY RESOURCES IN MICROGRIDS

ANDREA SCALFATI

TUTOR: PROF. MAURIZIO FANTAUZZI

PROF. DIEGO IANNUZZI

COORDINATOR: PROF. DANIELE RICCIO

XXX CICLO

SCUOLA POLITECNICA E DELLE SCIENZE DI BASE
DIPARTIMENTO DI INGEGNERIA ELETTRICA E TECNOLOGIE DELL'INFORMAZIONE

INDEX

Preface

This work is focused on the optimal sizing of the Distributed Energy Resources included in a Microgrid.

In recent years Microgrids are one of the most relevant research topics in electrical power systems. They are electricity distribution systems containing loads and distributed energy resources that can be operated in a controlled, coordinated way either while connected to the main power network or while islanded, and they are considered a key component of the smart grid scenario, aimed at obtaining better integration of distributed energy resources, increasing energy efficiency and reliability of the whole system, and providing the possibility to improve power quality and to achieve grid-independence to individual end-user sites.

Despite the strong consensus existing among researchers and stakeholders on the variety and importance of the advantages deriving from the implementation of the Microgrid paradigm in modern electrical distribution systems, their widespread diffusion is hindered from cost considerations and from the difficulties in conducting a comprehensive cost-benefit analysis and in identifying qualified modalities for system design and management.

Although the accurate evaluation of the economic results originating from the deployment of a μG is a demanding task, due to considerable uncertainties affecting the required input data, complexity of system model and market dynamics, difficult representation of the economic value for some outcomes, the identification of efficient methodologies for the optimal system design is important to allow appropriate analyses and informed choices on the opportunity and feasibility of μG realizations.

A fundamental aspect involved in the Microgrid design process, which constitutes the object of this work, is the choice and sizing of Distributed Energy Resources to be installed, including both Distributed Generators (DGs) and Electrical Energy Storage Systems (ESSs).

The thesis includes four chapters:

- Chapter 1 is an introduction to Microgrids, outlining their definition and main characteristics, the role they can play in present and future power systems, expected benefits and challenges related to their adoption and diffusion.
- Chapter 2 introduces different approaches applicable to the problem of optimally sizing the distributed energy resources included in a microgrid; a categorization is made distinguishing analytical approaches, mathematical programming approaches and heuristic

approaches, then various techniques used to deal with the uncertainty affecting design parameters are presented: sensitivity analyses, Stochastic Optimization, Sample Average Approximation, Robust Optimization and Decision Theory.

- Chapter 3 presents a new analytical approach aimed at the optimal sizing of energy storage systems in DC microgrids, pursuing the objective to improve the efficiency of energy supply through the minimization of line losses; the DC μG under study is characterized by the presence of loads, fossil and renewables based generation units and storage devices; numerical applications show the effectiveness of the method and allow implementing sensitivity analyses to identify ratios between costs of energy and cost of storage devices which make their installation convenient.
- Chapter 4 is focused on the application of mathematical programming approaches to the problem of optimally sizing, from an economic perspective, the Distributed Energy Resources included in a Microgrid; the proposed procedure is based on Mixed Integer Linear Programming and allows to determine the optimal sizes of Distributed Energy Resources, i.e. distributed generators and storage devices, which minimize the Microgrid Total Cost of Ownership, given location and load characteristics, also considering the opportunities of Load Management related to the presence of different quotes of controllable loads. Two variants of the sizing procedure are presented: the first uses a deterministic approach, not considering the uncertainties that affect design parameters, while the second uses a Robust Optimization approach to deal with them. In both cases, the performance of the sizing results against uncertainty are evaluated *a-posteriori* by means of Monte Carlo simulations. Numerical applications to a case study, referring to a DC μG with PV generation, storage and a certain amount of flexible load, are reported to show the effectiveness of the proposed methodology and allow different useful considerations.

Three appendices accompany the above mentioned chapters:

- Appendix A, linked to Chapter 3, presents an application of the superposition principle to derive a simple analytical expression of the power losses caused by the circulation of currents through the resistances of branch lines connecting the nodes of a DC network, depending on the nodal currents and the conductance matrix of the network;

- Appendix B details the calculations and operations made to adapt the standard AC LV CIGRE distribution network to be used as a DC test grid in the numerical applications of Chapter 3;
- Appendix C describes a well-established methodology of mathematical programming, useful to force different variables not to being simultaneously different from zero while preserving the linearity of the problem formulation, used in Chapter 4 to prevent solutions where energy is sold to the grid and bought from the grid at the same time (which is physically impossible on a single PCC).

Chapter 1

Microgrids

1.1 Introduction

This chapter is an introduction to Microgrids, outlining their definition and main characteristics, the role they can play in present and future power systems, expected benefits and challenges related to their adoption and diffusion.

1.2 The microgrid concept and its role in the future energy system

Microgrids (μGs) are defined by the Cigré C6.22 Working Group as "electricity distribution systems containing loads and distributed energy resources that can be operated in a controlled, coordinated way either while connected to the main power network or while islanded" [1], or similarly, as per the U.S. Department of Energy (DOE) definition, as "...group of interconnected loads and distributed energy resources (DERs) within clearly defined electrical boundaries that act as a single controllable entity with respect to the grid, and that can connect and disconnect from the grid to enable it to operate in both grid-connected and 'island' mode" [2].

The term microgrid was originally used in 2002 by R.H. Lasseter [3], to characterize the reformulation of an already existing concept, that of local power systems, well established in power distribution systems and originally used to increase the reliability of power supply for large institutions or for customers with limited access to the grid, by generating, distributing and regulating the supply of electricity, just like the main grid, but independently from it and on a local smaller scale.

In recent times, the changing energy landscape has driven a new and increasing interest in these systems, mainly related to the need to modernize the electricity system to allow:

- rising penetrations of interconnected distributed energy resources (DERs);
- increased levels of customer choice;
- chance to provide critical or emergency services enabling greater grid resiliency in response to more frequent extreme weather events.

Microgrids are now widely considered a fundamental building block of the future smart grid[1], and are expected to play a key role in allowing better integration of DERs, increasing energy efficiency and reliability of the whole system, and providing the possibility to improve power quality and to achieve grid-independence to individual end-user sites.

Microgrids are generally electrical based local energy systems (but they can include a thermal energy component), located at the distribution level of the Power System and usually operated at low voltage level, which incorporate three key components within a bounded and controlled network: generation, storage and demand [4]. They therefore fulfill all the necessary conditions to realize self-sustaining independent energy systems, that can be operated both not connected to the grid (i.e. in 'island' mode), or connected to the grid through a Point of Common Coupling (PCC), allowing bi-directional energy flow and provision of different services, while maintaining the balance between available supply and current demand through proper control of generators and storage systems and careful modulation of loads.

From the grid's perspective, the central advantage of a μG is that it can be regarded as a controlled entity within the power system that can be operated as a single aggregated load [5]. In other words, it can

[1] According to the European Technology Platform of Smart Grids [6], a smart grid is "an electricity network that can intelligently integrate the actions of all users connected to it – generators, consumers and those that assume both roles – in order to efficiently deliver sustainable, economic and secure electricity supplies".

establish binding contractual agreements with the bulk power provider covering its pattern of usage that are at least as strict as those covering existing customers, and it potentially could provide additional services.

Customers benefit from a μG because it is designed and operated to meet their local needs for heat and power as well as provide uninterruptible power, enhance local reliability, reduce feeder losses, and support local voltages/correct voltage sag. The pattern of exchange of energy services between the μG and the bulk power provider grid is determined by prevailing economic conditions.

1.3 Microgrid fundamentals

1.3.1 Basic microgrid architecture

The basic μG architecture reflects the concept of operating a set of loads and micro-sources (i.e. generators and storage devices) as a single system, by means of appropriate control and protection systems.

Power electronic plays a fundamental role in interconnecting micro-sources and loads to the distribution system and represents the critical distinguishing feature of a μG, providing the required flexibility to ensure the coordinated protection and operation which allows the μG to function as a semiautonomous power system, to present itself to the bulk power system as a single controlled unit, to enable simple 'plug-and-play' connection of micro-sources, and to meet the customers' local needs, including increased local reliability, security and affordability.

Figure 1-1 illustrates the basic μG architecture. The electrical system is assumed to be radial with three feeders – A, B, and C – and a collection of loads.

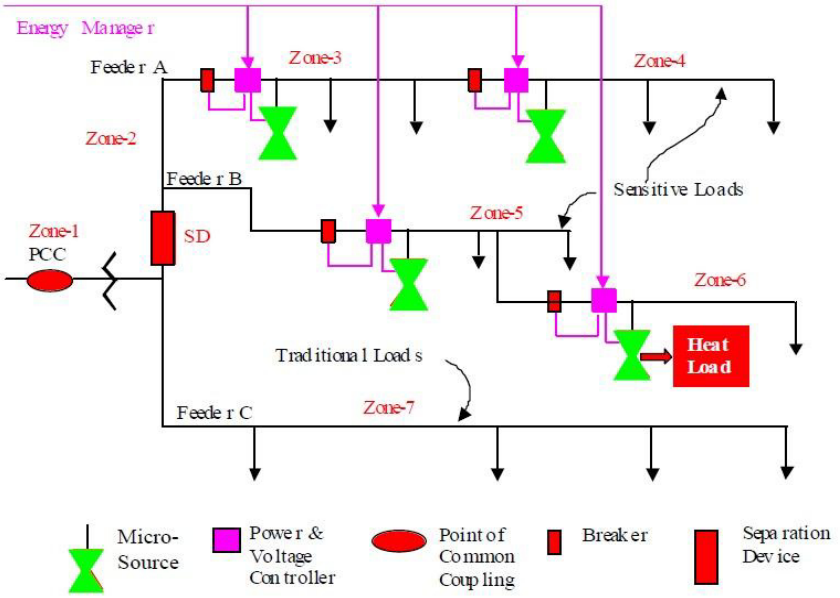

Fig. 1-1: Microgrid Architecture [5]

While feeder C supply ordinary loads that can be left to ride through grid disturbances, feeders A and B include critical loads and micro-sources, and can operate in island mode (within the limits imposed by micro-sources' capacities and possibly resorting to load curtailment) by opening the separation device SD. The presence of micro-sources along the feeders and near to the loads help also in reducing line losses and supporting voltage.

Key issues that are part of the µG structure include the interface, control and protection requirements for each micro-source, as well as µG voltage control, power flow control, load shedding during islanding, protection, stability, ability to operate smooth transition to and from the island mode and over all operation.

These issues are managed by means of power electronics (involved in micro-sources and load interfaces and in protection devices), control, and communications capabilities.

1.3.2 Hierarchical control

The complex control functions to be realized in a µG are usually based on a two-level hierarchical structure, that realizes a compromise between centralized and decentralized approaches:

- primary control is the first level and realizes the local control of single micro-sources, loads or protection devices (Power & Voltage Controller in fig. 1-1); it features the fastest response, relying only on local measurements to react instantaneously in predefined ways to local events, then requiring no communication;
- secondary control (Energy Manager in fig. 1-1), also referred to as μG Energy Management System (EMS), pursues the reliable, secure and economical operation of the microgrid, searching for the optimal Unit Commitment (UC) and dispatch of the available DER units, in the light of certain selected objectives, and sending correspondent calculated references for power and voltage to local controllers of the first level in the span of a few minutes.

A tertiary control level has been considered, which is responsible for coordinating the operation of multiple microgrids interacting with one another in the system, and communicating needs or requirements from the host grid (voltage support, frequency regulation, etc.). Yet, this control can be considered part of the host grid rather than the μG itself.

1.3.3 AC, DC and hybrid microgrids

Microgrids can be classified into AC μGs, DC μGs or hybrid μGs, depending on whether they transmit electricity in the form of alternate current or direct current, or with a combination of the two technologies.

AC μGs are more common because alternate current technology has been the traditionally dominant power delivery scheme, but DC and hybrid μGs are gaining interest both in academic and industrial world, because of potential benefits in terms of energy efficiency and capital savings and in terms of lower control system complexity (with positive consequences on system reliability and controllability).

Figure 1-2 shows a conceptual illustration of a hybrid AC-DC μG, interfaced to the main grid via a traditional voltage transformer, whereas the DC subsystem is interfaced to the AC one through a power electronic based AC/DC converter, which should be capable of allowing bi-directional energy flows between the two sub-systems if such energy exchanges are planned. For a DC μG connected to the

main AC grid, the (bi-directional) AC/DC converter would be the interfacing device on the PCC.

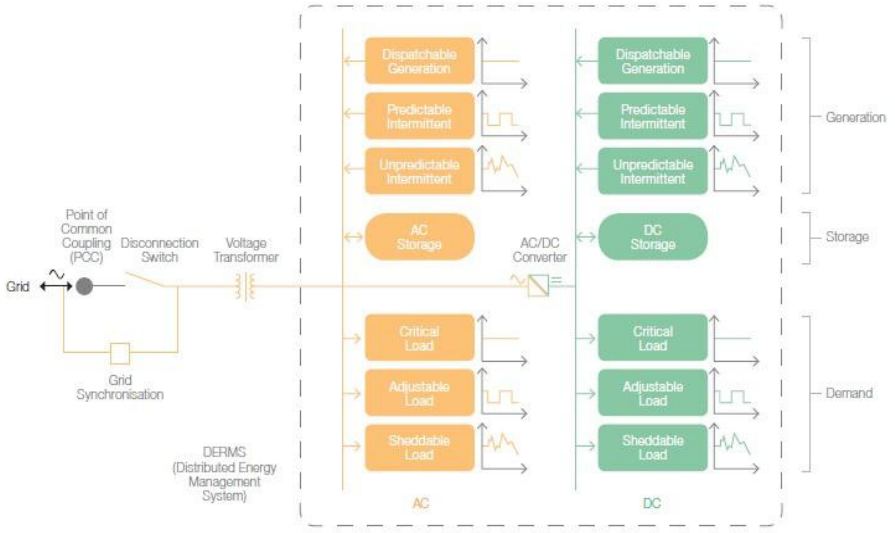

Fig. 1-2: Hybrid AC-DC Microgrid [4]

1.4 Microgrids and Distributed Energy Resources

One of the main features of μGs is that they offer a way to better control and integrate a variety of Distributed Energy Resources, usually located on the customer's side of the distribution system, and connected at low or medium voltage in front of the meter or behind the meter.

These DERs include Distributed Generation (DG) and Distributed Energy Storage (DES), that are more and more used by many customers to implement, on a local scale, effective alternatives to the main grid, as sources of high-quality, affordable and reliable electricity. Some defines DERs more broadly to include energy efficiency(EE) and energy management systems (EMS), Electrical vehicles (EV) and EV chargers, and demand response (DR).

The most important types of DERs often included in microgrids are [7]:

- Solar photovoltaics (PV)—Includes resources such as rooftop solar installations, which are typically small and have intermittent power output. These resources are widely dispersed on the grid and grid operators have little visibility or control over them. In addition to residential solar PV, community solar programs and commercial and industrial (C&I) PV are growing fast.
- Other distributed generation—In addition to solar PV, there are many other types of distributed generation resources connected to the grid, from combined heat and power (CHP) systems, to natural gas turbines, micro-turbines, wind turbines, biomass plants, and fuel cells.
- Energy storage—Energy storage includes many technologies, such as pumped hydro (scarcely likely to be deployed as DER), thermal storage, batteries, super-capacitors, fly-wheels. Storage resources can help provide grid flexibility since they can either draw power from or send power to the grid and provide grid services that help balance the system.
- Demand response—Includes a number of technologies and applications that adjust energy load to reduce peak demand and provide electricity services to the grid, such as frequency regulation. Demand response applications can be automated or manual and may control residential, commercial or industrial load. They are another source of flexibility that can help balance the grid, maintain reliability and reduce the need for new infrastructure.
- Electrical vehicles (EV) and EV chargers—Since they use batteries, electric vehicles can be seen as storage devices that can either draw electricity from the grid or provide stored electricity back to the grid. Several pilot programs and researches are exploring the capabilities of EVs and EV chargers to help balance the grid resources.
- Energy efficiency/energy management systems—Includes residential home energy management (HEM) systems that use smart thermostats to control energy use, sometimes in conjunction with demand response programs, as well as increasingly sophisticated building energy management systems for commercial and industrial (C&I) customers.

The continuously growing interest in these resources is mainly due to reasons which can be classified in three main categories: environmental, commercial and regulatory drivers [8].

Environmental drivers include the ability to limit greenhouse gas (GHG) emissions (by resorting to renewable energy resources and by making generators and loads closer so reducing transmission line losses), or avoid the construction of new transmission circuits and large generating plants.

Commercial drivers are for example the general uncertainty in electricity markets (which favors small generation schemes whose financial risk is commensurately small), or the cost-effectiveness of DG and DES based solutions to guarantee affordable energy with improved and controllable power quality and reliability levels.

Regulatory drivers are the increasing concern that has grown up amongst energy policy makers regarding energy security, and has pushed to establish norms which promote diversification of energy sources and their allocation near to load centers, or the support for competition policy, based on the idea that introduction of competition in generation and customer choice will deliver low energy prices and better service quality, requiring many players in the market.

DERs create opportunities for customers to self-provide energy, manage load profiles, improve power quality and resiliency, and help meet clean energy goals. At the same time, DERs can also potentially enhance the grid as a whole. Key motivating factors for the adoption of DER, for both customers and the grid, are often described with the following categories [9]:

- Economic Benefits. Avoided costs, increased efficiencies, and gained revenues. For customers owning DERs, benefits can be tied to incentive payments as well as avoided costs associated with electricity bills. For utilities, regulators, and ratepayers, benefits can be tied to more efficient utilization of the grid and deferred investments.
- Deferred or Avoided Network Investments. Avoided expansion of generation, transmission, or distribution facilities. This benefit applies to the grid which can indirectly benefit all ratepayers. Apart from providing economic benefits, DERs can also help avoid lengthy siting processes or can provide options

where technical challenges exist around traditional capacity expansion. In some cases, the utilization of DERs can provide a quick or novel means for addressing grid challenges

- Resiliency and Power Quality. Uninterrupted service in the event of loss of grid service and the ability to ride through transient and short-term interruptions. This can be applied to both customers who seek to reduce outage times or power quality events, and the utilities that are coordinating outage recovery efforts and managing grid power quality.
- Clean Energy. Social, regulatory, and economic reasons to invest in low or no-emission DERs. Many customers are motivated to purchase clean DERs to support clean energy goals. Likewise, many utilities are doing the same, often motivated by goals or explicit targets. The net effect on emissions, however, has to be investigated per system because the displacement of centralized generation can have different effects on total emissions.

Despite their benefits, the widespread diffusion of DERs also faces significative challenges, such as [9]:

- Complexity of policies, requirements and tariffs across jurisdictions, including interconnection standards, siting and permitting requirements and utility tariff agreements and eligibility.
- Determining fair compensation for the benefits of DERs to the grid, including which parties should receive financial compensation and how much. The benefits of DER can accrue to different stakeholders complicating the ability to identify compensation for these resources for their actions and thereby justify customer investments through potential revenue streams.
- Engineering can be costly and complex if no turn-key solution is available.
- Financing can be difficult to obtain, particularly where technologies are still gaining experience in the market or where no turn-key solutions are available.

- Customers must weigh the payback of investment in DERs versus the payback from investment in core business.
- Environmental and safety requirements can limit the installation or operations of some DER assets depending on their emissions profile or chemical make-up.

1.5 Microgrids: current status and future prospects

Regardless of the name, electrical systems with the essential characteristics of microgrids have been operating for decades, mainly to realize power supplies with increased levels of quality and availability, while in recent years the μG concept has been further developed to overcome the challenges of integrating more and more DER units in power systems, including conventional and renewable energy sources, electric vehicles (EVs), storage systems, etc., so that it now considered a key building block of the future Smart Grid.

Therefore, from the point of view of society as a whole, μGs play a fundamental role in the transition toward a more efficient, sustainable, economic and secure electricity supply.

At a lower level and at the same time, the μG concept aims at bringing advantages both to electricity end-users and utilities, but its widespread adoption also faces some significative challenges.

1.5.1 Benefits and challenges: the end-user perspective

From the end-user perspective, a microgrid is a way to simultaneously address energy security, affordability and sustainability through dispersed, locally controlled, independent energy systems precisely tailored to specific requirements [4]. Different end-users look at their energy supply systems in the light of different main goals, like supply security and reliability, sustainability and carbon footprint, affordability and/or profitability, and μGs can help in all these respects:

- *secure and reliable supply*: being a semi-autonomous system, a μG demonstrates a certain resilience to energy supply disruptions, that can be graduated to different levels regarding its timeframe

and extension, by means of proper sizing of internal generators and storage devices and of proper control of curtailable loads;

- *sustainable and low carbon supply*: the μG paradigm allows increasing penetration of renewable energy into the mix, helping to deal with consequent intermittency and supply/demand challenges; moreover, the local use of energy and the possibility of feeding DC loads from DC sources such as photovoltaics add a further contribute to conversion and network losses reduction and to a low carbon supply;
- *affordable and profitable supply*: a μG allows the user to select the most cost-effective system balance by selecting the optimal combination of indigenous supply and use, relying on grid or standby supply only when cost effective, fully employing the possibilities brought by all the available options like storage, load curtailment, bi-directional energy flows on the PCC; also, the minimization of conversion and line losses contributes to an affordable and possibly profitable power supply.

Figure 1-3 graphically represents the main results achievable by means of μG adoption. The balance between them will be stretched in one direction or another depending on the prevailing goals of different users.

Fig. 1-3: Main pros of μG adoption [4]

The main challenges to be faced when considering μG adoption, from the end-user perspective, are related to the difficulties in conducting a comprehensive cost-benefit analysis and in identifying qualified modalities for system design and management, besides the other challenges enumerated for DERs adoption in paragraph 1.4.

1.5.2 Benefits and challenges: the utility perspective

From the utility perspective, microgrids can be seen as a treat to the traditional business model, but also as a business opportunity. While microgrids have been around for a long time, they are expected in the near future to interact with the grid in increasingly sophisticated ways: islanding in an emergency, using black start capabilities, and selling demand response and ancillary services to the grid.

The main treat is related to the so-called "utility death spiral": the growing number of customers which reduce their grid-dependence by resorting to distributed energy resources, forces other customers to bear increasing costs for the maintenance of the utility-owned distribution system, with rates consequently going up and then pushing also these customers to leave it.

Despite this negative prospect, only about 50% of the American utilities surveyed in a recent study [10] foresee significant load loss from microgrids, while 97% consider microgrids as a business opportunity for them over the next decade.

This can be justified considering that approximately half of the utilities see themselves as microgrid owners, and in addition new business models, currently under study, can protect their economics as microgrids and distributed generation grow in presence on the grid. An important example of these possible new business model is the one which tends to establish utilities as distributed grid operators, acting as the manager of distributed energy assets, following a model analogous to that of Independent System Operators (ISOs) that now manage wholesale generation on the grid. For utilities, this would create a new business role and revenue source. The utilities surveyed clearly see potential in this model and named it as the best method to protect their revenue.

When it comes to customer rates, which could be expected to face an adverse impact from microgrids dissemination because of the costs to build new infrastructures, the majority of the utilities expect that microgrids will either lower or have no significant impact on them. In addition, while some have suggested that those key customers that especially need microgrids should be charged extra to cover the related costs, just over the half of utilities are against charging targeted premium rates for such service.

The majority of utilities do not see microgrids as a threat to grid reliability, like some microgrid critic does, even if approximately the half of them find current interconnection standards inadequate for safety purposes (they actually are in diverse cases dated and in need of change).

On the opposite, some microgrid supporters, also people from utilities, envision the possible future advantages, both in terms of system economics and availability, of pools of microgrids providing electricity and services to the grid as a virtual power plant (VPP).

Finally, while utilities want to own microgrids – and plan to get into the business – they say there are not enough financial incentives to spur them into action. They believe regulations should be changed to better incentivize microgrid installation. Regulators and policymakers who want to see more microgrids might heed this concern. Incentives have played a major role in developing other new electricity markets in the U.S., such as renewable energy and smart grids.

In conclusion, contrary to conventional wisdom, utilities are not the enemy of the microgrid. In fact, utilities see microgrids as a new business opportunity, with far more economic upside than downside. They want regulatory changes that will spur microgrid development, and they're willing to make concessions and adopt new business models to make it work. The microgrid, it turns out, could become a new utility asset in the not-so-distant future: a way to keep the power on during a storm and boost the utility bottom line.

But there are still many questions that need to be answered. Although the technology and equipment necessary for creating microgrids are available today, off-the shelf commercial solutions are rare. A number of technical, economic, and regulatory issues must be addressed to unlock the full potential of microgrids. For example:

- Technical: Considerable technical challenges exist when toggling a microgrid between grid connected and islanded modes. For example, during transition to island mode, phase and frequency drift is highly likely, which could cause loads and DERs to trip. Without a finely calibrated synchronization process, grid reconnection could damage generators and loads within the microgrid and in surrounding systems.

- Economic and regulatory: Determining standardized methods for valuing microgrids— from either the customer or utility perspective— is difficult due to an intersecting and fluid set of economic and regulatory issues. For example, regulatory and market uncertainties affect the upfront costs and life-cycle economics of microgrids and associated DER technologies. A second challenge is that a microgrid's costs and benefits can be difficult to monetize, or non-monetizable, thus complicating value stream calculations.
- Standards: Current technical standards offer guidance for microgrid development, but do not address more nuanced issues germane to system design. For example, further definition is required for protocols governing advanced protection coordination, multilayer-device communications and controls, microgrid-to-grid interactions, and grid resynchronization.

Microgrids can be justified across a wide variety of use cases based on a specific set of major drivers. Behind these use cases, the ownership and control of the component technologies range along a continuum between the extremes of customer and utility control. Since no two markets or utilities are alike, microgrids will continue to proliferate based on unique served loads, targeted drivers, and deployed technologies.

1.5.3 Main barriers and potential solutions for the microgrid paradigm implementation

The most common barriers to a wider implementation of the μG paradigm can be grouped into four categories: technical, regulatory, financial, and stakeholders [11].

Even if all the existing technical and regulatory issues would be alleviated, the commercialization of the microgrid concept heavily depends on the reduction of production costs of renewable energy generation, storage technologies, and energy management systems, to be achieved through more R&D. In addition, it could be useful to create long term plans to improve the local economy and capacity of the community, also approaching external parties for financial assistance that can mitigate the financial challenges associated with

microgrid implementation. Finally, market support for the advanced control functionalities, energy management systems and increased reliability of energy supply that are integral to the microgrid concept is also required.

As far as stakeholders are concerned, if incorporation of prosumers into the planning and implementation of microgrid projects is foreseen, some issues arise about gaining trust of local consumers, dealing with conflicting self-interest, and managing operations. In this respect, resorting to a qualified person to explain the microgrid vision and convince the community of the benefits that they can gain is a key factor to achieve wide social acceptance, as well as a comprehensive training of microgrid users and operators and contingency planning can mitigate the challenges of managing microgrid operations under planned conditions and even unplanned situations, like times of natural disasters.

1.5.4 Future Prospects

Despite the existing barriers outlined in previous paragraphs, the interest in microgrids is continuously growing and the outlooks on their market foresee a significative growth in the next years, as reported in Figure 1-4.

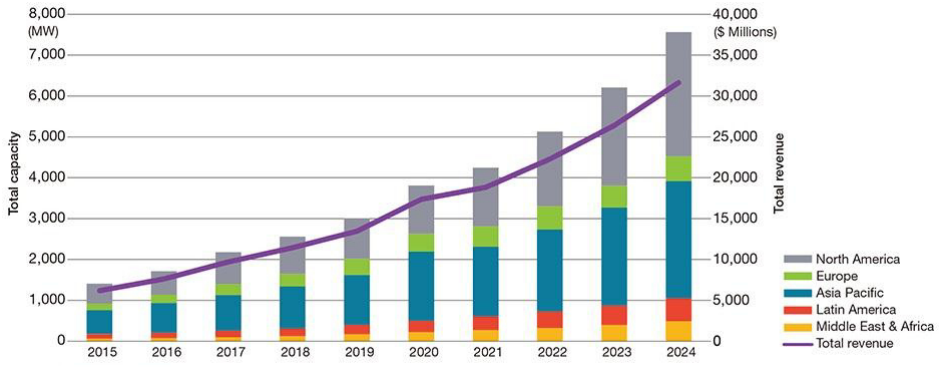

Fig. 1-4: Total Microgrid Capacity and Revenue, World Markets: 2015-2024

The primary reasons for this bright future prospect are likely to be found in the immense potential that microgrids have to facilitate the power system to become more secure, reliable and green, and in their

being the only affordable, sustainable and reliable option for electrification of the various regions of the world that still need it.

1.6 References

[1] http://c6.cigre.org/WG-Area/WG-C6.22-Microgrids.
[2] Dan T. Ton, Merrill A. Smith, "The U.S. Department of Energy's Microgrid Initiative", The Electricity Journal, Volume 25, Issue 8, October 2012, Pages 84-94.
[3] R. H. Lasseter, "MicroGrids", 2002 IEEE Power Engineering Society Winter Meeting. Conference Proceedings (Cat. No.02CH37309).
[4] ARUP, "Microgrids, Five minute guide".
[5] R. H. Lasseter et alii, "The CERTS MicroGrid Concept", 2002, Consortium for Electric Reliability Technology Solutions.
[6] European Commission, European Technology Platform, "SmartGrids, Vision and Strategy for Europe's Electricity Networks of the Future", 2006.
[7] "Managing variable and distributed energy resources: A new era for the grid", 2016, Deloitte Center for Energy Solutions.
[8] J.A. Pecas Lopes, N. Hatziargyriou, J. Mutale, P. Djapic, N. Jenkins, "Integrating distributed generation into electric power systems: A review of drivers, challenges and opportunities", Electric Power Systems Research 77 (2007) 1189–1203.
[9] "A Review of Distributed Energy Resources", September 2014, prepared for NYISO by DNV-GL.
[10] "The Utility view of Microgrids | 2014", Utility Dive.
[11] M. Soshinskaya, W. Crijns-Graus, J. Guerrero, J.C. Vasquez (2014). "Microgrids: Experiences, barriers and success factors", Renewable and Sustainable Energy Reviews. 40. 659-672. http://dx.doi.org/10.1016/j.rser.2014.07.198.

Chapter 2

Optimization techniques for the optimal sizing of Distributed Energy Resources in microgrids

2.1 Introduction

The optimal sizing of the distributed energy resources included in a microgrid is a typical constrained optimization problem, therefore this chapter introduces the topic of constrained optimization and present different techniques applicable to it, categorizing them into analytical approaches, mathematical programming approaches, heuristic approaches etc. A literature review on the application of optimization techniques to the planning of microgrids is presented. Finally, some techniques used to deal with the uncertainty affecting design parameters are described: sensitivity analyses, Stochastic Optimization, Sample Average Approximation, Robust Optimization and Decision Theory.

2.2 Generality on constrained optimization

The optimal sizing of the distributed energy resources included in a microgrid is a typical example of a constrained optimization problem, which can be generally written as follows:

$$\begin{aligned} &\min && f(\mathbf{x}) \\ &\text{subject to} && g_i(\mathbf{x}) = c_i \text{ for i=1, … ,n} \\ &&& h_j(\mathbf{x}) \geq c_j \text{ for j=1, … ,m} \end{aligned}$$

The above stated constrained optimization problem can be described as the process of optimizing an objective function f (cost or energy function to be minimized), with respect to some variables $\mathbf{x}$ (called decision variables) in the presence of equality constraints g_i and inequality constraints h_i on those variables[2].

Optimization has then the final goal of obtaining the best result under given circumstances, and is a continuously recurring task for planners involved in design, construction, and maintenance of any engineering system [1].

Since there isn't a single method capable of efficiently solving all kinds of optimization problems, a variety of methods have been developed for solving different types of optimization problems. These optimization techniques are useful in finding the minimum of a function of several variables under a prescribed set of constraints. In the following, the main classical and recent optimization techniques are briefly illustrated.

2.2.1 Analytical Techniques

These techniques are mostly based on the calculus of variations, an area of calculus that deals with the optimization of functionals, which are mappings from a set of functions to real numbers and are often expressed as definite integrals involving functions and their derivatives [2].

Physical system can be modeled by functionals, with which their variables can be optimized considering the constraints. Equality constraints can be managed by means of the method of Lagrange Multipliers [3], while the Karush-Kuhn-Tucker (KKT) conditions generalize it to include inequality constraints, resulting in non-linear formulations.

2.2.2 Mathematical Programming Techniques

Mathematical Programming is a set of techniques of mathematical optimization aimed at solve many real-world problems in many

[2] Constraints can be categorized as hard constraints (which set conditions that variables must satisfy) and soft constraints (which define some variable values that are penalized in the objective function if, and based on the extent that, the conditions on the variables are not satisfied).

different areas when they may be cast into the form of a Mathematical Programming problem: a set of decision variables, constraints over these variables and an objective function to be maximized or minimized [4].

Mathematical Programming problems are usually classified according to the types of the decision variables, constraints, and the objective function.

2.2.2.1 Linear programming

If the objective function and all of the hard constraints are linear, then the problem is a linear programming (LP) problem and it can be solved by efficient algorithms such as the simplex method (which usually works in polynomial time in the problem size but is not guaranteed to), or interior point methods (which are guaranteed to work in polynomial time) [5].

2.2.2.2 Mixed Integer Programming

Despite the fact that many application problems fit into the category of LP, it is obvious that continuous variables are insufficient to represent decisions of a discrete nature (‘yes’/‘no’ or 1,2,3,...), which are necessary in a number of applications.

This observation lead to the development of Mixed Integer Programming (MIP), where constraints and objective function are linear just as in LP and variables may have either discrete or continuous domains. To solve this type of problems, LP techniques are coupled with an enumeration (known as Branch-and-Bound) of the feasible values of the discrete variables.

Such enumerative methods may lead to a computational explosion, even for relatively small problem instances, so that it is not always realistic to solve MIP problems to optimality. However, in recent years, continuously increasing computer speed and even more importantly, significant algorithmic improvements (e.g. cutting plane techniques and specialized branching schemes) have made it possible to tackle ever larger problems, modeling ever more exactly the underlying real-world situations.

2.2.2.3 Quadratic Programming and Mixed Integer Quadratic Programming

Another class of problems that is relatively well-handled are Quadratic Programming (QP) problems: these differ from LPs in that they have quadratic terms in the objective function (the constraints remain linear). The decision variables may be continuous or discrete, in the latter case we speak of Mixed Integer Quadratic Programming (MIQP) problems.

2.2.2.4 Non-linear Programming

More difficult is the case of non-linear constraints or objective functions, Non-linear Programming (NLP) problems. Frequently heuristic or approximation methods such as Successive Linear Programming (SLP) are employed to find good (locally optimal) solutions.

2.2.3 Heuristic techniques

Heuristic techniques have been designed for solving a problem more quickly when classic methods are too slow, or for finding an approximate solution when classic methods fail to find any exact solution, by trading optimality, completeness, accuracy, or precision for speed.

Several heuristic tools have evolved in the past decades that facilitate solving optimization problems that were previously difficult or impossible to solve. Recently, these new heuristic tools have been combined among themselves and with knowledge elements, as well as with more traditional approaches such as statistical analysis, to build general-purpose meta-heuristic methods being able to solve extremely challenging problems [6].

These tools offers two major advantages when compared to traditional optimization techniques: (1) development time is much shorter and (2) the systems are robust, being relatively insensitive to noisy and/or missing data.

Some of the most used heuristic techniques are Genetic Algorithm (GA), Simulated Annealing (SA), Ant Colony Search Algorithm (ACS), Particle Swarm Optimization (PSO).

2.2.4 Multi-objective Optimization

Considering more than one objective function to be optimized simultaneously brings to a multi-objective optimization problem (MOO), which can be written in the general form:

find	$\mathbf{X} = \{x_1, x_2, \ldots, x_n\}$
which minimizes	$f_1(\mathbf{X}), f_2(\mathbf{X}), \ldots, f_k(\mathbf{X})$
subject to	$g_j(\mathbf{X}) \leq 0, j=1, 2, \ldots, m$

In general, no solution vector **X** exists that minimizes all the k objective functions simultaneously.

2.2.4.1 Utility Function method

A first simple solution to the multi-objective optimization problem is to define a utility function U, which is the sum of partial utility functions U_i obtained assigning a weighting factor w_i to each of the original partial objective functions $f_i(\mathbf{X})$, so that:

$$U = \sum_{i=1\ldots k} U_i = -\sum_{i=1\ldots k} w_i f_i(\mathbf{X})$$

This method, also called weighting function method, allows a simple reduction of the original multi-objective function to a single objective function, but has some drawbacks:

- it produces a unique solution which often does not adequately represent the complexity of the original problem and forces the decision maker leaving no room for his choice,
- it requires the definition of weighting factors w_i which is often very difficult and sometimes substantially impossible, when the differences between partial objective functions $f_i(\mathbf{X})$ are qualitative and do not allow a numerical comparison.

2.2.4.2 Pareto Front method

The Pareto Front method allows to identify a set of solutions as the best possible choices when compared to other solutions found in the

feasible region, through the concepts of dominated and non-dominated solutions.

A solution is dominated by another one when the second guarantees better results in one or more of the partial objective functions $f_i(\mathbf{X})$, while not performing worse with respect to all the remaining objectives, as it is shown in figure 2-1, for a bi-dimensional example case, where solutions A, C and E dominate solutions B and D.

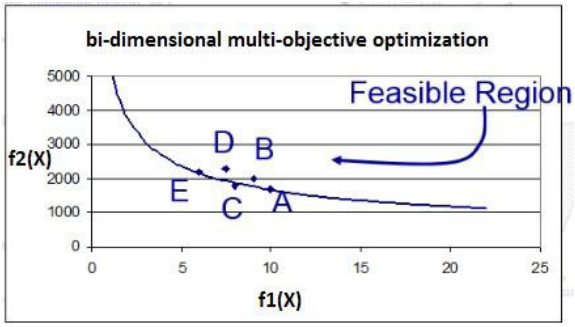

Fig. 2-1: Example of Pareto Front in a bi-dimensional case

The Pareto Front is the set of all non-dominated solutions, thus it provide a set of equally valuable solutions where the decision maker can make a choice by ranking the quality of the trade-offs based on the particular application, and according to his/her experience.

2.2.5 Game Theory

Game theory is a formal analytical as well as conceptual framework with a set of mathematical tools enabling the study of complex interactions among independent rational players. For several decades, game theory has been adopted in a wide number of disciplines ranging from economics and politics to psychology. More recently, game theory has also been applied to the design and analysis of communication systems and of power systems (specifically, smart grids and microgrids) [7].

2.2.6 Neural networks

The neural networks approach is based on the immense computational power of the nervous system to solve perceptional problems in the

presence of massive amount of sensory data, through its parallel processing capability,

2.2.7 Fuzzy optimization

Fuzzy optimization has been developed to solve optimization problems involving design data, objective function and constraints stated in imprecise form, involving vague and linguistic descriptions.

2.3 Dealing with uncertainty

The uncertainty of input data is a critical aspect to be considered in every planning and design process [8]. Whereas deterministic optimization problems are formulated with known parameters, the data of real world problems are very often uncertain or not exactly known at the time the problem is being solved, because of measurement and/or estimation errors (coming from the impossibility to measure and/or estimate exactly the data entries representing characteristics of physical systems, technological processes, environmental conditions, etc.) and of implementation errors (coming from the impossibility to implement a solution exactly as it is computed).

The presence of these uncertainties cannot be disregarded because sometimes even a small uncertainty in the data can heavily affect the quality of the nominal solution obtained using a deterministic approach to the optimization problem. Therefore, decision makers need methodologies capable of detecting these critical cases and generating solutions that are as much as possible immunized against the effect of data uncertainty [9].

The following paragraphs briefly describe the main techniques used to deal with uncertainties affecting planning problems.

2.3.1 Sensitivity analysis

Sensitivity analysis is aimed at correlating the uncertainty in the output of a mathematical model or system to different sources of uncertainty affecting its inputs [10].

Different approaches are used to perform sensitivity analyses; in general, however, most procedures follow these steps:

- Quantify the uncertainty in each input in terms of ranges, probability distributions, etc. (this can be a difficult task).
- Identify the model output to be analyzed.
- Run the model a number of times varying the input data following rules dictated by the method of choice and the input uncertainty.
- Using the resulting model outputs, calculate the sensitivity measures of interest.

Sensitivity analysis can be useful for a range of purposes, such as testing the robustness of the results of a model or system in the presence of uncertainty, increase understanding of the relationships between input and output variables, contribute to uncertainty reduction, through the identification of model inputs that cause significant uncertainty in the output and should therefore be the focus of attention in order to increase robustness.

2.3.2 Stochastic Optimization (SO) and Sample Average Approximation (SAA) methods

Stochastic programming models deals with situations where some or all of the parameters of the optimization problem are described by stochastic (or random or probabilistic) variables, when probability distributions governing the data are known or can be estimated. The goal is to find some policy that is feasible for all (or almost all) the possible data instances and maximizes the expectation of some function of the decisions and the random variables [11].

Depending on the nature of equations involved (in terms of random variables) in the problem, a stochastic optimization problem is called a stochastic linear, geometric, dynamic, or nonlinear programming problem. The basic idea used in stochastic programming is to convert the stochastic problem into an equivalent deterministic problem. The resulting deterministic problem is then solved by using familiar techniques such as linear, geometric, dynamic, and nonlinear programming.

2.3.2.1 Formulation of two-stage problems

The two-stage formulation is widely used in stochastic programming. Its basic idea is that decisions should be based on data available at the

time they are made and cannot depend on future observations (non-anticipativity constraint).

The general formulation of a two-stage stochastic programming problem is given by:

$$\min_{x \in X} \{g(x) = f(x) + E_\xi[Q(x, \xi)]\}$$

where Q(x,ξ) is the optimal value of the second-stage problem:

$$\min_{y} \{q(y, \xi) \mid T(\xi)x + W(\xi)y = h(\xi)\}$$

The classical two-stage linear stochastic programming problems can be therefore formulated as:

$$\begin{aligned} \min_{x \in \mathbb{R}^n} \quad & g(x) = c^T x + E_\xi[Q(x, \xi)] \\ \text{subject to} \quad & Ax = b \\ & x \geq 0 \end{aligned}$$

where Q(x, ξ) is the optimal value of the second-stage problem:

$$\begin{aligned} \min_{y \in \mathbb{R}^m} \quad & q(\xi)^T y \\ \text{subject to} \quad & T(\xi)x + W(\xi)y = h(\xi) \\ & y \geq 0 \end{aligned}$$

In such formulation $x \in R^n$ is the first-stage decision variable vector, $y \in R^m$ is the second-stage decision variable vector, and ξ(q,T,W,h) contains the data of the second-stage problem. It can be seen that at the first stage we have to make a "here-and-now" decision $\boldsymbol{x}$ before the realization of the uncertain data ξ, viewed as a random vector, is known. At the second stage, after a realization of ξ becomes available, we optimize our behavior by solving an appropriate optimization problem.

At the first stage we optimize the cost $\boldsymbol{c^T x}$ of the first-stage decision plus the expected cost of the (optimal) second-stage decision. We can view the second-stage problem simply as an optimization problem which describes our supposedly optimal behavior when the uncertain data is revealed, or we can consider its solution as a recourse action where the term $\boldsymbol{Wy}$ compensates for a possible inconsistency of the system $\boldsymbol{Tx} \leq$ h, and $\boldsymbol{q^T y}$ is the cost of this recourse action.

The considered two-stage problem is linear because the objective functions and the constraints are linear. Conceptually this is not

essential and one can consider more general two-stage stochastic programs. For example, if the first-stage problem is integer, one could add integrality constraints to the first-stage problem so that the feasible set is discrete. Non-linear objectives and constraints could also be incorporated if needed.

2.3.2.2 Discretization and scenarios

In stochastic programming it is assumed that a random vector ξ with known probability distribution describes the second stage data. To solve stochastic problems numerically, one often needs to assume that the random vector ξ has a finite number of possible realizations, called scenarios, say $\xi_1 \ldots \xi_k$, with respective probability masses $p_1 \ldots p_k$. Therefore, the expectation in the first-stage problem's objective function can be written as the summation:

$$E[Q(x,\xi)] = \sum_{k=1}^{K} p_k Q(x,\xi_k)$$

and the two-stage problem can be formulated as one large linear programming problem, called the deterministic equivalent of the original stochastic problem.
A limit to the straightforward application of this technique is that the volume of the search region generally grows geometrically with dimension, then a “naive” search in a high-dimensional problem will generally be absolutely impracticable.
This problem, called the “curse of dimensionality” after famous mathematician Richard Bellman, has been producing a strong effort in the research of techniques to circumvent it, such as Column generation techniques, Scenario reduction techniques and Scenario Tree Construction techniques.

2.3.2.3 Sample Average Approximation (SAA) Method

A common approach to reduce the scenario set of a stochastic optimization problem to a manageable size is by using Monte Carlo simulation.

This approach is particularly useful when the following three conditions occur (as it is often the case in real-world applications):

1. the expected value function g(x) cannot be written in a closed form, and/or its values cannot be easily calculated.
2. The function $Q(x,\xi)$ is easily computable for given x and ξ.
3. The set S of feasible solutions, although finite, is very large, so that enumeration approaches are not feasible[3].

Under these circumstances, the deterministic equivalent of the original stochastic optimization problem (intractable by means of *brute force* approaches) can be taken on by means of Monte Carlo techniques, generating a random sample $\xi_1 \ldots \xi_N$ and approximating the expected value function by the corresponding sample average function: the obtained sample average optimization problem is solved, and the procedure is repeated several times until a stopping criterion is satisfied [12].

2.3.3 Robust Optimization (RO)

Robust optimization is a modelling framework that can be used in optimization problems when the uncertainty in the input data is assumed to be bounded in a known set of values; this uncertainty set can be described by linear constraints, convex quadratic constraints, or as a discrete set of vectors of uncertain data.

Under this assumption, the RO paradigm rests on three implicit assumptions on the underlying decision-making environment [9]:

1. All entries in the decision vector represent “here and now” decisions: they should get specific numerical values as a result of solving the problem before the actual data reveals itself."
2. The decision maker is fully responsible for consequences of the decisions to be made when, and only when, the actual data is within a prespecified uncertainty set U.
3. The constraints of the uncertain optimization problem in question are “hard”, i.e. the decision maker cannot tolerate violations of constraints when the data is in U.

[3] if, for instance, ξ is a random vector with 100 stochastically independent components each having 3 realizations, then the total number of scenarios is $K= 3^{100}$.

In the following the basics of RO are described, referring for the sake of simplicity to linear problems. A generic LP can be written as:

$$\min_x \{c^T x: Ax \leq b\}$$

In Robust optimization, an uncertain LP is defined as a collection of LP programs with a common structure and actual values of parameters (c, A, B) varying in a given uncertainty set *U*:

$$\{\min x \{cTx: Ax \leq b\}: (c, A, B) \in U\}$$

By considering the three above mentioned assumptions, it follow that solutions to the uncertain LP program must remain feasible for whatever realization of (c, A, B) in U. Similar solutions are called robust feasible and are the only meaningful solutions in the given decision-making environment.

Concerning the value of the objective function, (which can also be uncertain), the "worst-case-oriented" philosophy underlying the RO paradigm makes it natural to quantify the quality of a robust feasible solution x by the guaranteed value of the original objective, that is, by its largest value:

$$\sup\{cTx: (c, A, B) \in U\}$$

Thus, the best possible robust feasible solution is the one that solves the optimization problem:

$$\min_x \left\{ \sup_{(c,A,b)\in\mathcal{U}} c^T x : Ax \leq b \ \forall (c, A, b) \in \mathcal{U} \right\}$$

or, which is the same, the optimization problem:

$$\min_{x,t} \left\{ t : c^T x \leq t,\ Ax \leq b \ \forall (c, A, b) \in \mathcal{U} \right\}$$

The latter problem is called the Robust Counterpart (RC) of the original uncertain problem. The feasible/optimal solutions to the RC

are called robust feasible/robust optimal solutions to the uncertain problem. The Robust Optimization methodology, in its simplest version, proposes to associate with an uncertain problem its Robust Counterpart and to use, as our “real life” decisions, the associated robust optimal solutions. The difference in objective function values between the original problem and the robust version is often referred to as the price of robustness [13].

The solvability of a robust optimization problem depends on whether the robust constraints in the model can be transformed into a form that can be solved by the available mathematical programming solvers.

2.3.4 Decision theory and Risk Analysis

Decision theory is the study of the reasoning underlying an agent's choices [14]. It is then strongly related to the role of decision makers (DMs).

The area of choice under uncertainty represents the heart of decision theory and has its basis in the concept of expected value is that, when faced with a number of actions, each of which could give rise to more than one possible outcome with different probabilities, the rational procedure is to identify all possible outcomes, determine their values (positive or negative) and the probabilities that will result from each course of action, and multiply the two to give an "expected value", or the average expectation for an outcome; the action to be chosen should be the one with the highest total expected value.

A recent effective approach to decision making is offered by the Risk Analysis (RA) paradigm, which indicates a preferred solution as one that minimizes the regret felt by a Decision Maker (DM) after verifying that the decisions he had made were not optimal, given the future that in fact has occurred [15].

The RA paradigm is attractive because it reflects well the way people think. In fact, the traditional models in planning, namely those working under the Probabilistic Choice (PC) paradigm (i.e. stochastic optimization), concentrate their analysis on the solutions of the problem, while the RA paradigm is mainly focused on decisions.

Factors as risk aversion or risk attraction, associated with DMs, the concept of hedging (paying an extra to avoid adverse futures) and the measurement of regrets felt, all are reflected in the RA way of

dealing with a problem, and are very well understood by those planners that have a daily contact with real and practical problems.

Therefore, from the point of view of Decision Making, the optimum on the average of futures (i.e. the one pursued by PC) may not be the best decision, because the perspective of unwanted or even catastrophic events contradicts the basic assumption behind the Probabilistic Choice paradigm: that bad situations will be compensated by good situations along time, so that one can evaluate a solution by its average behavior. However, if a catastrophic event or scenario occurs, no reasonable recovery will ever be possible and the PC assumption cannot be verified, then the PC paradigm in this case is not an useful context for decision making in planning.

2.4 Optimization techniques applied to microgrids planning problems

2.4.1 Generality

Despite the numerous advantages that the adoption of the microgrid paradigm in the power system can bring to utilities and customers, planning a cost-effective microgrid is a complex process, due to all alternatives to consider at any decision level, characterized by different specific constraints and goals which often conflict each other, and by uncertainties which represent a key factor in every planning process, acting as a powerful source of risks that system planners must control.

2.4.2 Structure of the optimization problem

The optimization problem of optimal DERs deployment in a microgrid is characterized, as any other resource allocation problem, by four set of entities: inputs, outputs, objectives and constraints; for each of them, in the following different possibilities (which can occur in any combination) are listed [18]:

- Inputs (given):
    - Number and type of DER units
    - Amount of land used

- Atmospheric conditions
- Technology of DER units
- Mode of operation
- Operational life
- Efficiency
- Operation and maintenance cost
- Meteorological conditions
- Geographic locations of renewable energy sources units
- DERs related custom inputs

- Outputs (to be found):

  - Total generated energy
  - Number and capacity of DER units
  - Total investment
  - Life time of the DERs
  - Operation and maintenance cost
  - Reliability of DER units
  - Expected profit
  - Estimated land use
  - Best mix of DER units
  - Best DER sizing and siting
  - DER units related custom variables

- Objectives:

  - Minimize: Total cost of the system
  - Minimize: Cost per unit of energy produced
  - Minimize: Power losses
  - Minimize: Land area
  - Minimize: Investment
  - Minimize: Total maintenance cost
  - Minimize: Noise and pollution emission
  - Minimize: Loss of power supply probability
  - Maximize: Thermal efficiency
  - Maximize: Total power generation
  - Maximize: Reliability of the system

  - Maximize: Profit
  - Maximize: Life span
  - Maximize: Total revenue
  - Maximize: DER units related custom objectives

- Constraints:

  - Environmental/atmospheric constraint
  - Demand/load management constraint
  - Economic/budget constraint
  - Storage capacity of the Energy Storage Systems
  - Charge and discharge rate constraint
  - Carbon dioxide emission constraint
  - Social/regulatory constraint
  - Loss of power supply probability constraint
  - Life time of components constraints
  - Power rating of DER units constraints
  - Maximum power flow limits of distribution lines
  - Land available for renewable energy sources installation
  - Types and sizes of available generating units
  - Cost of energy constraints
  - DER units related custom constraints

2.4.3 Conflicting objectives

In paragraph 2.4.2 many different possible objectives of the DERs optimization have been presented; considering more than one objectives simultaneously brings to a multi-objective optimization problem, which can be hard to solve because typically different objectives conflict with one another, as it is shown in figure 2-2 with reference to the optimal sizing of DERs [18].

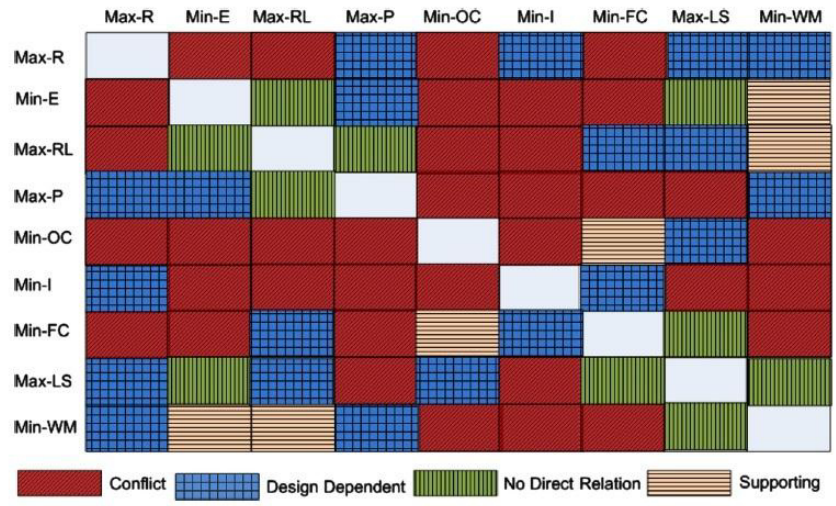

Relation between conflicting objectives. Max-R: maximize revenue, Min-E: minimize emissions, Max-RL: maximize reliability, Max-P: maximize production, Min-OC: minimize operating cost, Min-I: minimize investment, Min-FC: minimize fuel cost, Max-LS: maximize life span, Min-WM: minimize waste.

Fig. 2-2: Relation between conflicting objectives

2.4.4 Main sources of uncertainty in the microgrid planning problem

Significative uncertainties affect the input data of the microgrid/DERs planning problem, the main sources of them being the forecast errors for loads, variable renewable generation, market prices, and islanding incidents [16].

Long-term load forecasting constitute a significant source of uncertainty, being generally more challenging for microgrids than for conventional power systems, due to the low system inertia, related to its relatively small scale, and to its nature, characterized by the presence of fixed and flexible loads. This factors, together with different possible control strategies, produce an highly non-smooth and volatile behavior of the power demand time series, conditioned by a set of internal and external factors, such as variations in hourly prices, grid status, weather conditions, consumers' decisions.

Another important source of uncertainty is represented by variable renewable generation: microgrids are often characterized by large deployments of renewable energy resources, mainly wind and solar energy, which are intrinsically non-predictable and does not follow a

repetitive pattern in the daily operation, being highly dependent on weather conditions.

Market prices (i.e., the real-time electricity prices at the microgrid point of common coupling, both for buying and for selling energy) strongly affect the economics of the microgrid operation, because they have a direct impact on cash-flows related to energy exchanges between the microgrid and the grid, and they considerably impact the commitment and dispatch of DERs. Market prices forecasting introduce therefore an additional relevant source of uncertainty, being characterized by a high degree of error due to the presence of several non-deterministic factors such as market conditions, network contingencies, demand-response strategies implemented by other market participants (e.g. other prosumers).

A fourth significative source of uncertainty is related to microgrid islanding, as a result of network temporary disturbances or long outages, which are clearly unexpected and unpredictable events. Although such events are not frequent, they can be considered among the inputs of the planning problem when considering the social advantages (and possibly the correspondent economic value) of microgrid-based solutions which can contribute to power quality and grid resiliency.

In addition to the above mentioned sources of uncertainty, other non-deterministically predictable factors should be considered in the planning problem, some linked to technical issues (e.g. the evolution of prices and performances of various technologies applied to DERs and other microgrid components), some other related to economic and regulatory issues (e.g. green energy policies, or microgrid-to-grid interactions rules).

2.4.5 Review of recent works applying optimization techniques to microgrid planning problems

In recent years, numerous scientific works have been published on the application of optimization techniques to the optimal planning of microgrids and DERs, due to the strong and ever growing interest in these topics. Also, different review articles categorize and summarize the published works [17]-[22].

Beyond specific constraints and goals of each particular project, some planning problems can be considered common to every microgrid feasibility study [17]:

- Power generation mix selection and sizing is related to the responsibility of choosing the best available power system to satisfy demand requirements for a particular area, including power generation and energy storage equipment sizing, according to peak-load demand and cost effectiveness criteria; this problem must be considered among strategic issues for the system and there exist three main objectives to fulfil during this planning stage: high cost-effectiveness, low environmental impact and high reliability.
- Siting problem covers power sources allocation and power lines layout, in order to keep quality constraints, considering not only actual consumers but also future potential customers, pursuing high cost-effectiveness, high reliability and also low power losses.
- Scheduling problem is focused on available resources planning, such as generators and storage devices, and it is aimed at minimizing operational costs, environmental impact and quality keeping while demand is covered. Optimal operational conditions for different microgrid configurations are searched using different optimization techniques towards one or more than one objective optimization.

In the following a survey is presented of recent articles that apply optimization techniques to the first of the above listed planning problems, which is central to this thesis.

Economic issues are a high priority in the microgrid planning in order to address long-term establishment for the system. Main problems in technical papers at strategic planning level are power sources selection and sizing [23], energy storage devices selection and sizing [24] and siting. Determination of the real power outputs for the generators so that the total cost of the system is minimized is also known as the problem of economic load dispatch, and towards it are addressed power mix selection and sizing problems.

Traditional optimization techniques are used in [25] by M. Vafaei and M. Kazerani, selecting and sizing, different power generation technologies and storage devices for a microgrid, in order to minimize operational costs. The optimization model is formulated as a MIP (Mixed Integer Programming) problem in GAMS environment.

Also, a classical optimization method is reviewed towards microgrid modelling purposes in [26] by Augustine et al. They perform the power mix selection of four different types of microgrids by using the Reduced-Gradient Method for Economic Dispatch algorithm and Matlab software in order to simulate the system. In this paper the final selection is based on economic dispatch costs, taking into account renewable energy sources penetration, costs and receipts associated.

Y. Han et al. in [27] solve the ELD problem using the Karush-Kuhn-Tucker (KKT) conditions. Allowing inequality constraints, the KKT approach to nonlinear programming generalizes the method of Lagrange multipliers, which allows only equality constraints. The KKT approach guarantees to find the true optimum (versus heuristic search approaches), but is also readily capable of being extended with further realistic constraints/costs, versus purely analytic approaches.

In [28] T. Logenthiran compares a classical Integer Minimization Problem (IMP) with Evolutionary Strategy (ES) method (a generic population-based optimization metaheuristic algorithm) in order to size power equipment for an islanded microgrid. The optimization aim is to minimize the sum of the total capital, operational and maintenance cost of DERs.

Heuristics are widely used in sizing and power generation mix selection. Erdinc in [21] highlights some heuristic optimization techniques for hybrid renewable energy systems sizing such as: GA, PSO, SA and some promising techniques such as Ant Colony and AIS.

In [29] S.M.M. Tafreshi et al model a microgrid using MATLAB and GA to solve the sizing problem with some restrictions. They evaluate the system considering costs and benefits such as: the cost function annualized capital, replacement, operational, maintenance, fuel costs and annual earning by selling power to grid.

SA algorithm is used to solve the optimal sizing problem for renewable energy generations and combined heat and power (CHP)

units in a hybrid energy microgrid in [30]. Stochastic variability of renewable energy resources and the heat and power requirements are considered in order to meet customer requirements with minimum system annual cost.

Energy efficiency and renewable power sources are nowadays the guidelines to minimize the environmental impact of a microgrid. But since renewable power sources are not always ready to produce energy at their peak power, energy storage becomes an important topic in microgrids. Thus, sizing problem concerns not only to power sources but also to energy storage devices. These devices must be sized and located regarding cost-effectiveness, environmental impact, reliability and quality goals. This topic is introduced by S. Bahramirad et al. in [31] in which the optimal ESS sizing problem is proposed both for initial investment and expansion problems. The problem is analysed from an economical point of view, using a MIP approach in order to minimize investment in storage devices and microgrid operational costs.

S.X. Chen et al. propose in [24] a method based on the cost-benefit analysis for optimal sizing of an energy storage system in a microgrid. Time series and Feed-forward neural network techniques are used for forecasting the wind speed and solar radiations respectively. The main problem is formulated as a MILP, which is solved in AMPL (A Modelling Language for Mathematical Programming). A specific Artificial Neural Network algorithm is used for production forecasting, meanwhile a classical approach is used for the optimization problem.

An heuristic method is again used in [32] by Navaeefard et al. They introduce uncertainty in a microgrid sizing problem that includes photovoltaic PV/wind hybrid system with storage energy systems. Wind power uncertainty is proposed and reliability index are considered as a constraint. PSO algorithm is used to obtain global optimal solutions using MATLAB.

In [33] O. Menniti et al. propose a methodology to determine the optimum sizing and configuration of a grid-connected hybrid Photovoltaic/Wind system, including energy storage systems and ensuring that the system total cost is minimized while guaranteeing a highly reliable source of load power. They base their analysis on simulation techniques.

In [34] G. Carpinelli et al. present a three step procedure, based on GA and Decision Theory, applied to establish the best distributed generation siting and sizing on an MV distribution network.

In [35] Z. Wang et al. deal with the microgrid planning problem by means of a two-stage optimization approach, where the problem is formulated as a mixed-integer program (MIP) and the probabilistic nature of DG outputs and load consumption is considered under a robust approach, resorting to a column and constraint generation (CCG) framework to solve the problem.

In [36] H. Lofti and A. Khoadei present a microgrid planning model for determining the optimal size and the generation mix of distributed energy resources (DERs), as well as the microgrid type, i.e., ac or dc. The microgrid type is selected based on economic considerations, by means of a mixed integer programming formulation, where the planning objective includes the investment and operation costs of DERs, cost of energy purchase from the main grid, and the reliability cost. The impact of a variety of factors on planning results, including the ratio of critical loads, the ratio of dc loads, and the efficiency of inverters and converters, is investigated through numerical applications.

In [37] G. Muñoz-Delgado et al. address the incorporation of uncertainty and reliability in the joint expansion planning of distribution network assets and DG combining stochastic programming, mixed-integer linear programming and predictive reliability assessment.

In [38] R. Atia and N. Yamada implement a mixed integer linear program for the optimization of a hybrid renewable energy system with a battery energy storage system in residential microgrids, in which the demand response of available controllable appliances is considered in the proposed optimization problem with reduced calculation burdens.

In [39] S. Mashayekh et al. present a mixed-integer linear programming model for optimal microgrid design, including optimal technology portfolio, placement, and dispatch, for multi-energy microgrids, i.e. microgrids with electricity, heating, and cooling loads and resources, including integer linear models for electricity and heat transfer networks, as well as their physical and operational constraints.

In [40] A. Narayan et al. implement the two stage stochastic programming paradigm for microgrid planning, in the aim of providing economically and environmentally acceptable designs with specified reliabilities, and extended the two-stage stochastic programming model to a risk-averse model using the Markovitz objective function. The microgrid planning problem is considered as an investment problem where the risk is due to uncertainty in the resources and one can determine solutions of desirable risk with corresponding optimal expected values.

In [41] M. Quashie et al. propose a systematic approach for formulating and quantifying a microgrid business case, defining stakeholders, benefits and beneficiaries, determining the dependency of the business case on microgrid technologies and implementing a method to quantify and allocate benefits.

In [42] M. Asensio et al. presents a bi-level model for distribution network and renewable energy expansion planning under a demand response (DR) framework. In the upper-level problem the target , is to minimize generation and network investment cost, while meeting the demand. The upper-level problem is constrained by a lower-level problem, which stresses the importance of integrating DR to time-varying prices into investment models and pursues the minimization of overall payment faced by the consumers. Using the Karush-Kuhn-Tucker complementarity constraints, the proposed bi-level model is recast as a mixed-integer linear programming problem, which is solvable using efficient off-the-shelf branch-and-cut solvers.

In [43] M. Armendáriz et al. present a coordinated approach to the microgrid planning problem, where the system operator and the microgrid owner collaborate to improve the voltage control capabilities of the distribution network and increase the PV potential, which can be otherwise hindered by technical issues such as the over-voltages caused in distribution networks during the daylight periods.

2.5 References

[1] S. S. Rao, “Engineering Optimization: Theory and Practice”, Wiley, 4th edition, 2004.

[2] S. Kiranyaz, T. Ince, M. Gabbouj, "Multidimensional Particle Swarm Optimization for Machine Learning and Pattern Recognition", Springer, 2014.
[3] D.P. Bertsekas, "Constrained Optimization and Lagrange Multiplier Methods", Academic Press, New York, 1982.
[4] FICO™ Xpress Optimization Suite, "Getting Started with Xpress", Release 7, June 2009.
[5] K.G. Murty, "Linear programming", John Wiley & Sons Inc.1, 2000.
[6] K. Y. Lee (Editor), M. A. El-Sharkawi (Editor), "Modern Heuristic Optimization Techniques - Theory and Applications to Power Systems", March 2008, Wiley-IEEE Press.
[7] W. Saad, Z. Han, H. V. Poor, and T. Basar, "Game-Theoretic Methods for the Smart Grid: An Overview of Microgrid Systems, Demand-Side Management, and Smart Grid Communications", IEEE Signal Process. Mag., vol. 29, no. 5, pp. 86–105, 2012.
[8] B. Dodson, P. C. Hammett, R. Klerx, "Probabilistic Design for Optimization and Robustness for Engineers", First Edition, 2014 by John Wiley & Sons, Ltd.
[9] A. Ben-Tal, L. El Ghaoui, A. Nemirovski, "Robust Optimization", Princeton Series in Applied Mathematics, 2009; ISBN 978-0-691-14368-2.
[10] A. Saltelli, (2002). "Sensitivity Analysis for Importance Assessment", Risk Analysis. 22 (3): 1–12.
[11] A. Shapiro et alii, (2009). "Lectures on stochastic programming: Modeling and theory", MPS/SIAM Series on Optimization. 9. Philadelphia, PA, pp. xvi+436. ISBN 978-0-89871-687-0. MR 2562798.
[12] A. Kleywegt, A. Shapiro, T. Homem-de-Mello, "The sample average approximation method for stochastic discrete optimization", SIAM J. O PTIM. 2001 Society for Industrial and Applied Mathematics, Vol. 12, No. 2, pp. 479–502.
[13] D. Bertsimas and M. Sim, "The price of robustness", Operations research, 52(1):35–53, 2004.
[14] K. Steele, H.O. Stefánsson, "Decision Theory", The Stanford Encyclopedia of Philosophy (Winter 2015 Edition), Edward N. Zalta (ed.).

[15] V. Miranda, L.M. Proenca, "Why risk analysis outperforms probabilistic choice as the effective decision support paradigm for power system planning", IEEE Transactions on Power Systems, Volume: 13 Issue: 2, May 1998.
[16] A. Khodaei, S. Bahramirad, M. Shahidehpour, "Microgrid planning under uncertainty", IEEE Trans. Power Syst., 2015, https://doi.org/10.1109/TPWRS.2014.2361094.
[17] C. Gamarra, JM. Guerrero, "Computational optimization techniques applied to microgrids planning: a review", Renew Sustain Energy Rev 2015;48:413–24.
[18] M. Iqbal, M. Azam, M. Naeem, A.S. Khwaja, A. Anpalagan, "Optimization classification, algorithms and tools for renewable energy: A review", Renew Sustain Energy Rev 2014;39:640–54. http://dx.doi.org/10.1016/j.rser.2014.07.120.
[19] G. Mendes, C. Ioakimidis, P. Ferrão, "On the planning and analysis of Integrated Community Energy Systems: A review and survey of available tools", Renew Sustain Energy Rev 2011;15:4836–54.
[20] D. Connolly, H. Lund, B.V. Mathiesen, M. Leahy, "A review of computer tools for analysing the integration of renewable energy into various energy systems", Appl Energy 2010;87:1059–82. http://dx.doi.org/10.1016/j.apenergy.2009.09.026.
[21] O. Erdinc, M. Uzunoglu. "Optimum design of hybrid renewable energy systems: Overview of different approaches", Renew Sustain Energy Rev 2012;16:1412–25. http://dx.doi.org/10.1016/j.rser.2011.11.011.
[22] R. Baños, F. Manzano-Agugliaro, F.G. Montoya, C. Gil, A. Alcayde, J. Gómez, "Optimization methods applied to renewable and sustainable energy: A review", Renew Sustain Energy Rev 2011;15:1753–66. http://dx.doi.org/10.1016/j.rser.2010.12.008.
[23] K. Nishikawa, J. Baba, E. Shimoda, T. Kikuchi, Y. Itoh, T. Nitta et al., "Design methods and integrated control for microgrid", 2008 IEEE Power Energy Soc. Gen. Meet. - Convers. Deliv. Electr. Energy 21st Century, IEEE; 2008, p. 1–7. http://dx.doi.org/10.1109/PES.2008.4596065.
[24] S.X. Chen, H.B. Gooi, M.Q. Wang, "Sizing of energy storage for microgrids", IEEE Trans Smart Grid 2012;3:142–51.

[25] M. Vafaei, M. Kazerani, “Optimal unit-sizing of a wind-hydrogen-diesel microgrid system for a remote community”, 2011 IEEE Trondheim PowerTech, IEEE; 2011, p. 1–7. http://dx.doi.org/10.1109/PTC.2011.6019412.

[26] N. Augustine, S. Suresh et al., “Economic dispatch for a microgrid considering renewable energy cost functions”, Innovative Smart Grid Technologies (ISGT), 2012 IEEE PES.

[27] Y. Han, P. Young, D. Zimmerle, “Optimal selection of generators in a microgrid for fuel usage minimization”, 2013 IEEE Power Energy Soc. Gen. Meet., IEEE; 2013, p. 1–5. http://dx.doi.org/10.1109/PESMG.2013.6672746.

[28] T. Logenthiran, D. Srinivasan, A.M. Khambadkone, T. Sundar Raj, “Optimal sizing of an islanded microgrid using Evolutionary Strategy”, 2010 IEEE 11th Int. Conf. Probabilistic Methods Appl. to Power Syst., IEEE; 2010, p. 12–7. http://dx.doi.org/10.1109/PMAPS.2010.5528840.

[29] S.M.M. Tafreshi, H.A. Zamani, S.M. Ezzati, M. Baghdadi, H. Vahedi, “Optimal unit sizing of Distributed Energy Resources in MicroGrid using genetic algorithm”, 2010 18th Iran. Conf. Electr. Eng., IEEE; 2010, p. 836–41. http://dx.doi.org/10.1109/IRANIANCEE.2010.5506961.

[30] Y. Yang, W. Pei, Z. Qi, “Optimal sizing of renewable energy and CHP hybrid energy microgrid system”, IEEE PES Innov. Smart Grid Technol., IEEE; 2012, p. 1–5. http://dx.doi.org/10.1109/ISGT-Asia.2012.6303122.

[31] S. Bahramirad, W. Reder, A. Khodaei, “Reliability-Constrained Optimal Sizing of Energy Storage System in a Microgrid”, IEEE Trans Smart Grid 2012;3:2056–62. http://dx.doi.org/10.1109/TSG.2012.2217991.

[32] A. Navaeefard, S.M.M. Tafreshi, M. Barzegari, A.J. Shahrood, “Optimal sizing of distributed energy resources in microgrid considering wind energy uncertainty with respect to reliability”, 2010 IEEE Int Energy Conf 2010:820–5. http://dx.doi.org/10.1109/ENERGYCON.2010.5771795.

[33] D. Menniti, “A method to improve microgrid reliability by optimal sizing PV/Wind plants and storage systems”, CIRED 2009. 20th Int. Conf. Exhib. Electr. Distrib., 2009, p. 1–4.

[34] G. Carpinelli, G. Celli, F. Pilo, A. Russo, "Distributed Generation siting and sizing under uncertainty", 2001 IEEE Porto Power Tech Proc., vol. 4, 2001, p. 335–41. http://dx.doi.org/10.1109/PTC.2001.964856.

[35] Z. Wang, B. Chen et al., "Robust Optimization Based Optimal DG Placement in Microgrids", IEEE Transactions on Smart Grid, Volume: 5, Issue: 5, Sept. 2014.

[36] H. Lotfi, A. Khodaei, "AC Versus DC Microgrid Planning", IEEE Transactions on Smart Grid, vol. 8 no. 1 pp. 296-304 Jan. 2017.

[37] G. Muñoz-Delgado J. Contreras J. M. Arroyo, "Multistage generation and network expansion planning in distribution systems considering uncertainty and reliability", IEEE Trans. Power Syst., vol. 31 no. 5 pp. 3715-3728 Sep. 2016.

[38] R. Atia, N. Yamada, "Sizing and analysis of renewable energy and battery systems in residential microgrids", IEEE Trans. Smart Grid, 2016, 7(3), 1204–1213. https://doi.org/10.1109/TSG.2016.2519541.

[39] S. Mashayekh, M. Stadler, G. Cardoso, M. Heleno, "A mixed integer linear programming approach for optimal DER portfolio, sizing, and placement in multi-energy microgrids", 2017 Applied Energy, 187 , pp. 154-168.

[40] A. Narayan, K. Ponnambalam, "Risk-Averse Stochastic Programming Approach for Microgrid Planning Under Uncertainty", Renew. Energy 2017, 101, 399–408.

[41] M. Quashie, F. Bouffard, G. Joós, "Business cases for isolated and grid connected microgrids: Methodology and applications", Applied Energy 205 (2017) 105–115.

[42] M. Asensio, G. Muñoz-Delgado, J. Contreras, "Bi-Level Approach to Distribution Network and Renewable Energy Expansion Planning Considering Demand Response", IEEE Transactions on Power Systems, Volume: 32, Issue: 6, Nov. 2017.

[43] M. Armendáriz, M. Heleno, G. Cardoso, S. Mashayekh, M. Stadler, L. Nordström, "Coordinated microgrid investment and planning process considering the system operator", Applied Energy 200 (2017) 132–140.

Chapter 3

Application of an analytical approach for the optimal sizing of Energy Storage Systems in DC microgrids to minimize power losses

3.1 Introduction

In this chapter, an analytical approach that deals with the optimal sizing of energy storage systems (ESSs) in DC μGs is proposed [31]. The objective is to improve the efficiency of energy supply, through the minimization of line losses, in a DC μG characterized by the presence of loads, fossil and renewables based generation units and storage devices.

Based on the calculus of variations, an original matrix formulation which starts with the nodal representation of the direct current network is proposed. Two attractive closed-form solutions are presented for minimizing power losses, i.e., (1) a solution based on the approximation of considering the voltage constant at all the network's busses and (2) a solution based on the linear approximation of the load flow. In both cases, the goal is to minimize losses over a given time horizon (e.g., the daily cycle).

In the aim of providing an effective design tool that properly considers the economics, the proposed approach has finally been extended in a multi-objective formulation that considers both the expenses related to the installation of ESSs and the revenues due to the minimization of power losses.

The analytical procedure is formulated in a general manner that can be used for various storage technologies. Numerical applications demonstrate the feasibility and accuracy of the methodology.

3.2 State of the art and assessment of the proposed approach

In the recent literature, researchers have investigated the problem of converting existing AC distribution networks to DC networks in order to maximize the capacity of the overall system[1]–[8].

The DC paradigm avoids phase imbalances, which can occur if single-phase generators and loads are not properly distributed among three-phase AC distribution networks, and it also reduces power losses and improves the efficiency of DC appliances due to the absence of reactive power.

There is increased academic and industrial-sector interest in DC power distribution systems, due to the potential benefits of enhanced energy efficiency and capital savings [1], [9].

Buildings are one of the more interesting field of application for these technologies, because in presence of end-use loads natively DC (e.g., computers, solid-state lighting or variable speed drives for electric motors and HVAC systems), and of onsite renewable generation and distributed energy resources also mostly based on DC technology (e.g. PV or micro-wind generators, storage systems and electric vehicles), DC-based building microgrids can bring additional benefits, allowing direct coupling of DC loads and DC energy resources. DC microgrids can thus give a significative contribution to increase the energy efficiency of buildings (which are responsible for approximately 40% of total energy consumption and roughly 40% of greenhouse gas emissions in USA and in Europe) and to achieve the goal of Net Zero Energy Buildings (i.e. buildings that produce as much energy as they consume) [3]. In particular, due to the increasing electronic loads in homes and the continued growth of distributed solar photovoltaic generation in recent years, the economics of DC circuits in homes may have to be reconsidered by the industry [1]. This is due mainly to the fact that one of the main advantages driving the increased use of DC appliances is their potential for reducing both energy consumptions and costs [8]. Also, when considering the presence of onsite renewable energy resources, e.g., photovoltaic (PV) devices and wind turbines, as well as energy storage systems (ESSs) and plug-in electric vehicles, DC-based networks can bring additional

benefits that can be achieved by direct coupling of these resources with loads, all operating with DC [9]–[13].

With reference to ESSs, their emerging status as crucial elements in modern power systems must be highlighted. Actually, it is well recognized that storage devices are key elements in the overall electrical chain, i.e., generation, distribution, and utilization [11]–[14]. Several energy storage technologies are available for power system applications, such as flywheels, superconducting magnetic energy storage, supercapacitors, fuel cells, and batteries.

In the literature, the use of ESSs has been investigated extensively for both planning and operation stages, and they are used now in most innovative transportation and stationary applications [15]–[22]. ESSs can be considered as the most versatile devices among the components of electrical systems, and they also have a significant role in the control of power systems through the use of electronically-coupled devices.

In [11], the reduction of losses in both transmission and distribution systems was analyzed, and the authors demonstrated the advantages of using storage systems by shifting part of a load from the peak demand period to an off-peak period. In [13], the authors discussed the need for a new methodology for the optimal sizing of combined photovoltaic and energy storage systems aimed at minimizing energy losses in a commercial distribution system. In this scenario, we must redefine the traditional optimization methods used in both the planning and operational stages based on a comprehensive analysis of this new operational environment.

Recently, studies concerning new methodologies for the optimal sizing of ESSs in power systems have been proposed in the literature [23]–[30]. In [23], the grey wolf optimization method was used to determine the optimal sizing of ESSs aimed at minimizing the operational costs of microgrids in presence of distributed generators (DGs). A combined, multi-period, optimal power flow and minute-by-minute control procedure was proposed in [24] to determine the minimum sizes of ESSs that can reduce the curtailment of DGs in distribution networks. In [25], an intelligent scheduling system was developed for the ESSs in distribution systems, and it also is useful in determining the optimal sizes of ESSs in order to reduce peak load demands. In [26], a procedure focused on peak-shaving was used to

size ESSs in distribution networks. In [27], the authors solved a unit commitment problem using the particle swarm optimization method to determine the sizes ESSs in microgrids with the aim of minimizing the total cost and maximizing the total benefit. In [28], an optimal procedure based on an improved bat algorithm was proposed for sizing ESSs in microgrids in order to minimize the total operational costs. In [29], a methodology was proposed for the optimal design of supercapacitors coupled to DC networks with the aim of reducing losses and energy usage. In [30], an analytical design methodology based on the formulation of an optimization problem with isoperimetric constraints was proposed for sizing ESSs in DC networks with the goal of reducing power losses.

In this chapter a new analytical design methodology is proposed for the optimal sizing of ESSs with the aim of minimizing power losses in DC μGs. The analytical tool was derived by starting with the linear approximation of the load flow equations proposed in [32], combined with the isoperimetric constraints. Unlike the current methods described in the literature, such as those in [23]–[29], the proposed method produces an accurate, closed-form expression that generalizes the approach presented in [30]. The novelty of this approach is that, basing on the theory of the calculus of variations, it relies on an analytical formulation of the minimization of the losses in the DC network over a time horizon of interest, which has never been addressed analytically with a rigorous approach.

The closed forms that are derived can be easily used for sensitivity analyses and probabilistic investigations, both of which can be useful to supporting designers and decision-makers.

The main original contributions of the method presented here are summarized as follows:

- the proposal of an enhanced tool for the optimization of the analytical design of DC networks that focuses on saving energy and improving efficiency;
- the achievement of two closed-form expressions based on different approximations, i.e., constant voltage on the busbars and linear approximation of the load flow equations;
- the identification of a rational procedure for the accurate sizing of ESSs that allows, in a general way, taking into account the

different storage technologies and scenarios related to the costs of storage devices and the price of energy.

3.3 Minimization of Power Losses in DC Networks by means of Energy Storage Systems: an Analytical Solution

In the following, the proposed methodological approach for the optimal sizing of ESSs in a DC network that includes DGs, ESSs, and loads is presented. This method is based on the analytical evaluation of the current profile of the ESSs over a specified time period to minimize network losses. To achieve this goal, first, a generalized matrix model of DC networks is presented, and, then, the problem of minimizing losses is solved using an optimization problem formulation that involves isoperimetric constraints.

Two solutions are given and discussed based on (i) constant voltage approximation and (ii) linear approximation of load flow equations. Finally, the problem is re-formulated as a multi-objective optimization problem to include economical evaluations by comparison of costs and revenues caused by the installation of ESSs.

3.3.1 General modeling of a DC network

Power losses in DC networks can be expressed as a function of the nodal currents and a suitable resistance matrix, based on some general concepts of power system analysis.

Let us consider a DC network that includes DGs, ESSs and loads (Fig. 3-1), and is connected to the main distribution grid at the point of common coupling (PCC). This point is regarded as the slack bus (bus #0) with an assigned voltage reference value, E. The remaining busses can be classified as:

- n_L load busses;
- n_G generation busses;
- n_S storage busses.

Thus, $n_L + n_G + n_S = n$, where n is the number of internal busses of the DC network, ordered as:

$\{0, 1, \ldots, n_L, n_L+1, \ldots n_L+n_G, n_L+n_G+1, \ldots, n\}$.

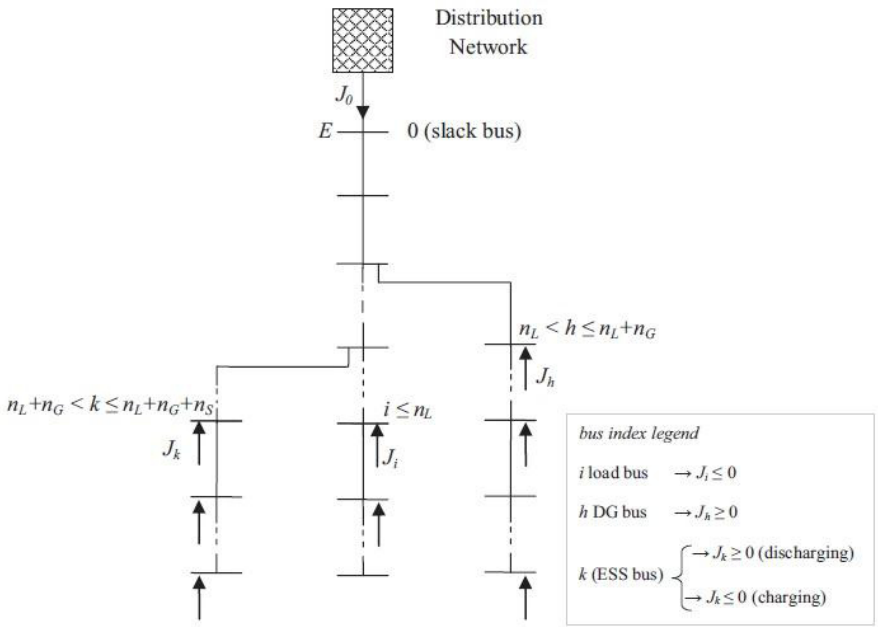

Fig. 3-1: Single line diagram of a typical network with DGs, ESSs, and loads

DGs, ESSs and loads are described in terms of their power profiles, which are assumed to be repetitive signals that have a common period of T (e.g., a day). These powers are assumed to be independent of the related bus voltages. The slack voltage E is assumed to be constant, and shunt conductances are assumed to be negligible.

The network, which interconnects all of the components, can be represented by the nodal conductance matrix **G**, which substantially summarizes the information related to the network nodal analysis. Matrix **G** is related to the branch conductance matrix $\mathbf{G_{br}}$ by the well-known relationship in (1) [33]:

$$\mathbf{G} = \mathbf{A}^{\mathbf{T}}\mathbf{G_{br}}\mathbf{A} \quad (1)$$

where **A** is the branch-to-node incidence matrix. It has to be highlighted that if the network has no shunt branches, e.g. a radial network, the following relation maintains:

$$\mathbf{G1=0} \quad (2)$$

where **1** is the vector of all ones, and, as a consequence, matrix **G** is singular. After matrix **G** is defined, the network can be described in a compact way as:

$$\begin{bmatrix} J_0 \\ --- \\ \mathbf{J} \end{bmatrix} = \mathbf{G} \begin{bmatrix} E \\ --- \\ \mathbf{V} \end{bmatrix} \tag{3}$$

where E and J_0 are the voltage and the injected current at the slack bus, respectively, **V** and **J** are the vectors of voltages and injected currents, respectively, at all busses except the slack bus. By starting with (3), the equivalent representation can be obtained by partitioning the symmetric matrix G, which is an (n+1)x(n+1) matrix:

$$\left[\begin{array}{c} J_0 \\ --- \\ \mathbf{J} \end{array}\right] = \left[\begin{array}{c|c} G_{00} & \mathbf{G_{0E}} \\ --- & --- \\ \mathbf{G_{E0}} & \mathbf{G_{EE}} \end{array}\right] \left[\begin{array}{c} E \\ --- \\ \mathbf{V} \end{array}\right] \tag{4}$$

where

$G_{\mathbf{00}} = G_{11}$,

$\mathbf{G_{0E}} = [G_{12}, \ldots\ldots G_{1n}]$,

$\mathbf{G_{E0}} = \mathbf{G_{0E}^T}$,

$$\mathbf{G_{EE}} = \begin{bmatrix} G_{22} & .. & .. & G_{2\,n+1} \\ .. & \ddots & & \\ .. & & \ddots & \\ G_{n+1\,2} & & & G_{n+1\,n+1} \end{bmatrix}.$$

It has to be emphasized that the matrix GEE is not singular.

Vectors **J** and **V** are related to injected powers **P** at the busses by the following rrlationship:

$$\mathbf{P} = diag(\mathbf{J})\mathbf{V} \tag{5}$$

where

$$diag(\mathbf{J}) = \begin{bmatrix} J_1 & 0 & . & 0 \\ 0 & J_2 & . & 0 \\ . & . & . & 0 \\ 0 & 0 & 0 & J_n \end{bmatrix} \tag{6}$$

By defining

$$\mathbf{R} = \mathbf{G_{EE}}^{-1} \tag{7}$$

we can write:

$$\mathbf{V} = E\mathbf{1} + \mathbf{RJ} \tag{8}$$

where **1** is the vector of all ones. In this case, it is straightforward to deduce a closed expression for the network power losses. In fact, by multiplying the vector **J** by $\mathbf{V^T}$, the following relationship is obtained:

$$\mathbf{V^T J} = E\mathbf{1^T J} + \mathbf{J^T RJ} = E\sum_{k=1}^{n} J_k + \mathbf{J^T RJ} \tag{9}$$

Since the following basic relationship applies:

$$J_0 + \sum_{k=1}^{n} J_k = 0 \tag{10}$$

It is obvious that

$$E\sum_{k=1}^{n} J_k = -EJ_0 \tag{11}$$

and consequently (9) becomes:

$$EJ_0 + \mathbf{V^T J} = \mathbf{J^T RJ} \tag{12}$$

which clearly put in evidence that the term $\mathbf{J^T RJ}$ corresponds to the network power losses (P_{loss}):

$$P_{loss} = \mathbf{J^T RJ} \tag{13}$$

Another straightforward justification of (13), based on the superposition principle, is detailed in Appendix A.

By using the linear approximation of the power flow solution proposed in [32], it follows that:

$$\mathbf{V} = E\mathbf{1} + \frac{\mathbf{RP}}{E} + \frac{\mathbf{R}\mu}{E^3} \tag{14}$$

where $\|\boldsymbol{\lambda}\| \le 4\|\mathbf{P}\|^2 \max_h \sqrt{\sum_k |R_{hk}|^2}$, being $\|\cdot\|$ the 2-norm vector and R_{hk} the resistance of the line between busses h and k.

This formulation clearly indicates that is possible to express the bus voltages as function of both injected active powers and slack bus voltage.

3.3.2 Matrix formulation of the power losses minimization problem with isoperimetric constraint

In this paragraph, the solution of the power losses minimization problem is derived in terms of the optimal current profiles at the busses where the ESSs are located. Based on (13), the minimization problem can be formalized as:

$$\min \int_0^T \mathbf{J}^{\mathrm{T}}\mathbf{R}\mathbf{J}\, dt \tag{15}$$

subject to:

$$\int_0^T diag\left(\mathbf{E}_{\mathrm{sto}}\right)\mathbf{J}_{\mathrm{sto}}\, dt = 0 \tag{16}$$

where $\mathbf{E}_{\mathrm{sto}}$ and $\mathbf{J}_{\mathrm{sto}}$ are the nodal vectors of voltages and injected currents, respectively, at the storage busses. Eq. (16) presents the

isoperimetric constraint that apply to the n_S busses where the ESSs are located. These constraints refer to the injected powers that must have null energy balance over the period T. According to the theory of the calculus of variations, the solution of the minimization problem shown in (15) and (16) can be derived by solving the following system:

$$\frac{d}{d\mathbf{J}_{sto}}(\mathbf{J}^{\mathrm{T}}\mathbf{R}\mathbf{J} + \boldsymbol{\lambda}^{\mathrm{T}}\mathbf{J}_{\mathrm{sto}}) = \mathbf{0} \tag{17}$$

$$\int_0^T diag(\mathbf{E}_{\mathrm{sto}})\mathbf{J}_{\mathrm{sto}}\, dt = 0 \tag{18}$$

where λ is an n_S-vector of Lagrange multipliers, and 0 is a zero n_S vector.

Two analytical approaches are applied to the minimization problem (17)-(18), based on different approximations of the DC bus voltage V:

- the first approach assumes a constant voltage E at all network busses (**V**=E**1**, which implies **J**=**P**/E) and allows finding a fast and straightforward analytical solution, which can be considered to be an extension of the results developed in [30];
- the second approach is based on the linear approximation of the load flow equations (**V**=E**1**+**RP**/E), which provides a more accurate analytical solution.

3.3.2.1 Solution 1: Constant voltage on all network busses

In the case in which constant voltages were assumed, (17) and (18) become:

$$\frac{d}{d\mathbf{J}_{sto}}(\mathbf{J}^{\mathrm{T}}\mathbf{R}\mathbf{J} + \boldsymbol{\lambda}^{\mathrm{T}}\mathbf{J}_{\mathrm{sto}}) = \mathbf{0} \tag{19}$$

$$\int_0^T \mathbf{J}_{\mathrm{sto}}\, dt = 0 \tag{20}$$

where $\mathbf{J}_{\mathrm{sto}}$ is the n_S-vector of currents injected at the storage nodes.

The system of 2 x n_S equations, i.e., (19) and (20), is the matrix formulation of the optimization problem with isoperimetric constraints. By applying the matrix differentiation theory and recalling that both $\mathbf{G_{EE}}$ and $\mathbf{R}$ are symmetric matrices, (19) can be written as:

$$2\mathbf{J}^{\mathbf{T}}\mathbf{R}\frac{d\mathbf{J}}{d\mathbf{J}_{\text{sto}}}+\boldsymbol{\lambda}^{\mathbf{T}}=0 \tag{21}$$

Since $\mathbf{J}_{\text{load}}$ and $\mathbf{J}_{\text{gen}}$ are not dependent on $\mathbf{J}_{\text{sto}}$, (21) can be rewritten as:

$$2\mathbf{J}^{\mathbf{T}}\mathbf{R}\begin{bmatrix}\mathbf{0}\\ \\ \mathbf{I}\end{bmatrix}+\boldsymbol{\lambda}^{\mathbf{T}}=0 \tag{22}$$

where $\mathbf{0}$ is the null matrix and $\mathbf{I}$ is the identity matrix. By transposing (22), a suitable equivalent formulation is provided:

$$2\begin{bmatrix}\mathbf{0} & \mathbf{I}\end{bmatrix}\mathbf{R}\,\mathbf{J}+\boldsymbol{\lambda}=2\begin{bmatrix}0 & \mathbf{I}\end{bmatrix}\mathbf{R}\begin{bmatrix}\mathbf{J}^{*}\\ \mathbf{J}_{\text{sto}}\end{bmatrix}+\boldsymbol{\lambda}=\mathbf{0} \tag{23}$$

where $\mathbf{J}^{*}=\begin{bmatrix}\mathbf{J}_{\text{load}}\\ \mathbf{J}_{\text{gen}}\end{bmatrix}$ is the (n_L + n_G) vector of currents injected at the load and generator busses. The product [**0 1**]**R** is equivalent to [$\mathbf{R_1}$ $\mathbf{R_2}$], and the elements of matrices $\mathbf{R_1}$ and $\mathbf{R_2}$ depend on the elements of matrix **R**, which, in turn, is related to the parameters of the assigned network, i.e.,:

$$\mathbf{R}_{\mathbf{1}i,j}=R_{(n_L+n_G+i,j)} \qquad i=1,...,n_S,\quad j=1,...,n_L+n_G \tag{24}$$

$$\mathbf{R}_{\mathbf{2}i,j}=R_{(n_L+n_G+i,n_L+n_G+j)} \quad i=1,...,n_S,\quad j=1,...,n_S \tag{25}$$

Thus, (23) becomes:

$$2\mathbf{R}_{\mathbf{1}}\,\mathbf{J}^{*}+2\mathbf{R}_{\mathbf{2}}\mathbf{J}_{\text{sto}}+\boldsymbol{\lambda}=\mathbf{0} \tag{26}$$

Vector Eq. (26) is a set of n_S scalar equations expressing $\mathbf{J}_{\text{sto}}$ as a function of $\mathbf{J}_{\text{load}}$, $\mathbf{J}_{\text{gen}}$, and $\boldsymbol{\lambda}$. The optimal profile of the injected currents at the ESSs' busses, $\mathbf{J}_{\text{sto}}$, can be derived as a function of $\mathbf{J}_{\text{load}}$

and $\mathbf{J}_{gen}$ by substituting (26) in (20) for the determination of the vector, $\boldsymbol{\lambda}$, of the Lagrange multipliers. Thus, the matrix form of the solution is given by:

$$\mathbf{J}_{sto} = \mathbf{R}_2^{-1}\mathbf{R}_1\left[\frac{1}{T}\int_0^T \mathbf{J}^* dt - \mathbf{J}^*\right] \tag{27}$$

The vector $\mathbf{J}_{sto}$ that can be obtained from (27) represents the profiles of injected currents at the ESSs' busses which allow the network power losses to be minimized. Note that the injected current profiles evaluated by (27) depend only on the matrix **R** of the DC network and on the currents injected at the load and generator busses. Moreover, in the particular case of the DC network of Fig. 3-2, which is characterized by one load bus, one storage bus, and no distributed generators, (27) reduces to:

$$J_{sto} = \frac{R_1}{R_1 + R_2}\left[\left(\frac{1}{T}\int_0^T \mathrm{J}_{load} dt\right) - \mathrm{J}_{load}\right] \tag{28}$$

where R_1 and R_2 are the resistances of the two lines of the network in Figure 3-2 (i.e., R_1 is the resistance of the line from bus #0 to bus #1, and R_2 is the resistance from bus #1 to bus #2). Formula (28) is the same as the formula obtained in [30].

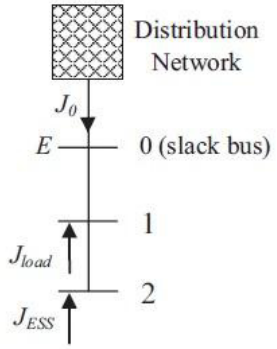

Fig. 3-2: DC network with one load bus and one ESS bus

Hence, the matrix formulation (27) is a generalized extension of that result to the case of a DC network with different loads, generators and storage busses operating as current sources, and a bus connecting the network to an upstream grid acting as a voltage source.

3.3.2.2 Solution 2: Linear approximation of load flow equations

In case the voltages of the busbars are not assumed to be constant, under the mild assumption of constant voltage at the ESS busses, again, the optimization problem with isoperimetric constraint is formulated through the system of Eqs. (17) and (18).

The currents injected at the load and generator busses are evaluated starting from their power profiles and the corresponding bus voltages, which can be obtained from the linear approximation:

$$\mathbf{V} = E\mathbf{1} + \frac{\mathbf{RP}}{E} \tag{29}$$

which can be rewritten as:

$$\mathbf{V} = E\mathbf{1} + \mathbf{R}'\frac{\mathbf{P}^*}{E} + \mathbf{R}''\mathbf{J}_{\text{sto}} \tag{30}$$

where **P*** is the vector of powers injected at the load and generator busses, and **R'** and **R''** are suitable partitions of **R**. By considering Eqs. (5) and (30), the current injected at the generic load bus or generator bus can be expressed as:

$$J^*_i = \frac{P^*_i}{V^*_i} = \frac{P^*_i}{E + \sum_{k=1}^{n_L+n_G} \frac{R'_{i,k}\cdot P^*_k}{E} + \sum_{h=1}^{n_S} R''_{i,h}\cdot J_{sto,h}} = \frac{P^*_i}{E\left[1 + \sum_{k=1}^{n_L+n_G} \frac{R'_{i,k}\cdot P^*_k}{E^2} + \sum_{h=1}^{n_S} \frac{R''_{i,h}\cdot J_{sto,h}}{E}\right]} \tag{31}$$

By considering that the terms in the denominator, i.e., $\sum_{k=1}^{n_L+n_G} \frac{R'_{i,k} \cdot P^*_k}{E^2}$ and $\sum_{h=1}^{n_S} \frac{R''_{i,h} \cdot J_{sto,h}}{E}$, assume small values, the approximation $\frac{1}{1+x} \cong 1-x$ (for small values of x) can be used, so we obtain:

$$J^*_i = \frac{P^*_i}{E}\left[1 - \sum_{k=1}^{n_L+n_G} \frac{R'_{i,k} \cdot P^*_k}{E^2} - \sum_{h=1}^{n_S} \frac{R''_{i,h} \cdot J_{sto,h}}{E}\right], \tag{32}$$

which is a more compact form that can be rewritten in the following matrix form:

$$\mathbf{J}^* = \mathbf{K_1} + \mathbf{K_2}\mathbf{J}_{\text{sto}} \tag{33}$$

where $\mathbf{K_1}$ and $\mathbf{K_2}$ are time-variant matrices that depend on the powers injected at the load and generator busses. However, $\mathbf{K_1}$ and $\mathbf{K_2}$ do not depend on the powers injected at the storage busses, so they can be calculated in advance if the power profiles at the load and generator busses are estimated.

By substituting (33) in (17), the following vector equation is obtained:

$$2\mathbf{J}^{\mathbf{T}}\mathbf{R}\begin{bmatrix}\mathbf{K_2}\\ \\ \mathbf{I}\end{bmatrix} + \boldsymbol{\lambda}^{\mathbf{T}} = \mathbf{0} \tag{34}$$

By comparing (34) and (22), it is clear that matrix $\mathbf{K_2}$ applies in (34) instead of the null matrix $\mathbf{0}$ appearing in (22). By transposing Eq. (34), the following equivalent formulation is obtained:

$$\begin{aligned} &2\begin{bmatrix}\mathbf{K_2}^{\mathbf{T}} & \mathbf{I}\end{bmatrix}\mathbf{R}\cdot\mathbf{J} + \boldsymbol{\lambda} = 2\begin{bmatrix}\mathbf{K_2}^{\mathbf{T}} & \mathbf{I}\end{bmatrix}\begin{bmatrix}\mathbf{R_{11}} & \mathbf{R_{12}}\\ \mathbf{R_{21}} & \mathbf{R_{22}}\end{bmatrix}\begin{bmatrix}\mathbf{K_1}+\mathbf{K_2}\mathbf{J}_{\text{sto}}\\ \mathbf{J}_{\text{sto}}\end{bmatrix} + \boldsymbol{\lambda} = \\ &2\begin{bmatrix}\mathbf{A_1} & \mathbf{A_2}\end{bmatrix}\begin{bmatrix}\mathbf{K_1}+\mathbf{K_2}\mathbf{J}_{\text{sto}}\\ \mathbf{J}_{\text{sto}}\end{bmatrix} + \boldsymbol{\lambda} = 0 \end{aligned} \tag{35}$$

where matrix **R** is conveniently partitioned in four blocks, i.e., $\mathbf{R_{11}}$, $\mathbf{R_{12}}$, $\mathbf{R_{21}}$, and $\mathbf{R_{22}}$, and matrices $\mathbf{A_1}$ and $\mathbf{A_2}$ are calculated as:

$$\mathbf{A_1} = \mathbf{K_2^T R_{11}} + \mathbf{R_{21}} \tag{36}$$

$$\mathbf{A}_2 = \mathbf{K_2^T R_{12}} + \mathbf{R_{22}} \tag{37}$$

Through (35), $\mathbf{J}_{sto}$ can be expressed as a function of **P*** and **λ**. Thus, by recalling the fundamental relationship (18), **λ** can be evaluated as a function of **P***. By trivial algebraic manipulations, $\mathbf{J}_{sto}$ can be stated definitively as:

$$\mathbf{J}_{sto} = -\mathbf{B_1} \cdot \mathbf{K_1} + \mathbf{B_2}\left[\int_0^T \mathbf{B_2} \mathrm{dt}\right]^{-1} \int_0^T \mathbf{B_1} \cdot \mathbf{K_1} \mathrm{dt} \tag{38}$$

where matrices B1 and B2 are evaluated as:

$$\mathbf{B_1} = \left[\mathbf{A_1 K_2} + \mathbf{A_2}\right]^{-1} \mathbf{A_1} \tag{39}$$

$$\mathbf{B}_2 = \frac{1}{2}\left[\mathbf{A_1 K_2} + \mathbf{A_2}\right]^{-1} \tag{40}$$

The vector $\mathbf{J}_{sto}$ obtained through (38) represents the profiles of injected currents at the ESSs' busses, which allow the minimization of the network's power losses. The obtained solution clearly indicates that the optimal ESS current profile strictly depends on the elements of the matrix **R**, which are characteristic parameters of the DC network, and on the powers injected at the load and generator busses. Finally, after the storage current profiles have been evaluated, the voltage profiles can be determined by (30).

By comparing Eqs. (38) and (27), it is to be expected that the slightly more complex closed-form solution (38) will be more accurate than solution (27), since in (38) the dependence of the injected currents on the voltage at both the load and DG busses is considered.

It is worth noting that the proposed procedure allows also the identification of the busses at which it is more convenient to connect

ESSs. In fact, if the optimal current profile at a specified bus is near zero, one can regard this result as a direct measure of the low sensitivity of the network power losses to power injection at that specified bus. Furthermore, another intrinsic measure of the sensitivity is just the vector of the Lagrange multipliers, which can provide additional useful information for identifying the most adequate busses for contemporaneously minimizing losses and reducing, the number of storage systems, if so desired.

3.3.3 Multi-objective Formulation for the Economic Evaluation of ESSs Installation

In this section, the optimal sizing of ESSs in DC networks is discussed by applying and extending the general methodology proposed for the analytical minimization of the power losses. In more detail, the proposed approach was modified to take into account the costs that are incurred when a specified ESS technology is used. An effort was made to retain the quadratic formulation of the minimization problem used in Section 2 in order to still obtain a closed form solution of the optimal sizing problem.

Based on the current literature on the technology and optimal sizing of ESSs, it is generally understood that the cost analysis for the use of a specified storage system must consider both the costs to maintain the system and the benefits it provides. The value of the total lifecycle costs related to the use of ESSs includes the total capital cost for purchase, installation, and delivery and the costs related to operation, maintenance, replacement, and disposal or recycling [20]–[22], [34], [35]. For the application being considered, the benefits obtained by using the ESS are related to the minimization of the costs associated with power losses, and these costs depend on the price of energy and on any incentives (if applicable) provided to save energy. Regarding the costs related to the use of an ESS, recently, several studies concerning the definition of suitable cost parameters and the calculation of their expected values based on extensive statistical reviews have been presented in the literature [20]–[22]. These studies indicated that the specific cost per stored unit of electricity depends on a variety of factors, e.g., efficiency, power-to-capacity ratio, self-discharge rate, depth of discharge, lifetime, specific capital cost,

operation cost, maintenance cost, and others. In addition, some other costs were related to financial and operational aspects, e.g., discounts and interest rates, yearly energy discharge, and the number of work cycles.

Without focusing on these aspects, which are outside the scope of this work, it is worth noting that it is possible to evaluate an expected specific cost of stored energy, depending on the chosen ESS technology and on the above mentioned factors, by means of the method of the levelized cost of energy provided by the ESS [20], also denoted as LCOS (levelized cost of storage). The LCOS is basically calculated dividing the total costs related to the storage system (including capital and operational expenditures, cost of input electricity and residual value of the components) by the sum of the annual energy outputs, and then it allows to perform detailed cost analyses depending on the considered technologies and business cases.

Therefore, in order to take into account the expenses related both to the use of ESSs and to power losses, the minimization problem in (15) and (16) must be rewritten as a multi-objective minimization problem that focuses on the minimization of two cost items, i.e., a) the cost of power losses and b) the specific cost of energy stored in the ESSs. The first cost item can be evaluated by means of a parameter that accounts for the price of energy (γ_1), and the second cost item can be evaluated by means of a parameter that accounts for the levelized cost of the energy provided by the ESS (γ_2) [20]–[22]. If γ_1 and γ_2 are known, it is easy to formulate the considered multi-objective problem as a single-objective minimization problem in which the objective function is given by a weighted sum of the costs related to both the power losses and the installation of ESSs:

$$\min \gamma_1 \int_0^T \mathbf{J}^{\mathrm{T}} \mathbf{R} \mathbf{J} \, dt + \boldsymbol{\gamma}_2^{\mathrm{T}} \int_0^T \frac{1}{2} diag\left(\mathbf{E}_{\mathrm{sto,rtd}}\right) \left|\mathbf{J}_{\mathrm{sto}}\right| dt \tag{41}$$

where $\boldsymbol{\gamma}_2$ is the vector of the levelized costs of energy delivered by the ESSs (in general, different technologies can be considered), $\mathbf{E}_{\mathrm{sto;rtd}}$ is the vector of the voltage rated values of the ESSs and the term,

$$\int_0^T \frac{1}{2} diag\left(\mathbf{E}_{\mathrm{sto,rtd}}\right) \left|\mathbf{J}_{\mathrm{sto}}\right| dt \tag{42}$$

represents the rated storage capacity of the ESSs.

In order to preserve the quadratic formulation of the minimization problem (41), the Chebyshev approximation to $f(x) = |x|$, $P(x)=x^2+1/8$ is used, where $P(x)$ is the min-max polynomial approximation of degree ≤ 3, that applies for x e [-1, 1] [36]. In our case, this approximation can be used easily by defining the function $J_{sto;i}/J_{max;i}$, for the ith ESS, where $J_{max;i}$ is the maximum value of the absolute value of the ESS current ($J_{sto;i}$) estimated through the application of formula (38).

Hence, with respect to the i[th] ESS, noting that a single term is detailed so the notation will be clear, the cost related to its use is:

$$\frac{1}{2}\gamma_{2,i}J_{max,i}\int_0^T E_{sto,rtd,i}\frac{|J_{sto,i}|}{J_{max,i}}dt \cong \frac{1}{2}\gamma_{2,i}J_{max,i}E_{sto,rtd,i}\int_0^T\left(\frac{J_{sto,i}^2}{J_{max,i}^2}+\frac{1}{8}\right)dt \qquad (43)$$

By splitting the right side of (43) into two terms, the cost item for the i[th] ESS becomes:

$$\gamma'_{2,i}\int_0^T J_{sto,i}^2 dt + \frac{1}{2}\gamma_{2,i}\frac{J_{\max,i}E_{sto,rtd,i}}{8}T \qquad (44)$$

where $\gamma'_{2,i} = \frac{1}{2}\gamma_{2,i}\frac{E_{sto,rtd,i}}{J_{\max,i}}$, and the constant term can be defined as: $\xi_i = \frac{1}{2}\gamma_{2,i}\frac{J_{max,i}E_{sto,rtd,i}}{8}T$. The complete matrix formulation that takes all of the ESSs into account can be then easily derived as:

$$min\,\gamma_1\int_0^T \mathbf{J}^{\mathrm{T}}\mathbf{R}\mathbf{J}\,dt + \int_0^T \mathbf{J}_{sto}^T\mathbf{\Gamma}\mathbf{J}_{\mathrm{sto}}\,dt + \Xi \qquad (45)$$

where $\mathbf{\Gamma} = diag\left(\gamma'_{2,i}\right)$ and $\Xi = \sum_{i=1}^{n_s}\xi_i$, and which obviously is still subject to the isoperimetric constraints:

$$\int_0^T diag\left(\mathbf{E}_{\mathrm{sto}}\right)\mathbf{J}_{\mathrm{sto}}\,dt = 0 \qquad (46)$$

The procedure described in Section 2 can be used also to solve the minimization problem (45) and (46), and the following matrix equation can be stated:

$$\frac{d}{d\mathbf{J}_{sto}}\left(\gamma_1\mathbf{J}^{\mathrm{T}}\mathbf{R}\mathbf{J}+\boldsymbol{\lambda}^{\mathrm{T}}\mathbf{J}_{\mathrm{sto}}+\mathbf{J}_{sto}^{T}\boldsymbol{\Gamma}\mathbf{J}_{\mathrm{sto}}+\Xi\right)=\mathbf{0} \tag{47}$$

This equation must be solved together with (46). By considering that Ξ is a constant value, the following vector equation is obtained:

$$2\gamma_1\mathbf{J}^{\mathbf{T}}\mathbf{R}\begin{bmatrix}\mathbf{K_2}\\ \mathbf{I}\end{bmatrix}+\boldsymbol{\lambda}^{\mathbf{T}}+2\mathbf{J}_{sto}^{T}\boldsymbol{\Gamma}=0 \tag{48}$$

By transposing Eq. (48), the following equivalent formulation is obtained:

$$2\gamma_1\begin{bmatrix}\mathbf{K_2}^{\mathbf{T}} & \mathbf{I}\end{bmatrix}\mathbf{R}\cdot\mathbf{J}+\boldsymbol{\lambda}+2\boldsymbol{\Gamma}\mathbf{J}_{\mathbf{sto}}=2\gamma_1\begin{bmatrix}\mathbf{A_1} & \mathbf{A_2}\end{bmatrix}\begin{bmatrix}\mathbf{K_1}+\mathbf{K_2}\mathbf{J}_{\mathbf{sto}}\\ \mathbf{J}_{\mathbf{sto}}\end{bmatrix}+\boldsymbol{\lambda}+2\boldsymbol{\Gamma}\mathbf{J}_{\mathbf{sto}}=0 \tag{49}$$

Then, it is apparent that the optimal solution is given by:

$$\mathbf{J}_{\mathrm{sto}}=-\mathbf{B}_1^{'}\cdot\mathbf{K_1}+\mathbf{B}_2^{'}\left[\int_0^T\mathbf{B}_2^{'}\mathrm{dt}\right]^{-1}\int_0^T\mathbf{B}_1^{'}\cdot\mathbf{K_1}\mathrm{dt} \tag{50}$$

where matrices $\mathbf{B'_1}$ and $\mathbf{B'_2}$ are evaluated as:

$$\mathbf{B}_1^{'}=\left[\mathbf{A}_1^{'}\mathbf{K_2}+\mathbf{A}_2^{'}\right]^{-1}\mathbf{A}_1^{'} \tag{51}$$

$$\mathbf{B}_2^{'}=\frac{1}{2}\left[\mathbf{A}_1^{'}\mathbf{K_2}+\mathbf{A}_2^{'}\right]^{-1} \tag{52}$$

where $\mathbf{A}_1^{'}=\gamma_1\mathbf{A}_1$, and $\mathbf{A}_2^{'}=\mathbf{A}_2+\boldsymbol{\Gamma}$.

The vector $\mathbf{J}_{sto}$ obtained through (50) represents the profiles of the currents injected at the ESS busses, which allows minimizing both network power losses and the cost of ESSs.

Based on a correct estimation of the cost parameters γ_1 and $\gamma_{2,i}$ ($i \in 1, \ldots n_s$), formula (50) allows to obtain the current profile of each ESS and, consequently, by means of formula (42), to obtain their storage capacity. The proposed approach is very general, and it allows designers to determine the optimal storage technology and size, because they can use formula (50) to evaluate any storage technology by using proper values of the parameter $\gamma_{2,i}$ [20-22].

Parametric analyses can be usefully performed based on the ratio $\rho_i=\gamma_{2,i}/\gamma_1$. In fact, different values of ρ_i related to different technologies can be assessed, and future perspectives for both storage costs and energy prices can be easily analyzed.

3.4 Numerical Applications to a DC Microgrid

In this paragraph, the proposed methodology is applied to an LV DC test Microgrid, as shown in the single line diagram in Fig. 3-3, derived with slight modifications from the AC LV CIGRE distribution network [37].

Three PV generators, one wind turbine (WT) generator, and one microturbine (MT) are connected to the grid. Table 3-1 provides the loads and DGs' rated sizes and locations.

Table 3-1: Rated powers of the DGs and loads

DGs			Loads	
Bus #	Type	Rated power [kW]	Bus #	Rated power [kW]
9	PV	10	9	47
11	PV	10	10	15
11	WT	10	11	50
13	PV	3	13	15
14	MT	30	14	72

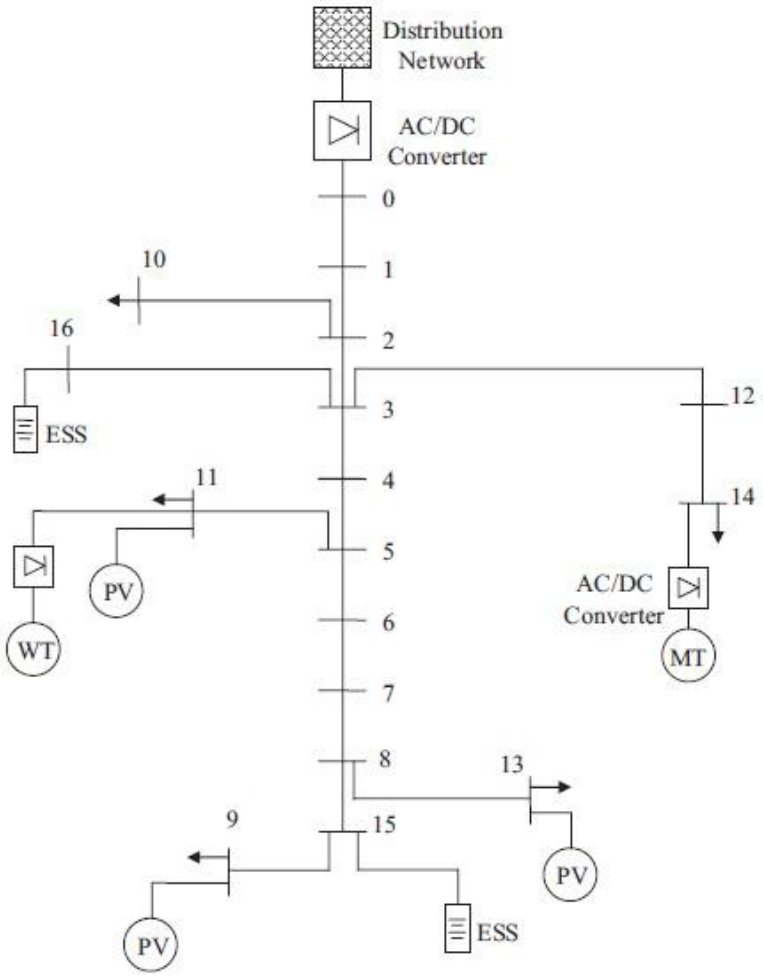

Fig. 3-3: DC LV test Microgrid

In order to allow the operation of the original network in DC, an AC/DC converter is required at the point at which the considered network is connected to the main distribution network. Also, converters are required to connect the AC loads, the WT and MT generators to the network. The AC/DC interfacing converters for PV generators and ESSs are replaced by DC/DC converters. A DC voltage level of 400 V was selected to facilitate the transition of the original network to DC since this value allowed us to maintain the

same cable characteristics and losses. More details are given in Appendix B about the use of the DC test grid.

In applying the proposed procedure, the daily profiles of loads and generators were considered. (The daily profiles were partitioned into 24 time intervals.) As examples, Fig. 3-4 shows the daily profile of the absorbed power at bus #10 [37]; Fig. 3-5 shows the daily profile of the injected power by both WT and PV generators connected at bus #11. These profiles were obtained from the hourly mean values of actual measured data taken over one year at a location in the southern part of Italy. With reference to the MT, we assumed a constant injected power equal to the 80% of the rated power.

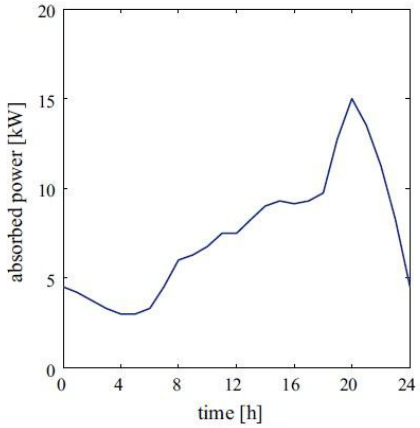

Fig. 3-4: Daily profile of the power demand of the load connected at bus #10

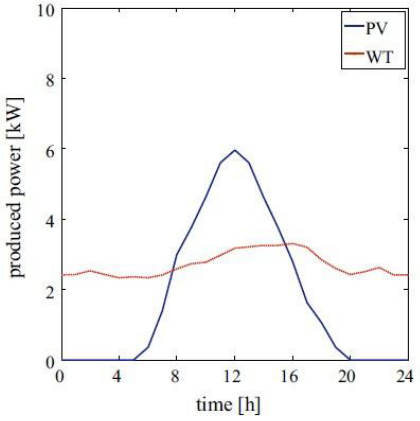

Fig. 3-5: Daily profile of the power produced by PV and WT at bus # 11

In this application, the analytical approaches proposed in paragraphs 3.3.2 and 3.3.3 were used to demonstrate the effectiveness and the feasibility of the proposed methodology for determining the optimal sizes of the ESSs located in busses #15 and #16.

To show the accuracy of the proposed analytical methodology, the optimal current profiles at busses #15 and #16 were evaluated first without considering the problem of optimal sizing. In this case, the results obtained using formulas (27) and (38) were used and compared to those obtained by rigorous load flow (LF) calculations.

In order to demonstrate the potential of the sizing procedure presented in paragraph 3.3.3, an additional application evaluated the optimal sizing of the ESSs based on formula (50). In this case, a

parametric analysis was performed with reference to the cost of the ESSs.

3.4.1 Accuracy of the analytical approach

Two case studies were analyzed to determine the accuracy of the analytical approach, respectively using formula (27), which refers to constant bus voltages, case (1.A), and formula (38), which refers to the linear approximation of bus voltages, case (1.B).

In both cases, LF calculations were done at each hour of the day, based on the same power profiles of the loads, DGs, and ESSs. The power profiles of the ESSs were assumed to be equal to those obtained by the proposed approaches in case (1.A) and case (1.B) respectively. In addition, cases with and without storage were analyzed.

Table 3-2 reports the energy losses in case (1.A) and in case (1.B).

Table 3-2: Energy losses in case (1.A) – (1.B)

Accuracy of the proposed approaches.

Case study		Energy Losses [kW h]		Percentage error (%)
		Proposed formula[a]	Load flow	
Case (1.A)	With ESSs	48.72	52.70	7.55
	Without ESSs	58.45	65.17	10.3
Case (1.B)	With ESSs	52.17	52.68	0.97
	Without ESSs	64.43	65.17	1.13

[a] In *case (1.A)*, formula (27); in case (*1.B*), formula (38).

Table 3-2 shows that, compared to the LF, the use of the constant voltage approximation (case 1.A) implies larger errors than the errors implied by the linear approximation (case 1.B). In fact, in case (1.B) with and without ESSs, the errors obtained were approximately 1%, confirming the accuracy of the proposed methodology.

To better emphasize the accuracy of case (1.B), Fig. 3-6 shows the voltage profile at hour 12 for all the busses, in the case 'with ESSs'. Figure 3-6 shows that slight differences between LF and formula (38) can be observed; by extending the comparison over the whole day, a mean value of the errors of about 1% is obtained.

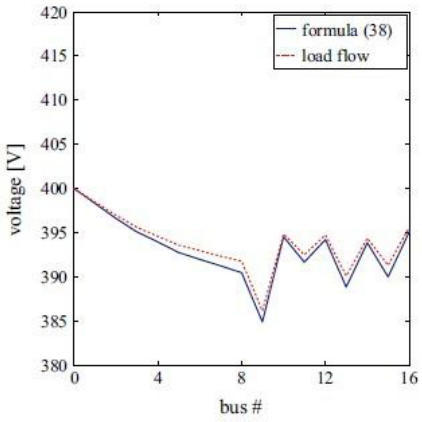

Fig. 3-6: Voltage levels on all busses at hour 12:00

The variation of the voltage on all busses during the whole day never exceeded 10% of the rated voltage (400 V). This demonstrated that the functional integration of the ESSs in the network did not affect the voltage profile dramatically. Also the line currents were maintained within admissible ranges.

Figure 3-7 shows the charging/discharging daily power profile of the ESSs.

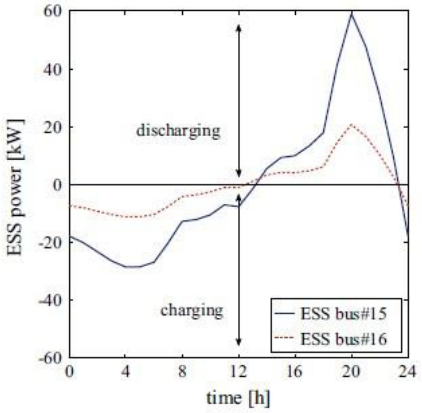

Fig. 3-7: ESSs daily charging/discharging cycle

The ESSs' power profiles reported in Fig. 3-7 clearly indicate that the ESSs are required to provide a charging/discharging cycle that is

essentially consistent with the load-demand profile. This must be done by charging during the low-demand hours and discharging during the peak-demand hours, which occur mainly in the evening according to the demand profile of Fig. 3-4. Moreover, Figure 3-7 indicates that the ESSs have only one charging/discharging cycle per day, which makes the use of batteries particularly suitable for this application [20]-[22]. According to the profiles of Fig. 7, the power and capacity requested to the ESSs are about 60 kW and 240 kWh, respectively, for the ESS at bus #15, and about 20 kW and 90 kWh, respectively, for the ESS at bus #16. A lower value of stored energy is requested for the ESS located at bus #16, which is the storage system located closest to the slack bus. Notably, these values refer to the general approach of paragraph 3.3.2, without considering the cost related to the use of ESSs.

Note that the charging/discharging profiles of both ESSs are far from zero, thus demonstrating that both busses (i.e., #15 and #16) are quite sensitive to reductions in power losses.

3.4.2 Optimal sizing of storage systems

In this case, the optimal sizing problem of the ESSs located at busses #15 and #16 is analyzed again by taking into consideration the cost related to the use of ESSs in the networks and the cost of the energy. To do that, the analytical procedure presented in paragraph 3.3.3 for the optimal sizing of an ESS is used through a proper parametric analysis obtained by means of formula (50).

For the sake of simplicity, it is assumed that the same technology is used for both ESSs, thus allowing the parametric analysis to be performed in terms of the ratio $\rho=\gamma_2/\gamma_1$, which varies within the range 0–20. Note that, once the energy price and the specified cost of the storage capacity are estimated, this range allows us to analyze the possibility of applying different technologies [20]-[22]. In addition, the inclusion of the value $\rho=0$ (i.e., $\gamma_2=0$) allows to consider the case analyzed in the previous paragraph where the cost related to the use of ESSs is not considered.

The results of the simulations are reported in Figs. 3-8, 3-9, 3–10: the optimal capacity of the ESSs is depicted in Fig. 3-8, whereas Fig. 3-9 shows the optimal rated power for the ESSs and Fig. 10 shows the reduction in power losses compared to the case without ESSs.

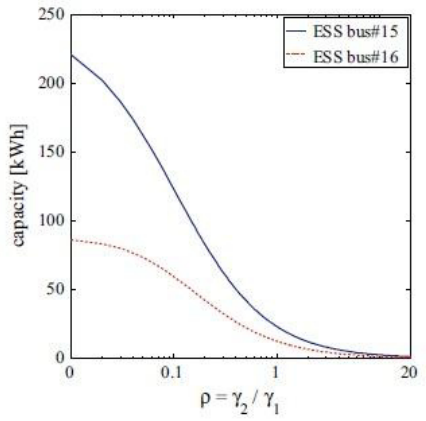

Fig. 3-8: Parametric evaluation of the optimal capacities of the ESSs

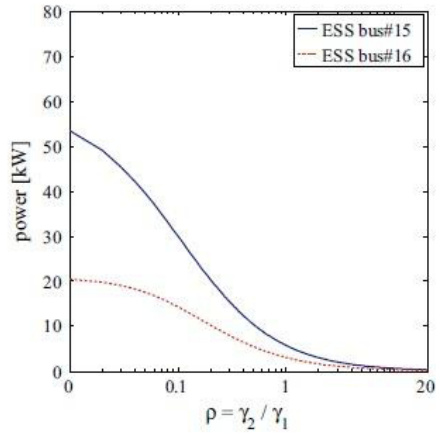

Fig. 3-9: Parametric evaluation of the optimal power of the ESSs

In Figs. 3-8 and 3-9, note that the lower is the value of ρ, the higher are the values of the rated capacity and power of the ESSs. However, for higher values of ρ, the resulting rated capacities and powers of the ESSs decreased significantly. These results are to be expected given that lower values of ρ imply substantially low cost for capacity and a high energy price, while higher values of ρ indicate just the opposite outcomes.

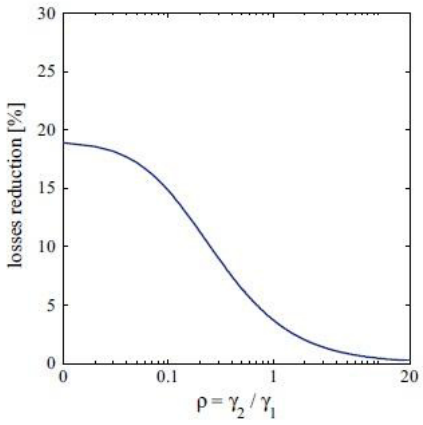

Fig. 3-10: Parametric evaluation of the reduction in power losses

In Figs. 3-8, 3-9, 3-10, the remarkable reductions of capacity, power, and losses are presented on a logarithmic scale for the parameter ρ. These results, which were consistent with results in the literature, demonstrate the feasibility and effectiveness of the proposed sizing method, and they provide an accurate and feasible tool that designers can use to deal with the problem of determining the optimal sizes of ESSs.

Based on the currently available data about the costs of ESSs and the price of energy, it must be highlighted that the expected value of ρ is rapidly approaching values less than 1 for some specific technologies, such as batteries for storing energy [20]-[22]. This is consistent with the tendency to consider the use of ESSs a valuable approach for decreasing losses and improving the efficiency of distribution networks. Fig. 3-10 also shows that decreasing the values of ρ, the reduction in power losses increases, which may justify policies that provide incentives for the use of ESSs to save energy.

Fig. 3-11 shows the optimal power profiles of the ESSs when ρ = 1. By comparing the profiles of Fig. 3-11 to those obtained in case of ρ = 0 (i.e., Fig. 3-7), it is obvious that the exchanges of power required of the ESSs are lower, which allows them to operate with a lower rated capacity. Specifically, the requested capacity of the ESSs was about 15 kW h (ESS located at bus #15) and 25 kW h (ESS located at

bus #16). Naturally, the reduction of power losses also decreases from about 20% (ρ = 0) to about 5% (ρ = 1).

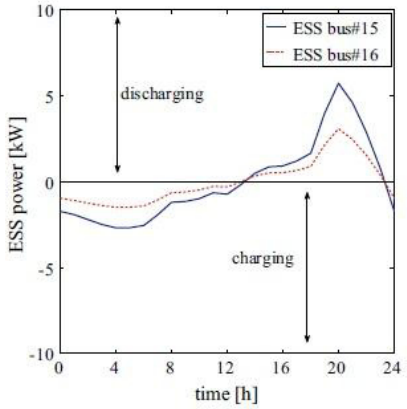

Fig. 3-11: ESSs daily charging/discharging cycle when ρ=1

By comparing Figs. 3-7 and 3-11, it appears that the shapes of the ESS power profiles are not substantially modified when the optimal rated values of power and energy decrease in the case of ρ = 1. This is because, while the optimal ESS rated capacity strictly depends on the values of ρ, the way in which the energy stored in the ESS is controlled (i.e., the ESS power profile) depends strongly on the network's characteristics and its loads and resources.

3.5 References

[1] B. Glasgo, I. Lima Azevedo, C. Hendrickson, "How much electricity can we save by using direct current circuits in homes? Understanding the potential for electricity savings and assessing feasibility of a transition towards DC powered buildings", Appl Energy 2016;180(15):66–75. http://dx.doi.org/10.1016/j.apenergy.2016.07.036.

[2] D. Antoniou, A. Tzimas S.M. Rowland, "Transition from alternating current to direct current low voltage distribution networks", IET Gener Transm Distrib 2015;9(12):1391–401. http://dx.doi.org/10.1049/iet-gtd.2014.0823.

[3] M. Fantauzzi, D. Iannuzzi, M. Pagano, A. Scalfati, M. Roscia, "Building DC microgrids: Planning of an experimental platform with power hardware in the loop features", IEEE International Conference on Renewable Energy Research and Applications, 2015. https://doi.org/10.1109/ICRERA.2015.7418659.

[4] A. Sannino, G. Postiglione, M.H.J. Bollen, "Feasibility of a DC network for commercial facilities", IEEE Trans Ind Appl 2003;39(5):1499–507. http://dx.doi.org/10.1109/TIA.2003.816517.

[5] Z. Liu, M. Li, "Research on energy efficiency of DC distribution system", AASRI procedia, vol. 7; 2014. p. 68–74. http://dx.doi.org/10.1016/j.aasri.2014.05.031.

[6] A.T. Elsayed, A.A. Mohamed, O.A. Mohammed, "DC microgrids and distribution systems: an overview", Electric Power Syst Res 2015;119:407–17. http://dx.doi.org/10.1016/j.epsr.2014.10.017.

[7] J.J. Justo, J. Mwasilu, J. Lee, J.W. Jung, "AC-microgrids versus DC-microgrids with distributed energy resources: a review", Renew Sustain Energy Rev 2013;24:387–405. http://dx.doi.org/10.1016/j.rser.2013.03.067.

[8] S. Pantano, P. May-Ostendorp, K. Dayem, "Demand DC – accelerating the adoption of DC in the home", Report in conjunction with CLASP and xergy consulting, May 2016. http://clasp.ngo/en/Resources/Resources/PublicationLibrary/2016/DemandDC (accessed on October 25, 2016).

[9] C. Keles, A. Karabiber, M. Akcin, A. Kaygusuz, B. Baykant Alagoz, O. Gul, "A smart building power management concept: smart socket applications with DC distribution", Int J Electr Power Energy Syst 2015;64:679–88. http://dx.doi.org/10.1016/j.ijepes.2014.07.075.

[10] A. Kumar Verma, B. Singh, D. Tekchand Shahani, C. Jain, "Grid-interfaced solar photovoltaic smart building with bidirectional power flow between grid and electric vehicle with improved power quality", Electr Power Components Syst 2016;44(5):480–94. http://dx.doi.org/10.1080/15325008.2015.1120818.

[11] A. Nourai, V.I. Kogan, C.M. Schafer, "Load leveling reduces T&D line losses", IEEE Trans Power Delivery 2008;23(4):2168-73. http://dx.doi.org/10.1109/TPWRD.2008.921128.

[12] M. Aneke, M. Wang, “Energy storage technologies and real life applications – a state of the art review”, Appl Energy 2016;179(1):350–77. http://dx.doi.org/10.1016/j.apenergy.2016.06.097.
[13] M. Bianchi, L. Branchini, C. Ferrari, F. Melino, “Optimal sizing of grid-independent hybrid photovoltaic–battery power systems for household sector”, Appl Energy 2014;136(31):805–16. http://dx.doi.org/10.1016/j.apenergy.2014.07.058.
[14] O. Palizban, K. Kauhaniemi, “Energy storage systems in modern grids—matrix of technologies and applications”, J Energy Storage 2016;6:248–59. http://dx.doi.org/10.1016/j.est.2016.02.001.
[15] G.L. Kyriakopoulos, G. Arabatzis, “Electrical energy storage systems in electricity generation: energy policies, innovative technologies, and regulatory regimes”, Renew Sustain Energy Rev 2016;56:1044–67. http://dx.doi.org/10.1016/j.rser.2015.12.046.
[16] X. Luo, J. Wang, M. Dooner, J. Clarke, “Overview of current development in electrical energy storage technologies and the application potential in power system operation”, Appl Energy 2015;137(1):511–36. http://dx.doi.org/10.1016/j.apenergy.2014.09.081.
[17] M. Farhadi, O. Mohammed, “Energy storage technologies for high power applications”, IEEE Trans Industry Appl, (in press) http://dx.doi.org/10.1109/TIA.2015.2511096.
[18] C. Chao, Z. Md Fadlullah, N. Kato, I. Stojmenovic, “On optimally reducing power loss in micro-grids with power storage devices”, IEEE J Selected Areas Comm 2014;32(7):1361–70. http://dx.doi.org/10.1109/JSAC.2014.2332077.
[19] A. Yu, Z. Chen, R. Maric, L. Zhang, J. Zhang, J. Yan, “Electrochemical supercapacitors for energy storage and delivery: advanced materials, technologies and applications”, Appl Energy 2015;153(1):1–2. http://dx.doi.org/10.1016/j.apenergy.2015.05.054.
[20] V. Jülch, “Comparison of electricity storage options using levelized cost of storage (LCOS) method”, Appl Energy 2016;183(1):1594–606. http://dx.doi.org/10.1016/j.apenergy.2016.08.165.

[21] B. Zakeri, S. Syri, "Electrical energy storage systems: a comparative life cycle cost analysis", Renew Sustain Energy Rev 2015;42:569–96. http://dx.doi.org/10.1016/j.rser.2014.10.011.
[22] B. Battke, T.S. Schmidt, D. Grosspietsch, V.H. Hoffmann, "A review and probabilistic model of lifecycle costs of stationary batteries in multiple applications", Renew Sustain Energy Rev 2013;25:240–50. http://dx.doi.org/10.1016/j.rser.2014.10.011.
[23] S. Sharma, S. Bhattacharjee, A. Bhattacharya, "Grey wolf optimisation for optimal sizing of battery energy storage device to minimise operation cost of microgrid", IET Gener Transm Distrib 2016;10(3):625–37. http://dx.doi.org/10.1049/iet-gtd.2015.0429.
[24] S.W. Alnaser, L.F. Ochoa, "Optimal sizing and control of energy storage in wind power-rich distribution networks", IEEE Trans Power Syst 2016;31(3):2004–13. http://dx.doi.org/10.1109/TPWRS.2015.2465181.
[25] C.J. Bennett, R.A. Stewart, J.W. Lu, "Development of a three-phase battery energy storage scheduling and operation system for low voltage distribution networks", Appl Energy 2015;146(15):122–34. http://dx.doi.org/10.1016/j.apenergy.2015.02.012.
[26] P.F. Lyons, N.S. Wade, T. Jiang, P.C. Taylor, F. Hashiesh, M. Michel, et al., "Design and analysis of electrical energy storage demonstration projects on UK distribution networks", Appl Energy 2015;137(1):677–91. http://dx.doi.org/10.1016/j.apenergy.2014.09.027.
[27] H. Khorramdel, J. Aghaei, B. Khorramdel, P. Siano, "Optimal battery sizing in microgrids using probabilistic unit commitment", IEEE Trans Ind Informatics 2016;12(2):834–43. http://dx.doi.org/10.1109/TII.2015.2509424.
[28] B. Bahmani-Firouzi, R. Azizipanah-Abarghooee, "Optimal sizing of battery energy storage for micro-grid operation management using a new improved bat algorithm", Int J Electr Power Energy Syst 2014;56:42–54. http://dx.doi.org/10.1016/j.ijepes.2013.10.019.
[29] D. Iannuzzi, F. Ciccarelli, D. Lauria, "Stationary ultracapacitors storage device for improving energy saving and voltage profile of light transportation networks", Trans Res Part C: Emerg Technol 2012;21(1):321–37. http://dx.doi.org/10.1016/j.trc.2011.11.002.

[30] G. Clemente, M. Fantauzzi, D. Lauria, "Energy savings in urban mass transit systems: a probabilistic approach for sizing electric energy storage devices", Proc. 4th int. conf. clean elect. power, Alghero, Italy. p. 610–3. http://dx.doi.org/10.1109/ICCEP.2013.6586933.

[31] M. Fantauzzi, D. Lauria, F. Mottola, A. Scalfati, "Sizing energy storage systems in DC networks: A general methodology based upon power losses minimization", Applied Energy, Volume 187, 1 February 2017, pp. 862-872, https://doi.org/10.1016/j.apenergy.2016.11.044.

[32] S. Bolognani, S. Zampieri, "On the existence and linear approximation of the power flow solution in power distribution networks", IEEE Trans Power Syst 2016;31(1):163–72. http://dx.doi.org/10.1109/TPWRS.2015.2395452.

[33] J.J. Grainger, W.D. Stevenson Jr, "Power system analysis", New York: McGraw-Hill; 1994.

[34] Electric Power Research Institute (EPRI), EPRI–DOE handbook of energy storage for transmission and distribution applications, Palo Alto, California: EPRI and U.S. Department of Energy (DOE); 2003.

[35] Sandia National Laboratories, DOE/EPRI 2013 Electricity Storage Handbook in Collaboration with NRECA, Sandia Report SAND2013-5131, Albuquerque, New Mexico 87185 and Livermore, California (US); 2013.

[36] F. Scheid, "Theory and problems of numerical analysis", schaum's outline series, 422. New York: McGraw-Hill; 1968.

[37] S. Papathanassiou, N. Hatziargyriou, K. Strunz, "A benchmark low voltage microgrid network", presented at the Cigre Symposium ''Power systems with dispersed generation: technologies, impacts on development, operation and performances," April 2005, Athens, Greece.

Chapter 4

Applications of Mixed Integer Linear Programming and Robust Optimization approaches for the optimal sizing of Distributed Energy Resources in smart microgrids

4.1 Introduction

This chapter presents some applications of mathematical programming approaches to the problem of optimally sizing, from an economic perspective, the Distributed Energy Resources included in a Microgrid, determining the optimal mix of Distributed Generators and Energy Storage Systems.

Despite the strong consensus existing among researchers and stakeholders on the variety and importance of the advantages deriving from μGs in modern electrical distribution systems, their widespread diffusion is hindered from cost considerations and from the difficulties in implementing a comprehensive cost-benefit analysis and in identifying qualified modalities for system design and management. The identification of efficient methodologies for the optimal system design is then important to allow appropriate analyses and informed choices on the opportunity and feasibility of μG realizations. An important point involved in the μG design process, which constitutes the object of this chapter, is the choice and sizing of distributed energy resources to be installed, including both Distributed Generators (DGs) and Energy Storage Systems (ESSs).

The proposed procedure is based on Mixed Integer Linear Programming and allows to determine the optimal sizes of Distributed Energy Resources which minimize the Microgrid Total Cost of

Ownership, given location and load characteristics. The opportunities of Load Management related to the presence of different quotes of controllable load are also considered and their impact on the sizing of DERs investigated.

The procedure is formulated as a quite general method that can be used for different microgrid architectures and different generation and storage technologies, although in this chapter it is applied to a grid-connected DC microgrid with PV generation and storage system.

Two variants of the sizing procedure are presented: the first uses a deterministic approach, not considering the uncertainties that affect design parameters, while the second uses a Robust Optimization approach to deal with them. In both cases, the performance of the sizing results against uncertainty can be estimated *a-posteriori* by means of Monte Carlo simulations.

Numerical applications to a case study, referring to a DC μG with PV generation, storage and a certain amount of flexible load, are reported to show the effectiveness of the proposed methodology. Various sub-cases highlight the effects of different levels of quality of forecasts for different sources of uncertainty, like PV generation and load profiles, and allow the comparison of results of the proposed methodology with those corresponding to an a-priori exclusion of DERs installation or to the lack of consideration of the possible Load Management during the design phase. In the last sub-case Monte Carlo simulations are employed to estimate the impact of uncertainties on the quality of results provided from both the deterministic and the RO approaches.

4.2 State of the art and assessment of the proposed approach

Recently, different studies on methodologies for the optimal sizing of ESSs and/or DGs in power systems and μGs have been proposed in the literature, pointing out various element of the sizing process. Studies [1-5] focus on different possible objective functions related to economic, environmental and system operational factors, sometimes resorting to multi-criteria optimization methods. Studies [6-8] draw attention to power quality and reliability perspectives, while studies

[9-11] deal with the uncertainties involved in the design process by using probabilistic techniques. Fewer studies consider the possible connection between the design stage and Smart Grid scenarios, including control of the electric load: in [12, 13] stochastic methods are employed to consider the demand uncertainty in the sizing process, while in [14] authors implement a mixed integer linear programming (MILP) model for the optimization of a hybrid renewable energy system in residential μGs considering also the demand response of available controllable appliances. A MILP formulation has also been adopted, from a control perspective, in [15] with reference to a hybrid μG, aimed at optimal one day ahead scheduling, followed by a very short-time predictive control, while in [16] the methodology has been extended to simultaneously minimize the energy costs and to compensate waveform distortions.

However, existing studies often don't guarantee an adequate representation of real conditions which affect the operation financial balance and thus the μG Total Cost of Ownership (TCO), underestimating relevant factors, e.g. the integration with smart grid scenarios like load management, the possibility to work both connected to the grid, allowing a bidirectional energy flow with correspondent costs and revenues, or in islanded mode, or even to potentially curtail sometimes non-critical loads, just to mention a few.

Compared to the above mentioned studies, the method presented here allows to properly take into account all the main factors affecting the economic impact of the μG DERs installation, including bidirectional energy flow to/from the main grid, proper consideration of the presence and effect of flexible loads in addition to the basic non-controllable load, calculation of optimal profiles for energy flows to/from the grid (purchase/sell of energy) and the ESSs (charge/discharge), possible curtailments of DGs power flows and of non-critical loads and control laws for flexible loads, bringing the following main contributions:

- integrated design approach which considers the presence of both controllable and non-controllable loads, technical and budget constraints, bidirectional energy flow to/from the grid, possible curtailment of renewable generation and non-critical load;

- development of a general procedure that might be used for sizing purposes (in parametric analyses considering different distributed generation and storage technologies and different scenarios related to costs of DER technologies and prices of energy) as well as for the μG management (i.e. one day-ahead scheduling of all energy flows to/from the grid and to/from storage devices, of potential load curtailments and of running times of flexible loads), when considering updated forecasts of non-controllable loads and of power generation from DGs and actual energy prices;
- efficient formulation of the sizing procedure as a Mixed Integer Linear Programming model, which benefits from guarantees of finite convergence to optimality and availability of efficient off-the-shelf software, and can contribute to the setting of an optimization framework suitable to deal with the various sources of uncertainty, while preserving computational solvability;
- development of an implementation of the procedure based on the Robust Optimization paradigm, which allows to easily consider different levels of uncertainty in the design phase.

4.3 Mixed Integer Linear Programming Formulation of DERs Optimal Sizing Problem

In this paragraph, the proposed methodological approach for the optimal sizing of μG DERs is presented, with reference to a DC microgrid which can include DGs, EESs, controllable and non-controllable loads and a connection to the main grid via a bidirectional AC-DC converter that allows bidirectional energy flows on the point-of-common-coupling (PCC) [17].

For the sake of brevity only one DG technology (i.e. a PV system) and only one ESS technology have been considered. The ESS is not precisely identified but merely associated with the capacity of storing energy, allowing charging and discharging energy flows between the limits imposed from minimum and maximum state of charge (SOC) and with a specified round-trip efficiency.

4.3.1 Nomenclature

Parameters:

NT	Number of considered discretization time steps in one year
NY	Years considered for life-cycle project assessments
Δt	Duration of the time-step (h)
$P_l(t)$	Load demand of non-controllable loads at time t
$P_{PV1}(t)$	Maximum generated power by 1kWp of installed PV at time t
$P_{ESS,max}$	Storage maximum charge/discharge power per kWh (kW)
N_{SL}	Number of types of shiftable loads
N_i	Number of appliances type i
N_{wi}	Number of work-cycles for shiftable load *i*
D_{wi}	Duration of each work-cycle for shiftable load *i*
P_i	Constant power of shiftable load *i*
$t_{in,i}$	Start of the time-window for shiftable load *i*
$t_{fin,i}$	End of the time-window for shiftable load *i*
PV_{acq}	PV system acquisition cost (€/kW)
$PV_{o\&m}$	PV system yearly O&M cost (€/kW)
ESS_{acq}	ESS acquisition cost (€/kWh)
$ESS_{o\&m}$	ESS yearly O&M cost (€/kWh)
$Conv_{acq}$	Converter acquisition cost (€/kW)
$Conv_{o\&m}$	Converter yearly O&M cost (€/kW)
GR_{ysc}	Grid connection yearly rent (€/kW)
$C_p(t)$	Cost of energy purchased from the grid at time t (€/kWh)
$C_s(t)$	Price of energy sold to the grid at time t (€/kWh)
C_{CU}	Cost of un-served load (€/kWh)
η_{Conv}	Bidirectional AC-DC Converter efficiency
η_r	ESS round-trip efficiency
CL_{ratio}	Ratio of critical load to total load
SoC_{min}	Minimum State of Charge of ESS
SoC_{max}	Maximum State of Charge of ESS
SoC_{in}	Initial State of Charge of ESS (at t=0)
$S_{PV,max}$	Maximum allowed size of PV system (kW)
$S_{Conv,max}$	Maximum allowed size of Bidirectional Converter (kW)
$S_{ESS,max}$	Maximum allowed size of ESS (kW)
$P_{PCC,max}$	Maximum allowed size of PCC (kW)
e	Escalation rate of grid energy price
v	Inflation rate
i	Interest rate

$Inv_{in,max}$	Maximum Initial Capital Investment (€)

Decision variables:

$P_{pg}(t)$	Power purchased from the grid at time t (kW)
$P_{sg}(t)$	Power sold to the grid at time t (kW)
$P_{ch}(t)$	Power charged to ESS at time t (kW)
$P_{dch}(t)$	Power discharged from ESS at time t (kW)
$P_{PV}(t)$	Power fed into the microgrid from the PV system at time t (kW)
$P_{CU}(t)$	Power of non critical load curtailed at time t (kW)
$W_{ESS}(t)$	Energy stored in ESS at time t (kWh)
u(t)	Status of energy flow to/from the grid (1: purchase; 0: sell)
S_{PV}	Size of PV system (kW)
S_{Conv}	Size of Bidirectional Converter (kW)
S_{ESS}	Size of ESS (kWh)
P_{PCC}	Maximum contractual power on PCC (kW)
$y_i(t)$	Number of controllable appliances type "i" running at time t
$k_i(t)$	Number of controllable appliances type "i" starting at time t

4.3.2 Objective function

The μG DERs optimal sizing problem consists in determining the optimal sizes of the bidirectional converter and of the DERs (DGs and ESSs) included in the considered μG, once all the necessary parameters are known; specifically, hourly demand profile of the basic load, PV productivity and energy prices are supposed to be known above the predefined time horizon (i.e. derived from appropriate forecasts).

The objective of the microgrid DERs optimal sizing is the minimization of the Total Cost of Ownership supported by the μG owner over a specified time horizon. With reference to the nomenclature reported in paragraph 4.3.1, the cost function to be minimized is then:

$$\begin{aligned} \mathrm{Cost} = {} & \mathrm{S_{PV}}\left(\mathrm{PV_{acq}} + \mathrm{PV_{o\&}}_{m}\mathrm{Act}\right) + \mathrm{S_{ESS}}\left(\mathrm{ESS_{acq}} + \right. \\ & \left.\mathrm{ESS_{o\&}}_{m}\mathrm{Act}\right) + \mathrm{S_{Conv}}\left(\mathrm{Conv_{acq}} + \mathrm{Conv_{o\&}}_{m}\mathrm{Act}\right) + \mathrm{P_{PCC}GR_{ysc}Act} + \\ & \sum_{\mathrm{t=1}}^{\mathrm{NT}}\left(\mathrm{C_p(t)P_{pg}(t)} - \mathrm{C_s(t)P_{sg}(t)}\right)\mathrm{Act_{en}} + \sum_{\mathrm{t=1}}^{\mathrm{NT}}\left(\mathrm{C_{CU}P_{CU}(t)}\right)\mathrm{Act} \end{aligned} \quad (1)$$

where the first three terms refer to the NPV (net present value) of the total cost of PV system, energy storage system, and bidirectional

converter respectively, the fourth term refers to the contractual cost for the grid connection on the PCC, while the fifth term refers to the sum of cost of energy purchased from the grid and profit of energy sold to the grid and the last term to the cost caused by the curtailment of some amount of non-critical load over the specified time horizon.

Costs borne year by year (i.e. O&M costs, grid connection costs and energy costs) are multiplied by suitable discount rates (Act and Acten) which consider interest rate, energy escalation rate, inflation rate, and are calculated as follows:

$$\mathrm{Act} = \sum_{y=1}^{NY} \left(\frac{1+v}{1+i}\right)^{y} \tag{2}$$

$$\mathrm{Act_{en}} = \sum_{y=1}^{NY} \left(\frac{1+e}{1+i}\right)^{y} \tag{3}$$

where v is the interest rate, i the inflation rate, e the energy escalation rate.

The decision variables of the optimization problem are listed in Section 2. Among them, scalar variables referred to sub-systems sizes (i.e.: SConv, SPV, SESS) and contractual power on the PCC (PPCC) are the answer to the μG optimal sizing problem. Other variables, which deal with the system optimal management, are calculated for each time step in the discretized planning horizon of the system (vector variables of dimension NT), and can be used for day-ahead scheduling of the various μG sub-systems.

4.3.3 Constraints

In the following the constraints that complete the optimization model are described.

4.3.3.1 Power Balance Constraint

The power balance constraint can be expressed at each time step as follows:

$$\eta_{\mathrm{Conv}} P_{\mathrm{pg}}(t) + P_{\mathrm{PV}}(t) + P_{\mathrm{dch}}(t) = \tag{4}$$

$$\left(\frac{1}{\eta_{Conv}}\right)P_{sg}(t)+P_{ch}(t)+P_{l}(t)+\sum_{i=1}^{N_{SL}}(y_i(t)P_i)-P_{cu}(t)$$

where the terms at the LHS refer, respectively, to powers imported from the grid, produced from the PV system and discharged from the ESS, while those at the RHS refer to powers sold to the grid, charged to the ESS, supplied to base load and to smart loads and finally to the curtailed load.

4.3.3.2 Constraints on power produced from the DGs

The power PPV(t) extracted from the PV system at each time step is always not greater than the specific productivity at the same time t multiplied by the size of the PV system:

$$P_{PV}(t)\leq S_{PV}P_{PV1}(t) \quad (5)$$

4.3.3.3 Constraints on charging and discharging power of ESSs

At each time step the power of the ESS must be in the allowed range limited by the ESS capacity (SESS) and the parameter PESS,max (ESS maximum charge/discharge power per kWh):

$$P_{ch}(t)\leq P_{ESS,max}S_{ESS} \quad (6)$$

$$P_{dch}(t)\leq P_{ESS,max}S_{ESS} \quad (7)$$

4.3.3.4 Constraints on energy stored in ESSs

The following constraints are related to the energy stored in the ESS at each time step:

$$W_{ESS}(1)=SoC_{in}S_{ESS}+\left(\eta_r P_{ch}(1)-P_{dch}(1)\right)\Delta t \quad (8)$$

$$W_{ESS}(t)=W_{ESS}(t-1)+\left(\eta_r P_{ch}(t)-P_{dch}(t)\right)\Delta t \quad (9)$$

$$W_{ESS}(t)\geq SoC_{min}S_{ESS} \quad (10)$$

$$W_{ESS}(t)\leq SoC_{max}S_{ESS} \quad (11)$$

Equations (8) and (9) calculate the level of energy stored in the ESS at each time t based on the level of energy of the preceding time-step and on the power used to charge or discharge the ESS. Inequalities (10) and (11) force the level of energy in the ESS at each time t to respect limits based on predefined min and max SoC.

4.3.3.5 Constraints on size of sub-systems

The size of individual sub-systems can be limited due to different causes, like restrictions in available space or various regulatory, technical or physical constraints, other than for financial reasons that will be addressed later.

A set of inequalities is then used to express these limits:

$$S_{PV} \leq S_{PV,max} \tag{12}$$

$$S_{Conv} \leq S_{Conv,max} \tag{13}$$

$$S_{ESS} \leq S_{ESS,max} \tag{14}$$

$$P_{PCC} \leq P_{PCC,max} \tag{15}$$

4.3.3.6 Constraints on power exchanged with the grid

The power exchanged with the grid in both input and output directions at each time step has to abide by constraints pertinent to the bidirectional converter size (i.e. nominal power in kW) and to the contractual power on the PCC:

$$P_{pg}(t) \leq \mathrm{Min}(S_{Conv,p}(t), P_{PCC}) \tag{16}$$

$$P_{sg}(t) \leq \mathrm{Min}(S_{Conv,s}(t), P_{PCC}) \tag{17}$$

Inequalities (16) and (17) make use of auxiliary variables $S_{Conv,p}(t)$ and $S_{Conv,s}(t)$ that, starting from the value of S_{Conv} and making use also of the binary variable u(t), were modeled in such a way to prevent $P_{pg}(t)$ and $P_{sg}(t)$ to be simultaneously different from zero (see Appendix C), i.e. to prevent solutions where energy is sold to the grid and bought from the grid at the same time, which is physically impossible on a single PCC.

4.3.3.7 Constraints on controllable loads

The following set of equalities and inequalities is used to model the mode of operation and the scheduling of controllable loads, which have to complete each day a given number of working cycles of given duration throughout fixed time windows:

$$\sum_{t=t_{in,i}}^{t_{fin,i}} y_i(t) = N_i Nw_i Dw_i \quad (18)$$

$$\sum_{t=t_{in,i}}^{t_{fin,i}-Dw_i} k_i(t) = N_i Nw_i \quad (19)$$

$$y_i(t_{in,i}) = k_i(t_{in,i}) \quad (20)$$

$$y_i(t) = y_i(t-1) + k_i(t) \quad (21)$$

for all t in (tin,i+1.. tin,i+ Dwi-1),

$$y_i(t) = y_i(t-1) + k_i(t) - k_i(t-Dw_i) \quad (22)$$

for all t in (tin,i+Dwi .. tfin,i),

$$y_i(t) \leq N_i \quad (23)$$

for all t in (tin,i .. tfin,i).

Equations (18)-(23) have to be implemented for each day of the considered time horizon and for all i in (1 .. N_{SL}). The integer variable $y_i(t)$ represent the number of appliances of type i running at time t, whereas the integer variable $k_i(t)$ represent the number of appliances of type i starting at time t.

Equation (18) guarantees that all the appliances complete their working-cycles in the time horizon of the prefixed shifting window. Equation (19) guarantees that all the appliances start their working-cycles in the time horizon of the prefixed shifting window. Equations (20)-(22) state the balance of working appliances at each time-slot t, while equation (23) limits the number of appliances of type i working in each time-slot with respect to the total number of type-i appliances.

4.3.3.8 Constraints on load curtailment

The load potentially not served at each time step t must always be limited by the proportion of critical load (which, by definition, cannot be curtailed):

$$P_{CU}(t) \leq (1 - CL_{ratio})P_l(t) \quad (24)$$

According to (24), the curtailable load is the proportion of non-controllable load which is considered not critical.

4.3.3.9 Constraints on initial investment cost

The following inequality guarantees that the initial acquisition cost for DERs and bidirectional Converter is not bigger than the fixed maximum capital available for investment:

$$S_{PV}PV_{acq} + S_{ESS}ESS_{acq} + S_{Conv}Conv_{acq} \leq Inv_{in,max} \quad (25)$$

4.4 Scenario Based Robust Formulation of the Microgrid DERs Optimal Sizing Problem

This Section presents a straightforward scenario based Robust Optimization (RO) variant of the optimal sizing procedure described in Section 4.3; in Section 4.5, results of the two approaches (i.e. deterministic and robust) will be compared with reference to a case study.

As is well known, RO is a viable optimization technique when uncertainty in the input data can be bounded within a well described region, and focuses on finding a solution that is always feasible when uncertain quantities take values within that region and optimal with respect to the worst case of all their admissible realizations [18].

Among different bounding techniques of the uncertainty set (i.e. the region in which uncertain quantities can take values), scenarios are an efficient way of characterizing robust optimization problems when historical realizations of the uncertain quantities are available. Under these circumstances, one can impose that one or more constraints are satisfied for each record of the uncertain quantities in the database of historical data, looking for robustness against them.

4.4.1 Modifications of the MILP formulation to achieve scenario-based robustness against load variations

In the following, scenario based robustness against variations of the non-controllable load Pl(t) will be considered. We assume to know

hourly realizations of the non-controllable load Pl(t) for a certain number of years in the past, and intend to achieve robustness of sizing results against realizations of the non-controllable load within this historical database.

To characterize the uncertainty of the power demand from electrical loads, we introduce the uncertain variable UD(t), which represent the possible deviation of the actual non-controllable load at time t, say $Pl_{act}(t)$, from its forecasted value Pl(t), and, following the rules of the scenario based approach, can take values in the set of all available past realizations of $Pl_{act}(t)$-Pl(t).

That being said, in the formulation of the optimal sizing problem (1)-(25), the power balance constraint (4) must be reformulated as follow:

$$\begin{aligned} &P_l(t) + UD(t) \leq \eta_{Conv} P_{pg}(t) + P_{PV}(t) + P_{dch}(t) + \\ &- \left(\frac{1}{\eta_{Conv}}\right) P_{sg}(t) - P_{ch}(t) - \sum_{i=1}^{N_{SL}} (y_i(t) P_i) + P_{cu}(t) \end{aligned} \tag{4'}$$

No other relation of the original formulation needs to be modified, if only uncertainties on the demand from non-controllable loads are considered, and we don't want to modify the constraint (24) on the maximum amount of curtailable load. It's worth noting that, while the variable Pl(t) is not used in the formulation of the objective function (1), it equally affects its value through the constraints.

4.5 Numerical applications

4.5.1 Case Study

In this section, the proposed μG DERs optimal sizing procedure is applied to the DC μG shown in Figure 4-1, which includes a DC bus connected to the main grid on the PCC via a bidirectional converter, non-controllable and controllable loads, a PV system and an ESS.

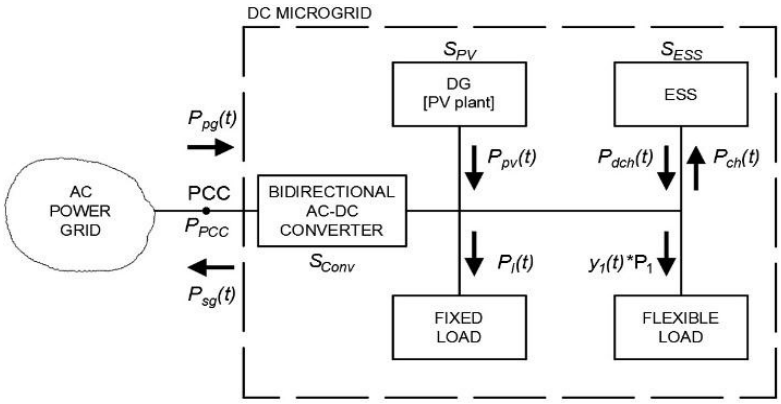

Fig. 4-1: Considered DC Microgrid

4.5.2 Input data

4.5.2.1 Parameters Values

Table 4-1 reports values for the general parameters involved in the MILP model, while Table 4-2 reports values for the cost parameters.

Table 4-1: General parameters

Parameter	Value	Parameter	Value
NT	8760	η_{Conv}	0.93
NY	25	η_r	0.86
Δt	1 h	SoC_{min}	0.2
$P_{ESS,max}$	0,5 kW/kWh	SOC_{max}	0.95
N_{SL}	1	SoC_{in}	0.5
		$S_{PV,max}$,	
N_1	10	$S_{Conv,max}$, $P_{PCC,max}$	1 MW
Nw_1	2	$S_{ESS,max}$	1 MWh
Dw_1	2 h	e	0.025
P_1	5 kW	v	0.015
$t_{in,1}$	10:00	i	0.020
$t_{fin,1}$	23:00		

Table 4-2: Cost parameters

Parameter	Value
PV_{acq}	1.500 €/kW [19]
$PV_{o\&m}$	20 €/kW
ESS_{acq}	500 €/kWh
$ESS_{o\&m}$	10 €/kWh
INV_{acq}	500 €/kW [14]
$INV_{o\&m}$	10 €/kW
GR_{ysc}	20 €/kW
$C_p(t)$	0.120 €/kWh from 0:00 to 6:00 and from 23:00 to 24:00 0.233 €/kWh from 7:00 to 23:00 [20]
$C_s(t)$	0.039 €/kWh [21]
C_{CU}	15 €/kWh [22]
$Inv_{in,max}$	10,000,000 €

4.5.2.2 Electrical Load

The forecast of load profiles is a critical point which can strongly affect results of the design process: a better knowledge of the electrical load could allow more suitable predictions of load profiles and better results from the design process, as it can be intuitively understood and will be showed from simulation data. On the other side, in most cases there aren't sufficient available data to properly characterize the electrical load along with hourly profiles of power demand.

For the considered case study (referring to an industrial facility located near Naples), ten years of registrations of power absorption were available. The mean yearly total energy demand has amounted to 393.000 kWh and for DERs sizing purposes it has been split in two parts, one related to the non-controllable load, set to 320.000 kWh, and one related to the controllable load that, given the characteristics stated in Tab. 4-1, requires 73.000 kWh per year.

Table 4-3 reports the detail of yearly energy demands for each year from 2007 to 2016.

Table 4-3: Yearly energy demands (2007-2016)

Year	Energy demand non-controllable load (kWh)	Energy demand controllable load (kWh)	Energy demand total load (kWh)
2007	307.200	73.000	380.200
2008	332.800	73.000	405.800
2009	310.400	73.000	383.400
2010	313.600	73.000	386.600
2011	320.000	73.000	393.000
2012	307.200	73.000	380.200
2013	352.000	73.000	425.000
2014	310.400	73.000	383.400
2015	324.800	73.000	397.800
2016	321.600	73.000	394.600

From the processing of raw data, three different daily profiles of hourly power demand from non-controllable loads were derived for the typical days (i.e. working day, non-working day and day before a holiday). Data were not differentiated among various months because there was little difference in the monthly energy demands.

A fourth hourly profile of power demand has been calculated, in order to consider situations where detailed information on the μG load is unavailable: an "average day" profile has then been derived from data provided by the Italian Transmission System Operator (TSO), related to the whole power demand on the national grid, that are publicly available via the website of the European Network of Transmission System Operators for Electricity [23].

Figure 4-2 shows the above described hourly profiles and points out the different patterns in power absorption between the various typical days, which are obviously disregarded when one considers only the average day.

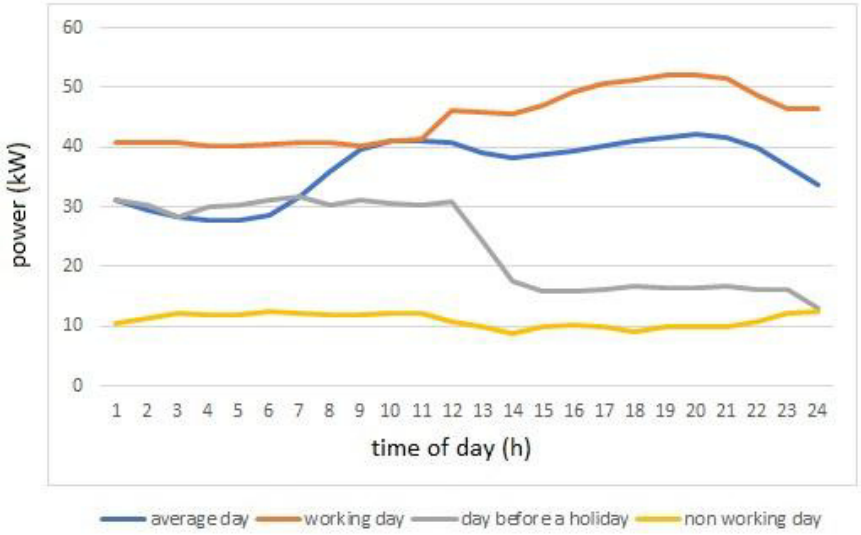

Fig. 4-2: Hourly power demand in typical days

4.5.2.3 PV Production

The hourly specific production of the PV generator has been calculated starting from data derived from the Photovoltaic Geographical Information System of the European Community, (PVGIS) [24], which provides, for a given location and for specified PV technology and modules orientation, the expected specific production along with the hourly solar irradiation of the typical day for each month.

The location of Naples (Italy) has been chosen, with crystalline silicon PV technology and the optimal inclination and orientation suggested from the PVGIS application:

- Latitude: 40°51'6" North
- Longitude: 14°16'5" East
- Inclination of modules (tilt): 34 deg.
- Orientation (azimuth) of modules: -1 deg.

The forecasted productivity (yearly specific production) for a PV system with the above listed characteristics amounts to 1464 kWh/kW.

Table 4-4 reports the average daily production data provided from PVGIS for each month.

Table 4-4: Average daily electricity production Ed (kWh/kW) from PV system

Month	Ed	Month	Ed
1	2.48	7	5.31
2	3.28	8	5.14
3	4.10	9	4.47
4	4.54	10	3.79
5	4.85	11	2.69
6	5.09	12	2.43

Figure 4-3 shows hourly production data for the average day of each month, calculated from the total daily production by scaling it proportionally to hourly irradiation levels.

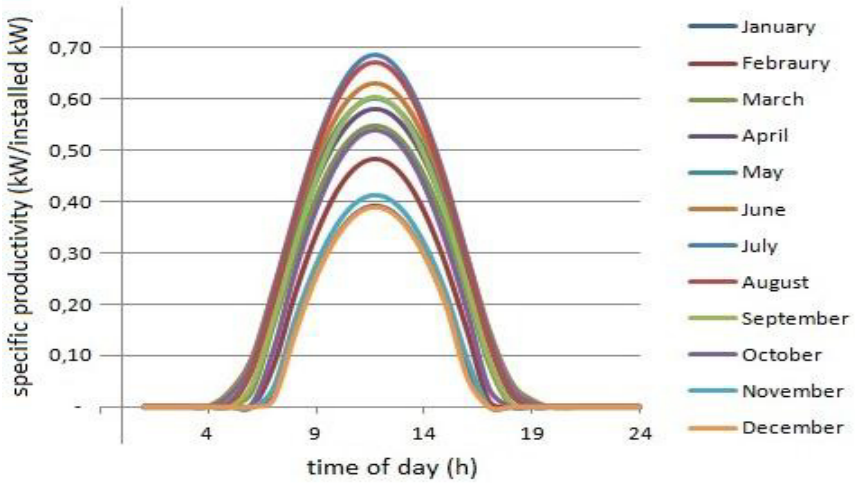

Fig. 4-3: Power produced by 1 kW of PV in the average day of each month

It shall be noted that, while the curves of Figure 4-3 seem to refer solely to clear sky conditions, they are only used in the design phase to evaluate the expected contribution of PV generation, whereas in Monte Carlo tests of par. 5.3.4 the actual power produced at each time

from the PV system is calculated altering the mean values provided by these curves by way of suitable probability distribution functions (PDFs).

4.5.3 Results

4.5.3.1 Case 1: reference case

Table 4-5 reports the results of the deterministic optimal sizing procedure that has been run two times with load profiles based on those described in paragraph 4.5.2 (case 1a: average day, case 1b: typical days).

Table 4-5: Optimal sizing results for Case 1

Item	Value Case 1a	Value Case 1b
TCO (€)	1,020,110	1,112,140
Annualized cost (€)	40,805	44,486
Contractual Power on PCC (kW)	31	44
Converter size (kW)	31	44
PV system size (kW)	249	270
ESS size (kWh)	396	446
Total Initial Cost (€)	587,000	650,000

Table 4-5 shows the effect of a less regular load evolution along the days of the week, with case 1b characterized by a TCO about 9% greater than the one of case 1a. On the other hand, the use of more pertinent load patterns commits to more robust results, as it will be shown in paragraph 4.5.3.5, then Case 1b will be used in the following as the reference case.

Table 4-6 reports the yearly energy balance for Case 1b. As expected, the algebraic sum of all input and output energy flows on the DC bus is null (considering the AC-DC converter efficiency), while the ratio between the energy related to ESS discharging and charging is equal to the assigned roundtrip efficiency of the ESS.

Table 4-6: Yearly energy balance for case 1b

Parameter	Value [kWh]
Energy used by loads	393,000
Energy produced by PV system	394,320
Energy purchased from the grid	75,619
Energy sold to the grid	49,692
Energy for ESS charging	130,088
Energy from ESS discharging	111,876
Energy not supplied to loads (load curtailment)	0

Results from Table 4-6 also show that no load curtailment has been operated (then it has been proved to be uneconomical, at least with the assigned parameter values) and that the renewable generator (i.e. the PV system) fulfils the large majority of the μG energy demand, as less than 20% of it is purchased from the grid.

Figure 4-4 shows power profiles of the main microgrid sub-systems during three consecutive typical days (i.e. from Friday to Sunday) for case 1b. Continuous lines represent power output from the DC bus, dashed lines represent power input to the DC bus.

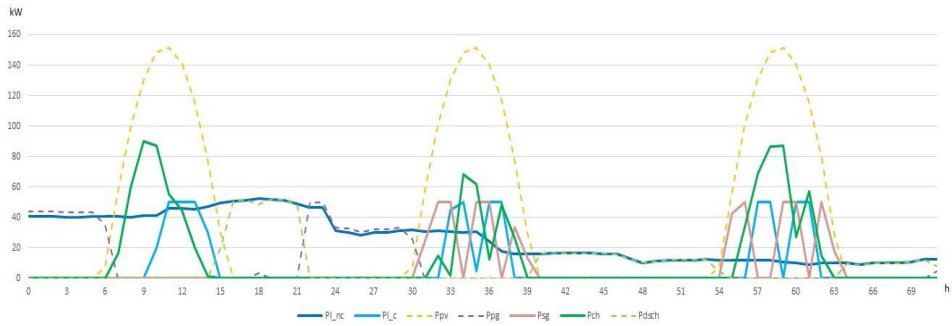

Figure 4-4. Power profiles of main microgrid sub-systems

It is worth noting that in the daylight hours the power produced from the PV system (Ppv) is used to feed both controllable (Pl_c) and non-controllable (Pl_nc) loads while charging the ESS (Pch) and selling the excess power to the grid (Psg), whereas when there is no PV production the load is fed by power bought from the grid in hours of low energy price and obtained from the discharging of the ESS in

hours of high energy price. It is then demonstrated that the described optimization procedure produces a proper dispatching of the various μG sub-systems.

4.5.3.2 Case 2: a priori exclusion of DERs installation

The deterministic optimal sizing procedure is repeated three times, with reference to the same μG and the same load and PV power profiles of Case 1b, but imposing respectively the absence of the PV System (Case 2a), of the Energy Storage System (Case 2b) and of both of them (Case 2c). Table 4-7 reports the results of Case 2 and the comparison with those of Case 1b.

Table 4-7. Optimal sizing results for Case 2

Item	Value Case 2a	Value Case 2b	Value Case 2c	Value Case 1b
TCO (€)	2,370,850	1,338,080	2,383,160	1,112,140
Annualized cost (€)	94,834	53,524	95,326	44,486
PCC Contractual Power (kW)	61	56	72	44
Converter size (kW)	61	56	72	44
PV system size (kW)	0	187	0	270
ESS size (kWh)	144	0	0	446
Total Initial Cost (€)	102,500	308,500	36,000	650,000

The comparison of results from cases 1 and 2 clearly shows the advantage deriving from increasing degrees of freedom in the planning phase: indeed, the installation of optimally sized DERs causes a greater initial cost (i.e. the cost of acquisition of PV system, ESS and bidirectional converter), but enlarges the possibilities of supplying the load, allowing a better energy management during the μG operation and finally the reduction of its TCO.

4.5.3.3 Case 3: no control of smart loads

In Case 3 the deterministic optimal sizing procedure has been applied as in Case 1b, except because there is no control of smart loads. The total yearly energy demand has been maintained equal to that of Case 1b through an appropriate increase of the non-controllable load, preserving the hourly profiles of the typical days.

Table 4-8 reports the results of Case 3 and the comparison with those of Case 1b.

Table 4-8. Optimal sizing results for Case 3.

Item	Value Case 3	Value Case 1b
TCO (€)	1,257,410	1,112,140
Annualized cost (€)	50,296	44,486
PCC Contractual Power (kW)	54	44
Converter size (kW)	54	44
PV system size (kW)	270	270
ESS size (kWh)	560	446
Total Initial Cost (€)	712,000	650,000

Results show the advantage brought by the optimal management of the flexible loads: the reduction of costs with proper control of flexible loads is around 13%; an increased percentage of the controllable load (that in the selected case study represent a few less than 20% of the total demand) would most likely allow more significant savings, as well as the eventual opportunity to activate part of the controllable load in off-peak hours.

It's worth noting that, if the optimization procedure is run again, allowing the optimal control of flexible loads but with DERs sizes fixed at values calculated in Case 3, the resulting TCO amounts to € 1,170,550, which is only 5% bigger that the one of Case 1b. The advantage of considering the chance to optimally manage the flexible loads already from the sizing phase seems then to be confirmed but could be further investigated and quantified.

4.5.3.4 Case 4: sensitivity analyses

This paragraph presents results of sensitivity analyses implemented to highlight the effect of variations of diverse input data on the overall results of the optimal sizing procedure. The aim is to identify the parameters whose variation mainly affects the results of the optimization procedure, both in terms of DERs sizing and of economic system performance achievable with DERs sizes fixed to nominal values.

Sensitivity analyses have been implemented against variation of the following parameters:

- PV / ESS / Converter acquisition cost (PVaq / ESSaq / CONVaq);
- cost of energy purchased from the grid (Cp);
- solar irradiation (PVirr), which affects the PV specific productivity;
- global demand of non-controllable and controllable loads (PLoad).

Each of the above mentioned parameters has been independently varied between -50% and +50% of the nominal value used in Case 1b, and the optimization procedure has been run two times, the first one to calculate the correspondent optimal DERs sizes and annualized TCOs (ATCO), the second one with DERs sizes fixed to the values calculated in Case 1b and allowing only the optimal management of the system to derive the correspondent annualized TCO (ATCO'). Tables 4-9a – 4-9f and Figures 4-5a – 4-5f, 4-6a – 4-6f show results of the sensitivity analyses in terms of optimal DERs sizes and ATCOs.

Table 4-9a:Variation of Optimal DERs Sizes and ATCOs against PVaq

		SESS [kW]	*SCONV [kW]*	*SPV [kW]*	*ATCO*	*ATCO'*
PVaq	*-50%*	489	44	335	€ 36.001	€ 36.390
	-40%	495	44	300	€ 37.970	€ 38.010
	-30%	474	44	278	€ 39.703	€ 39.630
	-20%	447	44	275	€ 41.231	€ 41.250
	-10%	448	44	270	€ 42.910	€ 42.870
	0%	446	44	269	€ 44.486	€ 44.490
	10%	483	43	272	€ 46.414	€ 46.110
	20%	481	43	269	€ 48.074	€ 47.730
	30%	457	44	264	€ 49.490	€ 49.350
	40%	479	43	263	€ 51.237	€ 50.970
	50%	479	43	263	€ 52.815	€ 52.590
	Var%[4]	11%	3%	27%	38%	36%

[4] Var% = (Max-Min)/Nom, with reference to maximum, minimum and nominal values of each column, where the nominal value is that of the reference Case 1b

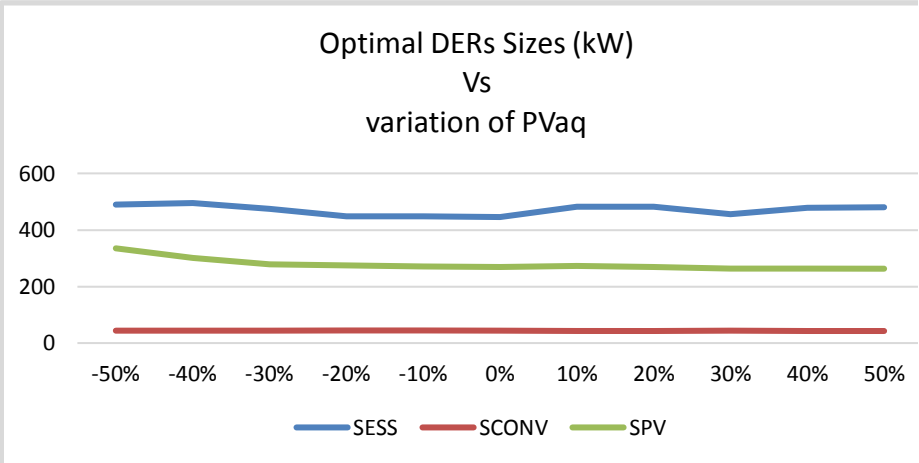

Figure 4-5a: Variation of Optimal DERs Sizes (kW) against PVaq

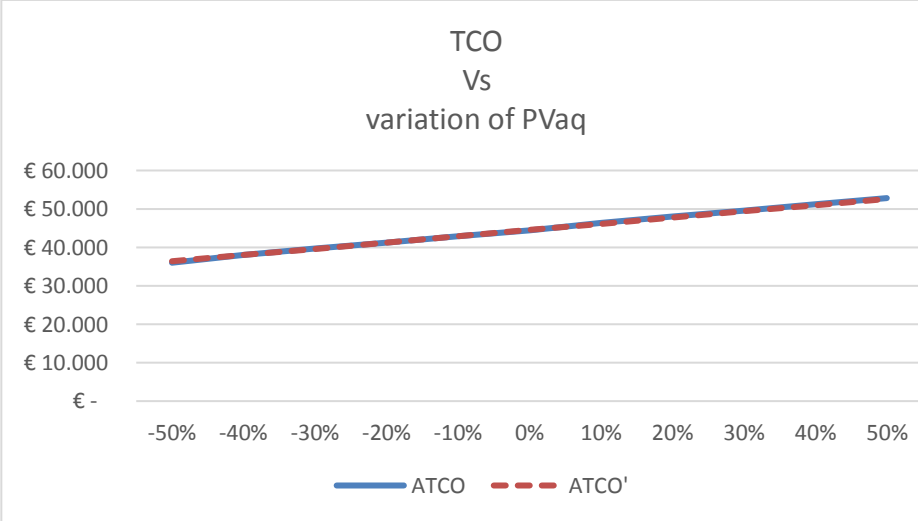

Figure 4-6a: Variation of annualized TCOs against PVaq

Table 4-9b: Variation of Optimal DERs Sizes and ATCOs against ESSaq

		SESS [kW]	SCONV [kW]	SPV [kW]	ATCO	ATCO'
ESSaq	-50%	568	35	296	€ 39.951	€ 40.030
	-40%	495	43	281	€ 40.855	€ 40.922
	-30%	476	43	272	€ 41.918	€ 41.814
	-20%	460	43	273	€ 42.699	€ 42.706
	-10%	448	44	271	€ 43.603	€ 43.598
	0%	446	44	269	€ 44.486	€ 44.490
	10%	456	44	267	€ 45.561	€ 45.382
	20%	456	44	267	€ 46.465	€ 46.274
	30%	456	44	267	€ 47.371	€ 47.166
	40%	456	44	268	€ 48.245	€ 48.058
	50%	435	44	266	€ 48.980	€ 48.950
	Var%	30%	20%	11%	20%	20%

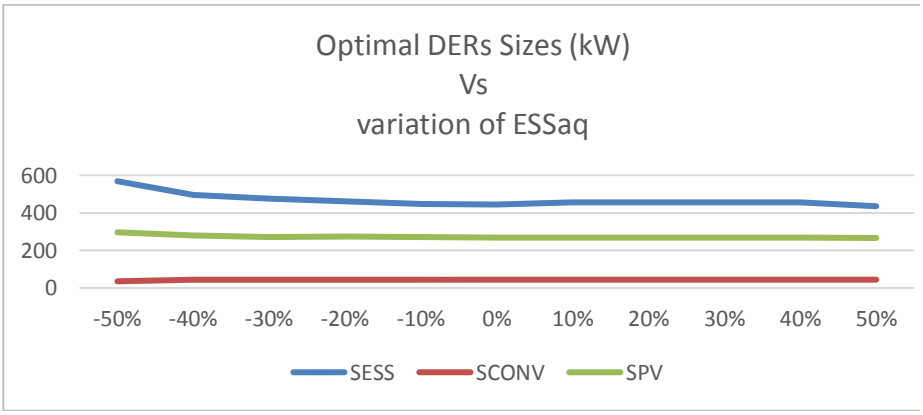

Figure 4-5b: Variation of Optimal DERs Sizes (kW) against ESSaq

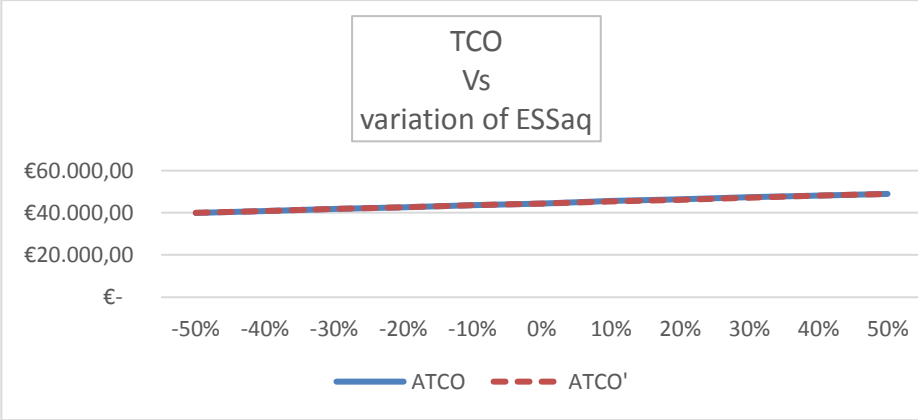

Figure 4-6b: Variation of Annualized TCOs against ESSaq

Table 4-9c: Variation of Optimal DERs Sizes and ATCOs against CONVaq

		SESS [kW]	*SCONV [kW]*	*SPV [kW]*	*ATCO*	*ATCO'*
CONVaq	*-50%*	469	44	270	€ 44.268	€ 44.050
	-40%	456	44	267	€ 44.305	€ 44.138
	-30%	475	44	272	€ 44.467	€ 44.226
	-20%	469	43	270	€ 44.528	€ 44.314
	-10%	469	43	270	€ 44.597	€ 44.402
	0%	446	44	269	€ 44.486	€ 44.490
	10%	452	43	270	€ 44.640	€ 44.578
	20%	446	44	269	€ 44.677	€ 44.666
	30%	446	44	269	€ 44.763	€ 44.754
	40%	446	44	270	€ 44.842	€ 44.842
	50%	446	44	271	€ 44.933	€ 44.930
	Var%	7%	1%	2%	1%	2%

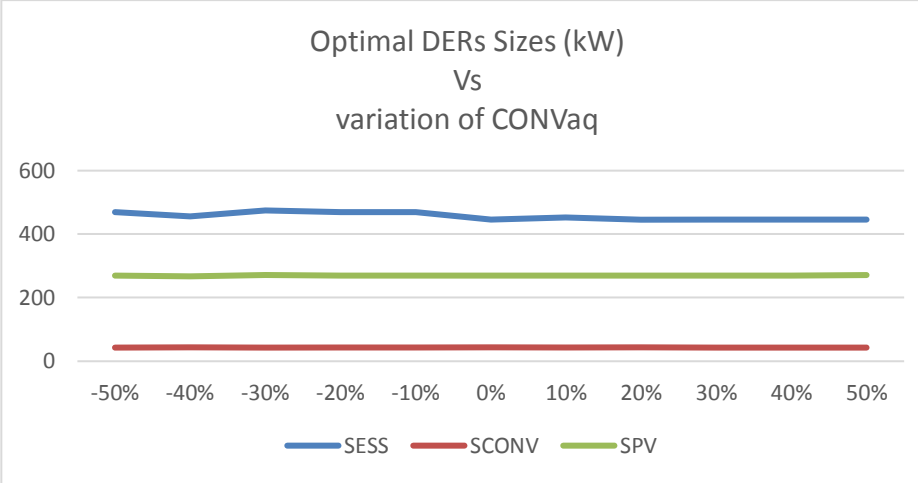

Figure 4-5c: Variation of Optimal DERs Sizes (kW) against CONVaq

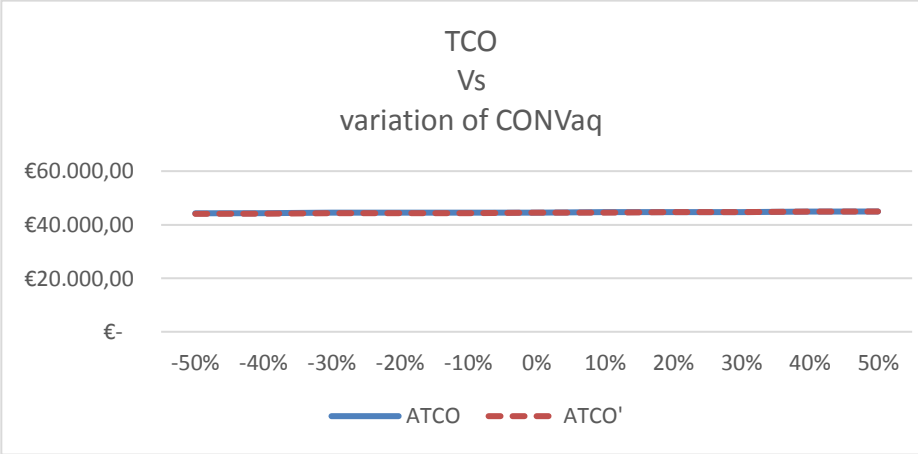

Figure 4-6c: Variation of Annualized TCOs against CONVaq

Table 4-9d: Variation of Optimal DERs Sizes and ATCOs against Cp

		SESS [kW]	*SCONV [kW]*	*SPV [kW]*	*ATCO*	*ATCO'*
Cp	*-50%*	51	51	169	€ 34.647	€ 40.492
	-40%	85	49	176	€ 37.996	€ 41.292
	-30%	219	44	209	€ 41.068	€ 42.092
	-20%	447	44	262	€ 43.128	€ 42.891
	-10%	456	44	267	€ 43.765	€ 43.691
	0%	446	44	269	€ 44.486	€ 44.490
	10%	465	44	276	€ 45.272	€ 45.290
	20%	476	43	281	€ 45.946	€ 46.089
	30%	536	44	291	€ 46.957	€ 46.889
	40%	603	33	312	€ 47.111	€ 47.688
	50%	659	29	325	€ 47.346	€ 48.488
	Var%	136%	49%	58%	29%	18%

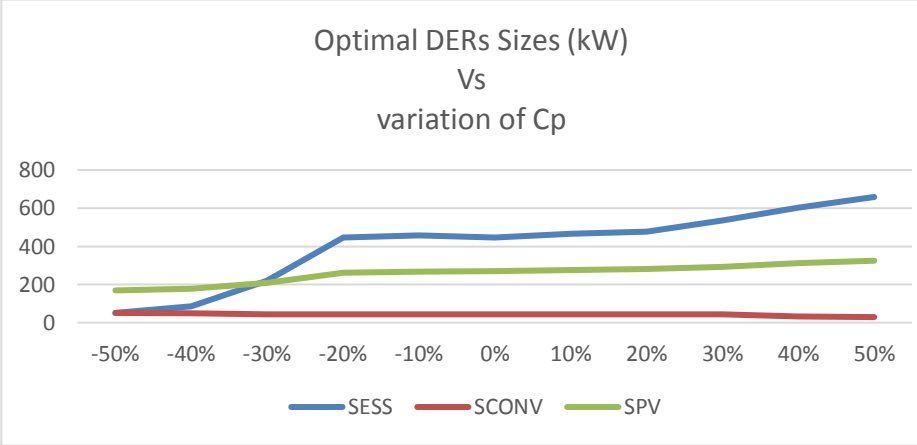

Figure 4-5d: Variation of Optimal DERs Sizes (kW) against Cp

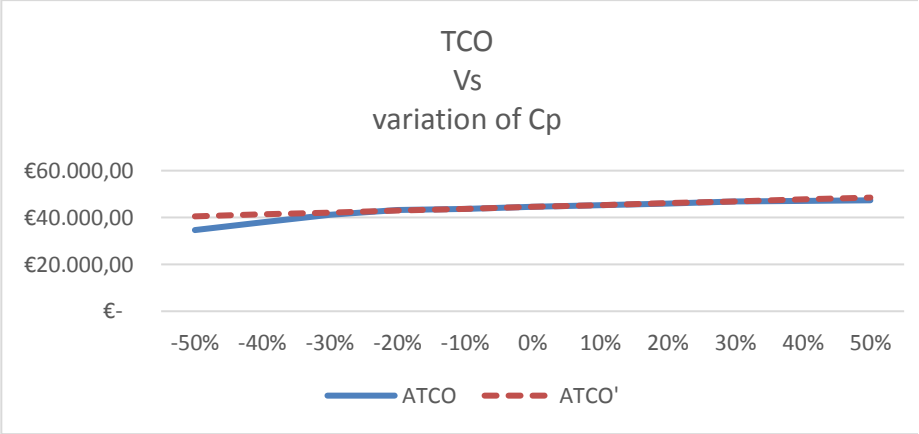

Figure 4-6d: Variation of Annualized TCOs against Cp

Table 4-9e: Variation of Optimal DERs Sizes and ATCOs against PVirr

		SESS [kW]	*SCONV [kW]*	*SPV [kW]*	*ATCO*	*ATCO'*
PVirr	*-50%*	252	50	403	€ 64.051	€ 75.848
	-40%	471	44	426	€ 58.632	€ 67.360
	-30%	454	45	369	€ 53.584	€ 60.419
	-20%	457	44	328	€ 49.910	€ 54.159
	-10%	480	44	298	€ 47.256	€ 48.012
	0%	446	44	269	€ 44.486	€ 44.490
	10%	447	44	249	€ 42.570	€ 42.843
	20%	448	44	229	€ 40.916	€ 41.417
	30%	461	44	213	€ 39.622	€ 40.201
	40%	473	44	217	€ 38.299	€ 39.377
	50%	473	44	198	€ 37.234	€ 38.961
	Var%	51%	14%	85%	60%	83%

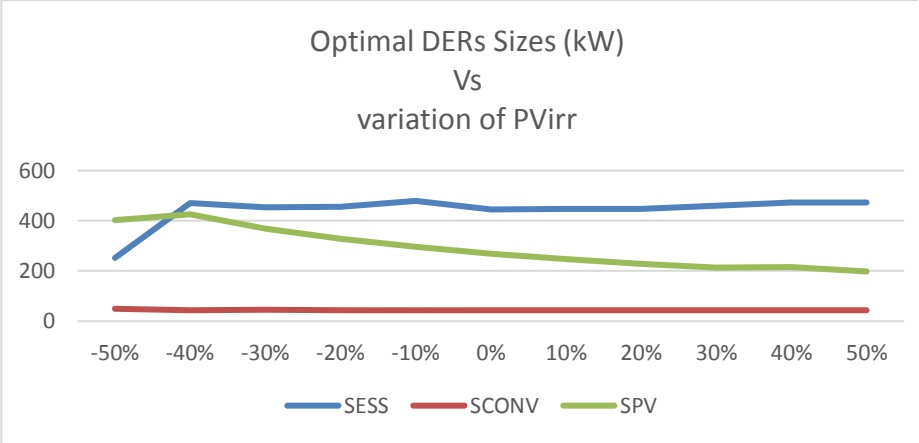

Figure 4-5e: Variation of Optimal DERs Sizes (kW) against PVirr

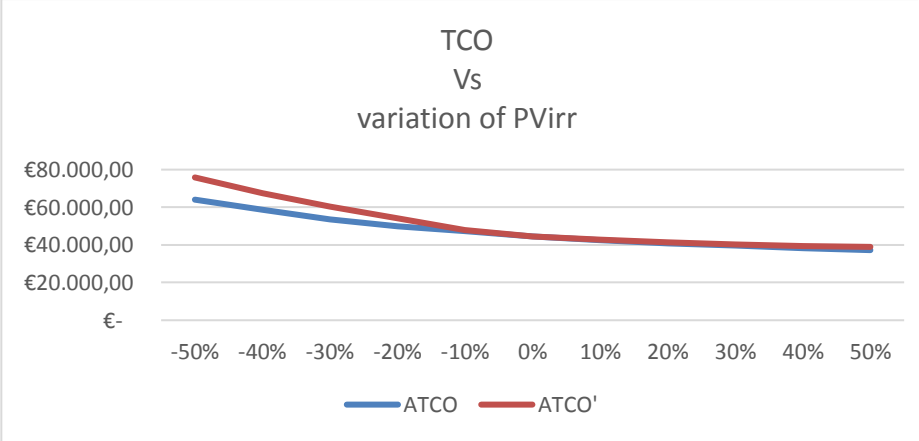

Figure 4-6e: Variation of Annualized TCOs against PVirr

Table 4-9f: Variation of Optimal DERs Sizes and ATCOs against PLoad

		SESS [kW]	SCONV [kW]	SPV [kW]	ATCO	ATCO'
PLoad	-50%	228	22	134	€ 22.323	€ 29.672
	-40%	281	26	165	€ 26.755	€ 31.678
	-30%	335	31	191	€ 31.313	€ 34.534
	-20%	358	35	215	€ 35.627	€ 37.650
	-10%	426	39	244	€ 40.259	€ 40.811
	0%	446	44	269	€ 44.486	€ 44.490
	10%	502	48	294	€ 49.112	€ 50.321
	20%	557	53	329	€ 53.487	€ 57.668
	30%	593	57	349	€ 58.010	€ 65.658
	40%	639	61	374	€ 62.502	€ 76.299
	50%	703	65	412	€ 66.888	€ 176.832
	Var%	107%	98%	103%	100%	331%

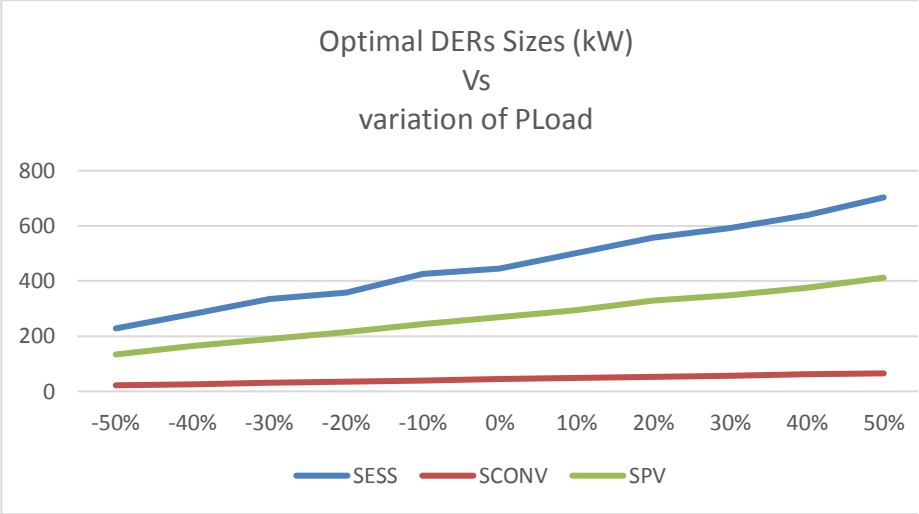

Figure 4-5f: Variation of Optimal DERs Sizes (kW) against PLoad

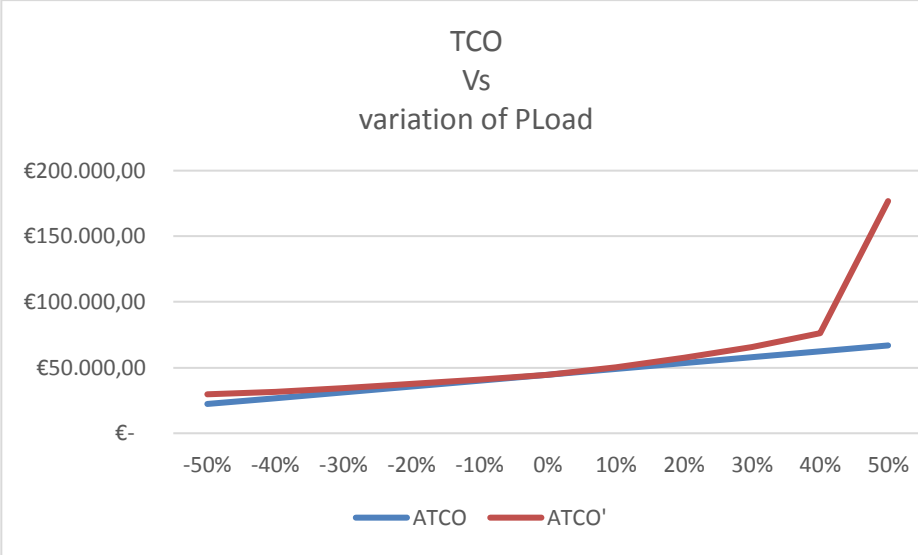

Figure 4-6f: Variation of Annualized TCOs against PLoad

By observing the results of sensitivity analyses reported in the previous tables and figures, the following considerations can be made:

- the linear variation of acquisition costs for the PV system and for the ESS produce a quasi-linear decline in the optimal size of the same DER and a quasi-linear increase in the resulting ATCOs; the difference between results in terms of ATCOs between the system with optimally sized DERs and the system with DERs fixed to values calculated in Case 1b is negligible;
- the variation of DERs sizes and ATCOs correspondent to a variation of acquisition costs for the bidirectional converter is almost negligible;
- the variation of energy costs produce a correspondent quasi-proportional increase of PV and ESS sizes and a quasi-linear decline of the bidirectional converter size; indeed, if the cost of energy is low it can be convenient to purchase it from the grid rather than produce and store it locally, while the opposite is true if the cost of energy is high;
- variations of solar irradiation and of electrical loads global energy demand produce the strongest variations in optimal DERs sizes and ATCOs, and non-negligible differences

between ATCOs correspondent to DERs optimally sized and DERs fixed to values calculated in Case 1b[5]; therefore, those parameters are strong candidates to be further investigated in their effects on the optimal sizing procedure.

4.5.3.5 Case 5: Monte Carlo tests on the deterministic sizing

In this paragraph, the Monte Carlo method is applied to verify the results of the deterministic sizing procedure against the uncertainties affecting the input data of the optimization problem (specifically, among the various uncertain parameters, only deviations of hourly load and solar radiation against the expected values considered in the design phase have been considered).

The Monte Carlo method is applied considering Gaussian probability distribution functions (PDFs) both for the non-controllable load and for the solar radiation. For each instance, values extracted from the above-mentioned PDFs are used to modify the profiles of non-controllable load and of PV system productivity, then the optimization model is solved using these modified profiles and maintaining the sizes of the bidirectional converter, the PV system and the ESS found in cases 1a and 1b, thus allowing only the optimal management of the μG, with deterministically sized DERs.

Figure 4-7 shows the overlapping of load profiles of typical days (used as the basis for the optimal sizing) with those corresponding to the first instance of Monte Carlo simulations.

[5] The dramatic increase of ATCO reported in table 4-9f for the case with +50% variation of global energy demand from loads and DERs sized as in Case 1b is due to the fact that these DERs sizes don't allow to fulfill the increased energy demand and then a large amount of electrical load is curtailed, resulting in a very high cost for unserved load.

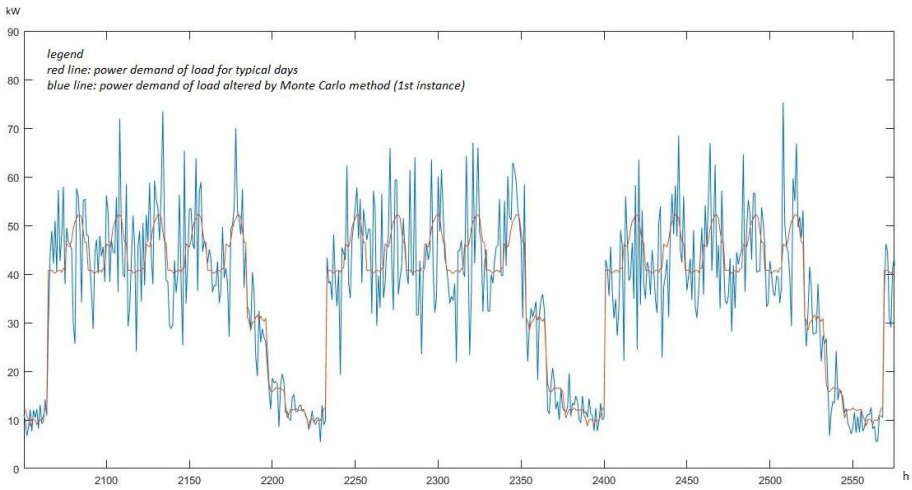

Figure 4-7: Typical days load profiles Vs Monte Carlo modified load profiles (1st instance)

Table 4-10 reports results of Monte Carlo simulations based on modifications of load profiles described in paragraph 4.5.2.2 for the typical working day, non-working day and day before a holiday, for the following subcases:

- Case 5a: DERs sized as in case 1a (based on the average day), standard deviations of the Gaussian PDFs set at 10%,
- Case 5b: same as case 5a except for DERs sized as in case 1b (based on typical days),
- Case 5c: same as case 5b except for standard deviations of the Gaussian PDFs set at 20%,
- Case 5d: same as case 5c except for total energy demand from non-controllable loads increased by 20%.

Monte Carlo simulations have been implemented, for each sub-case, with size of 100 samples for each instance, obtaining standard deviations in resulting TCOs lesser than 1% of the mean value[6].

[6] Monte Carlo tests with size of 1000 samples for instance showed no significative improvements regarding the stability of results in terms of standard deviations of the calculated TCOs

Table 4-10: TCOs for Case 5 and comparison with previous cases

Case	TCO (€)
Case 5a (sizing based on average day, σ=0.10)	
mean	1,175,800
ratio to TCO of case 1a (€ 1,020,110)	+15.3%
Case 5b (sizing based on typical days, σ=0.10)	
mean	1,120,066
ratio to TCO of case 1b (€ 1,059,380)	+0.7%
Case 5c (sizing based on typical days, σ=0.20)	
mean	1,136,671
ratio to TCO of case 1b (€ 1,059,380)	+2.2%
Case 5d (sizing based on typical days, σ=0.20, load x1.2)	
mean	1,417,342
ratio to TCO of case 1b (€ 1,059,380)	+27.4%

Table 4-10 highlights the dependency of the optimization results from the accuracy of load profiles used as input data.

Results show that the sizing based on load profiles of typical days performs quite well, even considering increasing uncertainty levels, with resulting TCOs not far from that of the corresponding optimal deterministic sizing (cases 5b and 5c), and seems to be sufficiently resilient also again an unpredicted increase of the total demand (case 5d), while the sizing based on less sophisticated input data is not equally efficient (case 5a).

It is then confirmed that the availability of suitable predictions of load power profiles is a key factor to achieve best results from the optimal sizing process. However, the comparison of tables 4-7 and 4-10 demonstrates that the optimal sizing procedure, also when based on less sophisticated input data, brings to economic results much better than those produced from an a priori exclusion of the DERs installation.

4.5.3.6 Case 6: scenario based Robust Optimization against load uncertainties

In this paragraph, the scenario based RO sizing procedure described in paragraph 4.4 is applied to the case study.

In order to study the effect of different degrees of uncertainty, 5 series of 10 years of hourly demands from the non-controllable load have been artificially created starting from the typical days of Case 1b, by adding to each value of Pl(t) a quantity determined by the multiplication of a random number (with values in the interval [0,1]) and an "uncertainty level" ul (with values in {0, 10%, 20%, 30%, 40%} for cases 6a-6e). Finally, the real historical values derived from the available registrations of power demand were considered for the non-controllable load (case 6f).

Tables 4-11 reports the results of the scenario based RO sizing procedure, described in paragraph 4.4, applied to the case study on the basis of the above-mentioned modalities.

Table 4-11: Optimal sizing results for Case 6

	Case 6a	**Case 6b**	**Case 6c**	**Case 6d**	**Case 6e**	**Case 6f**
Uncertainty level (ul)	**0**	**10%**	**20%**	**30%**	**40%**	**n.a.**
Converter size (kW)	44	48	52	56	60	64
PV system size (kW)	270	290	310	330	350	361
ESS size (kWh)	446	489	527	569	610	616
Total Initial Cost (€)	650,000	703,500	754,500	807,500	860,000	881,500
	100%	*108%*	*116%*	*124%*	*132%*	*136%*

The Total Initial Cost refers, as usual, to the sum of acquisition costs of the bidirectional converter, the PV system and the ESS, and its evolution along with the uncertainty level shows the correspondently increasing "price of robustness". On the other hand, the bigger sizes of DERs calculated with the RO approach for each different uncertainty level allow the reduction of operation costs, thanks to more energy produced by the PV system and more flexibility in storing and exchanging electric energy with the grid.

It's worth noting that DERs sizes pretty similar to those of Table 4-11 (generally a bit larger) can be obtained by adopting the deterministic formulation of the optimal sizing procedure, if each hourly value of the non-controllable load Pl(t) is incremented by percentages equal to the uncertainty levels considered in case 6.

To investigate the overall effect of bigger initial costs and reduced operating costs, a new round of Monte Carlo simulations has been implemented, testing all the sizings reported in Table 4-11 against variations of PV productivity and load profiles, obtained from Gaussian PDFs with standard deviations set at 20%, as in Case 5c, per different levels of increase of the total energy demand from non-controllable loads (i.e. load scaling factor, *lsf*).

Table 4-12 reports results of Monte Carlo simulations (again implemented with size of 100 samples for each instance) in terms of mean TCOs. In correspondence with each level of *lsf*, the minimum of the mean TCOs for sub-cases 6a-6f is highlighted. Moreover, for each value of mean TCO, two percent values are listed for comparative purposes: the first one is to be read on a "per row" basis and shows, for each value of *lsf*, the ratios of TCOs of all sub-cases 6a-6e to the minimum of them; the second percent value is to be read on a "per column" basis and shows, for each sub-case, the trend of increase of the TCO along with the *lsf*.

Table 4-12. Mean TCOs (€) of Monte Carlo tests with DERs optimal sizes from results of Case 6.

Load scaling factor (*lsf*)	Case 6a	Case 6b	Case 6c	Case 6d	Case 6e	Case 6f
1.0	**1,136,671** *100% - 100%*	1,137,997 *100% - 100%*	1,156,122 *102% - 100%*	1,180,254 *104% - 100%*	1,206,222 *106% - 100%*	1,218,178 *107% - 100%*
1.1	1,269,337 *102% - 113%*	1,243,602 *100% - 109%*	**1,241,253** *100% - 107%*	1,255,863 *101% - 106%*	1,279,179 *103% - 106%*	1,290,648 *104% - 106%*
1.2	1,417,342 *105% - 126%*	1,375,228 *102% - 121%*	1,349,135 *100% - 117%*	**1,343,637** *100% - 114%*	1,356,302 *101% - 112%*	1,366,568 *102% - 112%*
1.3	1,627,709 *112% - 146%*	1,525,183 *105% - 134%*	1,482,342 *102% - 128%*	1,453,466 *100% - 123%*	**1,446,997** *100% - 120%*	1,453,510 *100% - 119%*
1.4	2,523,879 *162% - 234%*	1,715,910 *110% - 151%*	1,631,221 *104% - 141%*	1,589,662 *102% - 135%*	1,561,079 *100% - 129%*	**1,557,913** *100% - 128%*

Different interesting points can be made by observing results of Case 6 in Table 4-12:

- as expected, when lsf increases, minimum values of TCO are found with increased level of uncertainty considered in the sizing phase (which implies bigger sizes of DERs);
- considering the row for lsf=1.0, the first percent values of TCOs show the effect of compensation between bigger initial costs and smaller operating costs, so that the price of robustness in terms of TCOs seems to be much less significant than it appeared in Table 4-11 (for example, the comparison of sub-cases 6e and 6a points out a ratio of TCOs equal to 106%, whereas the ratio of initial costs is 132%);
- considering the values of TCOs in each column, the second percent values have a quasi-linear trend for all sub-cases and demonstrate the positive effect of more robust sizings, which guarantee smaller ratios between lsf and the increase of TCO; there is an exception for Case 6a, where the value of TCO for lsf=1.4 show a dramatic increase, because of the inability of the under-sized bidirectional converter and DERs to fulfill the electrical demand, which causes a considerable amount of load curtailment and consequently a large cost due to the high value set for the parameter C_{CU};
- knowledges of decision theory could be applied to the results reported in Table 4-12 to help a decision maker in the choice among various sizing alternatives, for example by attributing a probability to each value of lsf and then calculating different indices like the expected value of the mean TCO or suitable regret functions.

4.5.4 Software used and computational effort

The MILP formulation of the sizing problem through equalities and inequalities (1)-(25) has been implemented on FICO XPress Optimization Suite®, while the setting up of input data has been implemented in Matlab®.

Each instance of the complete deterministic formulation, with Δt=1h and NT=8760, uses circa 90,000 variables, including 8,760 binary variables (i.e. u(t)) and 17,520 integer variables (i.e. y(t) and k(t)), and usually converges to an optimal solution in less than 5 min

on a Windows® based notebook with Intel Core i5® processor and 16 Gb of RAM.

4.6 References

[1] M. Alsayed, M. Cacciato, G. Scarcella, G. Scelba, "Multicriteria optimal sizing of photovoltaic-wind turbine grid connected systems", IEEE Trans. Energy Convers., 2013, 28(2), 370–379. https://doi.org/10.1109/TEC.2013.2245669.

[2] R. Rigo-Mariani, B. Sareni, X. Roboam, "Integrated optimal design of a smart microgrid with storage", IEEE Trans. Smart Grid, 2017, 8(4), 1762–1770. https://doi.org/10.1109/TSG.2015.2507131.

[3] J. Vasiljevska, J. A. P. Lopes, M. A, Matos, "Evaluating the impacts of the multi-microgrid concept using multicriteria decision aid", Electric Power Systems Research, 2012, 91, 44–51. http://dx.doi.org/10.1016/j.epsr.2012.04.013.

[4] S. Chen, H.B. Gooi, M. Wang, "Sizing of energy storage for microgrids", Proceedings of the IEEE Power & Energy Society (PES) General Meeting, San Diego, CA, USA, 22-26 July 2012. https://doi.org/10.1109/PESGM.2012.6345233.

[5] P. Karimyan, G.B. Gharehpetian, M. Abedi, A. Gavili, "Long term scheduling for optimal allocation and sizing of DG unit considering load variations and DG type", International Journal of Electrical Power & Energy Systems, 2014, 54, 277–287. http://dx.doi.org/10.1016/j.ijepes.2013.07.016.

[6] S. Bahramirad, W, Reder, A. Khodaei, "Reliability-constrained optimal sizing of energy storage system in a microgrid", IEEE Trans. Smart Grid, 2012, 3(4), 2056–2062. https://doi.org/10.1109/TSG.2012.2217991.

[7] N. Khalesi, N. Rezaei, M.R. Haghifam, "DG allocation with application of dynamic programming for loss reduction and reliability improvement", International Journal of Electrical Power & Energy Systems, 2011, 33(2), 288–295. http://dx.doi.org/10.1016/j.ijepes.2010.08.024.

[8] A. Barin, L.N. Canha, A.R. Abaide, R.Q. Machado, "Methodology for placement of Dispersed Generation Systems by

analyzing its Impacts in Distribution Networks", IEEE LatAmTrans, 2012, 10(2), 1544–1549, https://doi.org/10.1109/TLA.2012.6187598.

[9] M. Kefayat, A. Lashkar Ara, S.A. Nabavi Niaki, "A hybrid of ant colony optimization and artificial bee colony algorithm for probabilistic optimal placement and sizing of distributed energy resources", Energy Conversion and Management, 2015, 92, 149–161. http://dx.doi.org/10.1016/j.enconman.2014.12.037.

[10] A. Khodaei, S. Bahramirad, M. Shahidehpour, "Microgrid planning under uncertainty", IEEE Trans. Power Syst., 2015. https://doi.org/10.1109/TPWRS.2014.2361094.

[11] P. Dehghanian, S.H. Hosseini, M. Moeini-Aghtaie, A. Arabali, "Optimal siting of DG units in power systems from a probabilistic multi-objective optimization perspective", Electr.Power.Energy. Syst, 2013, 51, 14–26. http://dx.doi.org/10.1016/j.ijepes.2013.02.014.

[12] S. Kahrobaee, S. Asgarpoor, W. Qiao, "Optimum sizing of distributed generation and storage capacity in smart households", In Proceedings of the IEEE Power & Energy Society (PES) General Meeting, National Harbor, MD, USA, 27-31 July 2014. https://doi.org/10.1109/PESGM.2014.6939014.

[13] A. Arabali, M. Ghofrani, M. Etezadi-Amoli, M.S. Fadali, "Stochastic performance assessment and sizing for a hybrid power system of solar/wind/energy storage", IEEE Trans. Sustain. Energy, 2014, 5(2), 363–371. https://doi.org/10.1109/TSTE.2013.2288083.

[14] R. Atia, N. Yamada, "Sizing and analysis of renewable energy and battery systems in residential microgrids", IEEE Trans. Smart Grid, 2016, 7(3), 1204–1213. https://doi.org/10.1109/TSG.2016.2519541.

[15] A. Bracale, P. Caramia, G. Carpinelli, E. Mancini, F. Mottola, "Optimal control strategy of a DC micro grid", International Journal of Electrical Power & Energy Systems, 2015, 67, 25–38. http://dx.doi.org/10.1016/j.ijepes.2014.11.003.

[16] L. Alfieri, A. Bracale, P. Caramia, G. Carpinelli, "Distributed Energy Resources to Improve the Power Quality and to Reduce Energy Costs of a Hybrid AC/DC Microgrid", Chapter from the book "Development and Integration of Microgrids", InTech,

https://www.intechopen.com/books/development-and-integration-of-microgrids.

[17] A. Scalfati, D. Iannuzzi, M. Fantauzzi, M. Roscia "Optimal Sizing of Distributed Energy Resources in Smart Microgrids: a Mixed Integer Linear Programming Formulation", presented at 6th IEEE International Conference on Renewable Energy Research and Applications, 2017, San Diego.

[18] A. Ben-Tal, L. El Ghaoui, A. Nemirovski "Robust Optimization", Princeton Series in Applied Mathematics, 2009; ISBN 978-0-691-14368-2.

[19] International Energy Agency – TRENDS 2016 in Photovoltaic Applications.
Available online: http://iea-pvps.org/fileadmin/dam/public/report/national/Trends_2016_-_mr.pdf (accessed on 06 December 2017)

[20] AEEGSI – Memoria 21 Aprile 2015 174/2015/I/COM: Indagine conoscitiva sui prezzi finali dell'energia elettrica e del gas naturale.
Available online: http://www.autorita.energia.it/allegati/docs/15/174-15.pdf (accessed on 06 December 2017).

[21] GSE – Aggiornamento dei prezzi minimi garantiti per l'anno 2016.
Available online: http://www.autorita.energia.it/allegati/comunicati/160201tab.pdf (accessed on 06 December 2017).

[22] Estimating the Value of Lost Load, Briefing paper prepared for the Electric Reliability Council of Texas, Inc. by London Economics International LLC, June 17th, 2013.
Available online: http://www.ercot.com/content/gridinfo/resource/2014/mktanalysis/ERCOT_ValueofLostLoad_LiteratureReviewandMacroeconomic.pdf (accessed on 23 June 2017).

[23] European Network of Transmission System Operators for Electricity.
Available online: https://www.entsoe.eu/Pages/default.aspx (accessed on 06 December 2017).

[24] PV potential estimation utility. Available online: http://re.jrc.ec.europa.eu/pvgis/apps4/pvest.php?lang=en&map=europe (accessed on 06 December 2017).

Appendix A

Power losses in DC network, a simple analytical expression derived by application of the superposition principle

The aim of this paragraph is to derive a simple analytical expression of the power losses caused by the circulation of currents through the resistances of branch lines connecting the nodes of a DC network, depending on the nodal currents and the conductance matrix of the network.

We consider a DC network like the one described in paragraph 3.3.1 and for the sake of simplicity here we assume that the voltage on the DC bus is maintained at the constant value E fixed by the voltage source connected to the slack bus, so that devices connected to all other nodes act as current sources with a current profile proportional to the respective power profile, known for i=1...n and t (0,T).

It is worth mentioning that power losses on line resistances depend only from the currents injected in the nodes where current sources are connected, and not from the voltage level E fixed by the voltage source. To prove that, we consider figure A1, where a DC network with the above-mentioned characteristics is depicted (fig. A1a), together with the two sub-networks it can be divided into by applying the superposition principle (fig. A1b, A1c):

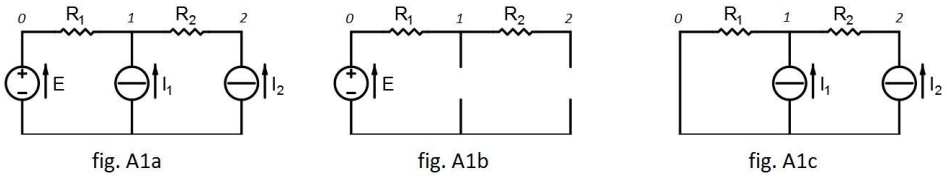

Fig. A1 - System cabling in a 4-wire cable; AC (a) and DC (b)

First consider the whole network of fig. A1a: the power losses on the network are equal to the sum of all power injections calculated for each node of the network:

$$P_{losses} = \Sigma V_i J_i = \text{ for } i=1...n+1 \quad \text{(A1)}$$

This can be expressed in a matrix form as:

$$P_{losses} = \boldsymbol{V}^T \boldsymbol{J} \quad \text{(A2)}$$

where $\boldsymbol{J}$ is the (n+1)-vector of currents injected in the network (currents exit the nodes) and $\boldsymbol{V}$ is the (n+1)-vector of potentials of these nodes compared to the reference node.

As it is well known from the node-voltage method, the following equation applies:

$$\boldsymbol{J} = \mathbf{G}\ \boldsymbol{V} \quad \text{(A3)}$$

where **G** is the (n+1)x(n+1) conductance matrix of the network, which has the following properties:

- **G** is symmetric;
- diagonal elements of **G** are positive and off-diagonal elements are negative;
- diagonal elements G_{ii} are equal to the sum of all conductances connected to node i;
- off-diagonal elements G_{ij} are sum of conductances directly connecting nodes i and j.

Unfortunately, the matrix **G** is singular, because KCL imposes that one equation in system (a3) is linear-dependent from other equations, so it is not possible to calculate power losses in terms of node currents by inverting (A3) and substituting in (A2).

Now we write again the equation for power expressed in terms of nodal currents and voltages, but considering only nodes from 1 to n (i.e. forgetting node 0, where the voltage source E is connected), and referring to the two sub-networks of figures A1b and A1c, and make the following considerations:

- first of all, the total power injected in nodes from 1 to n must equal the sum of the power exported to (or imported from) the grid, say P_{slack}, plus the power lost in line resistances, say P_{losses};

- second, while in the DC network of fig. A1b there is no circulation of current, and the voltage is equal to E in every node, for the network of fig. A1c nodal currents are the same of that circulating in the whole network of fig. A1a, and node voltages are that caused only by the circulation of those currents through network lines resistances.

Then we can write:

$$P_{slack} + P_{losses} = \boldsymbol{V}^T \boldsymbol{J} \tag{A4}$$

$$\boldsymbol{V} = \boldsymbol{V'} + \boldsymbol{V''} = \boldsymbol{E} + \boldsymbol{\Delta V} \tag{A5}$$

$$\boldsymbol{J} = \boldsymbol{J'} + \boldsymbol{J''} = \boldsymbol{0} + \boldsymbol{J} \tag{A6}$$

where $\boldsymbol{V}$ and $\boldsymbol{J}$ are now n-vectors of voltage and current of nodes from 1 to n, $\boldsymbol{V'}$, $\boldsymbol{J'}$ and $\boldsymbol{V''}$, $\boldsymbol{J''}$ refer respectively to the sub-network of fig. A1b and A1c, $\boldsymbol{E}$ and $\boldsymbol{0}$ are n-vectors with all elements respectively equal to E and 0, $\boldsymbol{\Delta V}$ is an n-vector with elements corresponding to the voltage drops caused on each node, with reference to node 0, by the circulation of currents on line resistances.

By substituting (A5) and (A6) in (A4) it follows:

$$P_{slack} + P_{losses} = \boldsymbol{V}^T \boldsymbol{J} = [\boldsymbol{E} \quad \boldsymbol{\Delta V}]^T [\boldsymbol{0} \quad \boldsymbol{J}] = \boldsymbol{E}^T\boldsymbol{J} + \boldsymbol{\Delta V}^T\boldsymbol{J} \tag{A7}$$

Now it's easy to understand that the first term corresponds to the power exchanged with the grid in the slack bus, and the second term corresponds to network power losses:

$$P_{slack} = \boldsymbol{E}^T\boldsymbol{J} \tag{A8}$$

$$P_{losses} = \boldsymbol{\Delta V}^T\boldsymbol{J} \tag{A9}$$

Now applying again the node-voltage method we have:

$$\boldsymbol{\Delta V} = \mathbf{G}^{-1} \boldsymbol{J} \tag{A10}$$

where $\mathbf{G}$ is the conductance matrix of the network in fig. A1c, that is not singular and therefore invertible.

Finally, by substituting (A10) in (A9), the total network power losses can be expressed as:

$$P_{losses} = \boldsymbol{J}^T \mathbf{R}\, \boldsymbol{J} \qquad \text{(A11)}$$

where $\boldsymbol{J}$ is the n-vector of currents injected in all load, generation and storage nodes and $\mathbf{R}$ is the inverse of the reduced conductance matrix $\mathbf{G}$, which derivates from the total admittance matrix of the network by deleting the first row and the first column related to the slack bus.

Appendix B

Conversion of the standard AC LV Cigré distribution network to be used in DC

The data of the test LV network are reported in tables B.1 and B.2. Compared to the original AC benchmark network provided from the CIGRE, the network's lines #14 (connects bus #3 to bus #12) and #15 (connects bus #12 to bus #14) were modified to make the network more usable with a DC supply. In the modifications, symmetrical cables were substituted for both lines, which originally were not symmetrical. In so doing, all of the lines in the considered LV network were made of 4 conductors of the same size (Table B.2).

Table B.1. Lines of the network

	Line of the Network		**Line type**	**Line length**
n.	**from bus #**	**to bus #**		**[m]**
1	0	1	L_1	35
2	1	2	L_1	35
3	2	3	L_1	35
4	3	4	L_1	35
5	4	5	L_1	35
6	5	6	L_1	35
7	6	7	L_1	35
8	7	8	L_1	35
9	8	15	L_1	35
10	15	9	L_2	30
11	8	13	L_3	30
12	5	11	L_4	30
13	3	16	L_2	30
14	3	12	L_1	105
15	12	14	L_5	30
16	2	10	L_3	30

Table B.2. Typologies of the lines used in the network

Line type	Cable type	Resistance [Ω/km]
L_1	4 × 120 mm^2	0.284
L_2	4 × 16 mm^2	1.380
L_3	4 × 6 mm^2	3.690
L_4	4 × 25 mm^2	0.871
L_5	4 × 50 mm^2	0.397

The 4-conductors' lines (3 phases and 1 neutral) used in the test network were made by 4-core cables that, in the original benchmark LV grid, were used in a three-phase system at 400 V (Fig. B1a).

To achieve the transition of the original network to DC (Fig. B1b), the DC voltage was 400 V, since this value provides the same cable characteristics and losses, and it is widely adopted in current efforts toward the standardization of LV DC networks.

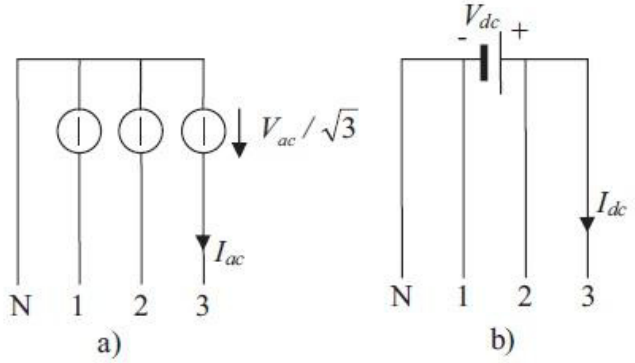

Fig. B1 - System cabling in a 4-wire cable; AC (a) and DC (b)

With reference to the symbols of Fig. B1, the equality of the line losses can be written as:

$$4RI_{dc}^2 = 3RI_{ac}^2 \tag{B.1}$$

where R is the line resistance and I_{dc} and I_{ac} are the line currents in the DC and AC case, respectively. From (B.1), the following relationship can be derived:

$$I_{dc} = \sqrt{\frac{3}{4}} I_{ac} \tag{B.2}$$

By denoting the rated AC and DC voltage as V_{ac} and V_{dc}, respectively, the equality of the transferred power in AC and DC, i.e.

$$2V_{dc}I_{dc} = \sqrt{3}V_{ac}I_{ac} \tag{B.3}$$

gives:

$$V_{dc} = V_{ac} \tag{B.4}$$

Thus, since the original network operates at the rated voltage of V_{ac} = 400 V, it follows that the rated voltage in DC is V_{dc} = 400 V.

Appendix C

Mixed Integer Linear Programming: Linearization of the product of decision variables

To prevent solutions where energy is sold to the grid and bought from the grid at the same time (which is physically impossible on a single PCC), three auxiliary variables were used in constraining the power exchanged with the grid:

- u(t): binary variable which is 1 when energy is purchased from the grid and 0 when energy is sold to the grid,
- $S_{Conv,p}$ (t): real variable which is equal to S_{Conv} when u(t)=1 and is 0 when u(t)=0,
- $S_{Conv,s}$ (t): real variable which is equal to S_{Conv} when u(t)=0 and is 0 when u(t)=1.

Once these variables are available, constraints on the power exchanged with the grid can be easily expressed by means of equations C1 and C2:

$$P_{pg}(t) \leq \mathrm{Min}(S_{Conv,p}(t), P_{PCC}) \quad \text{(C1)}$$

$$P_{sg}(t) \leq \mathrm{Min}(S_{Conv,s}(t), P_{PCC}) \quad \text{(C2)}$$

which force a unidirectional energy flow (limited by the size of the converter and the contractual power on the PCC), considering that only one variable between $S_{Conv,p}$ (t) and $S_{Conv,s}$ (t) can be different from zero at each time-step t.

The link among values of $S_{Conv,p}$ (t), $S_{Conv,s}$ (t) and the binary variable u(t) can be easily expressed as:

$$S_{Conv,p}(t) = S_{Conv}\, u(t) \quad \text{(C3)}$$

$$S_{Conv,s}(t) = S_{Conv}\,(1 - u(t)) \quad \text{(C4)}$$

Unfortunately, equations (C3) and (C4) contain products of decision variables, therefore they are incompatible with the desired linear formulation of the problem.

This difficulty can be resolved by resorting to the following set of linear inequalities (to be applied at each time t):

$$S_{Conv,p}(t) \leq BigM\ u(t) \quad (C5)$$
$$S_{Conv,p}(t) \leq S_{Conv} \quad (C6)$$
$$S_{Conv,p}(t) \geq S_{Conv} - BigM\ (1 - u(t)) \quad (C7)$$
$$S_{Conv,s}(t) \leq BigM\ (1 - u(t)) \quad (C8)$$
$$S_{Conv,s}(t) \leq S_{Conv} \quad (C9)$$
$$S_{Conv,s}(t) \geq S_{Conv} - BigM\ u(t) \quad (C10)$$

where BigM is a "sufficiently large" constant. Therefore, when u(t)=1, constraints (C5) and (C10) are relaxed, while constraints (C6) and (C7) force $S_{Conv,p}(t)= S_{Conv}$ and constraint (C8) forces $S_{Conv,s}(t)=0$. On the contrary, when u(t)=0, constraints (C7) and (C8) are relaxed, while constraints (C9) and (C10) force $S_{Conv,s}(t)= S_{Conv}$ and constraint (C5) forces $S_{Conv,p}(t)=0$.